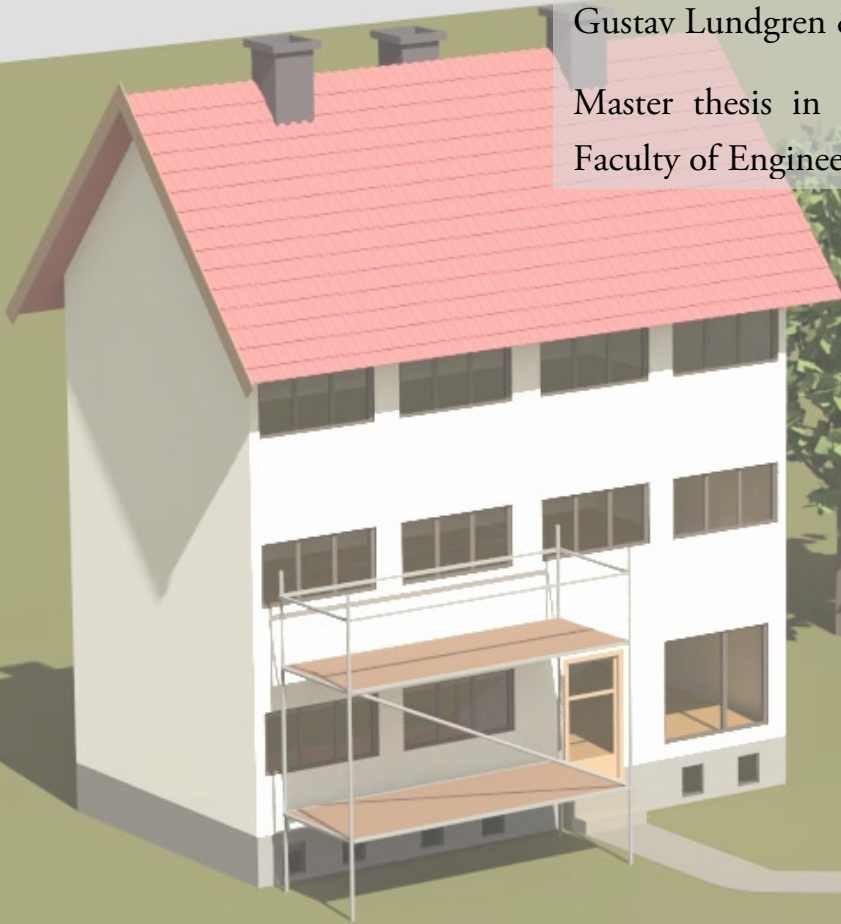


Evaluating retrofit options for specific buildings with low energy-performance in Skåne, Sweden

Focusing on energy use, environmental impact, profitability, and thermal comfort

Gustav Lundgren & Rohullah Hussaini

Master thesis in Energy-efficient and Environmental Buildings
Faculty of Engineering | Lund University



Lund University

Lund University, with eight faculties and a number of research centres and specialized institutes, is the largest establishment for research and higher education in Scandinavia. The main part of the University is situated in the small city of Lund which has about 112 000 inhabitants. A number of departments for research and education are, however, located in Malmö. Lund University was founded in 1666 and has today a total staff of 6 000 employees and 47 000 students attending 280 degree programmes and 2 300 subject courses offered by 63 departments.

Master Programme in Energy-efficient and Environmental Building Design

This international programme provides knowledge, skills and competencies within the area of energy-efficient and environmental building design in cold climates. The goal is to train highly skilled professionals, who will significantly contribute to and influence the design, building or retrofitting of energy-efficient buildings, taking into consideration the architecture and environment, the inhabitants' behaviour and needs, their health and comfort as well as the overall economy.

The degree project is the final part of the master programme leading to a Master of Science (120 credits) in Energy-efficient and Environmental Buildings.

Examiner: Pieter de Wilde (Division of Energy and Building Design)

Supervisor: Jouri Kanters (Division of Energy and Building Design), Ricardo Bernardo (Division of Energy and Building Design).

Keywords: Life Cycle Assessment, Life Cycle Cost, Energy use, Thermal comfort, Retrofitting, Buildings, Parametric analysis.

Publication year: 2024

Abstract

In pursuit of energy efficiency and sustainable development, goals have been set by the EU and Sweden to improve the energy performance of buildings and reduce their environmental impact. Renovating the existing building stock is a path to achieving the energy and climate goals. This study investigates and analyses various retrofitting options for multifamily residential buildings in Skåne, Sweden, concerning energy performance, life cycle cost, life cycle assessment, and thermal comfort.

Two multifamily buildings in Skåne with the lowest energy performance were chosen from the Swedish National Board of Housing, Building and Planning's database. Information about the buildings was gathered from relevant literature, respective building owners, and city planning offices to create an energy model for both buildings, suited for simulation. A detailed parametric analysis was conducted, creating 560 cases for each of the buildings, and included measures such as insulating the façade and roof, new windows, implementation of mechanical ventilation, and heat pump system. The results from the parametric analysis were used to evaluate the retrofitting options in different categories, namely, operational energy, profitability (life cycle cost), environmental impact (life cycle assessment), and thermal comfort (overheating hours). The energy model was created in Rhinoceros 3D and the parametric simulations were done with Grasshopper plug-in. Data for costs were collected from Wikell's database and manufacturers, while the input data for environmental impact calculations were collected from relevant EPDs and the climate database of the Swedish National Board of Housing, Building, and Planning.

The results indicate that the best-retrofitted cases are different, depending on what factors are being analyzed and given priority. The best energy performance was achieved when all the measures were combined. Similarly, the retrofitting options with the lowest environmental impact consisted of all measures that reduce the operational energy and its impacts. Moreover, the combination with roof and façade insulation proved to be the most profitable option, due to the low investment cost relative to the energy savings. While other measures were less desirable when economic efficiency was the main aim. The implementation of mechanical ventilation with heat recovery was also a less desirable option from an environmental standpoint, due to its high embodied impact. On the contrary, heat pump systems and mechanical ventilation systems with heat recovery are preferred when prioritizing energy savings. The best thermal comfort can be achieved by using a mechanical ventilation system in combination with window replacement or roof insulation for building A and building B respectively. Consequently, the insulation of the roof proved to be a common measure in winning cases across all categories, while other measures varied across analysis categories.

Acknowledgments

Imagine having a cup of coffee like every other morning for the last six months, raising your head from the computer, and realizing it is time to turn in the report which you have been pouring your soul into, keeping you up and awake for many nights. The weight is still there on your shoulders, but the imagination of how light you can be is not surreal. Firstly, as authors of this study, we would like to thank each other for the great effort and dedication put into this report, which is a product of approximately 1 800 hours of work. Hopefully, we both can look back and appreciate the time spent in creating this study.

We would like to express our deepest gratitude to our supervisors Jouri Kanters and Ricardo Bernardo. For their support, and the invaluable hours they put into guiding us on a path, that would lead to the end-product of this report. This research would not have been possible without their assistance throughout the journey.

We extend our heartfelt gratitude to Stefan Carlsson from GK for providing insightful ideas and data for this study, and Ilia Iarkov from Lunds University, whose exhaustive responses created clarity and guidance whenever we needed help. Furthermore, we would like to highlight René Andersson from HSB Landskrona and Oliver Gerlach from BRF Sofielund. For their help in assisting us with data collection and access to the buildings. They did not expect anything in return but alas, they provided us with both their time and interest.

Finally, we express our heartfelt appreciation to our dear families for their unwavering support throughout the last two years, and especially this journey. We would also like to thank all the professors and teachers in this master's program for teaching us and providing us with the knowledge necessary to complete this study.

Abbreviations

ACH – Air change per hour
ADP – Abiotic depletion potential
AHU – Air handling unit
AP – Acidification potential
BBR – Boverket’s building regulations
Boverket - The Swedish National Board of Housing, Building and Planning
CAV – Constant air volume
CDB – Climate database
COP – Coefficient of performance
CS – ClimateStudio
DDY – Design day year
DH – District heating
DH-system – Hydronic system with district heating
DHW – Domestic hot water
DVUT – Design winter outdoor temperature
EEM – Energy efficient measure
EP – Eutrophication potential
EPD – Environmental product declaration
EPW-file – EnergyPlus weather file
GH – Grasshopper
GWP – Global warming potential
GWP-GHG – Global warming potential, excluding absorption and emission of biogenic carbon dioxide
HP – Heat pump
HP-system – Hydronic system with air-to-water heat pump
HR – Heat recovery
HVAC – Heating, ventilation, and air conditioning
LCA – Life cycle assessment
LCC – Life cycle cost
MEV – Mechanical extract ventilation
MVHR – Balanced mechanical ventilation with heat recovery
NPV – Net present value
ODP – Ozone depletion potential
POCP – Photochemical oxidant creation potential
Rhino – Rhinoceros 3D
SCOP – Seasonal coefficient of performance
SFP – Specific fan power
U-value – Heat transfer coefficient
VAV – Variable air volume
WUFI – Wärme und feuchte instationär

Table of Contents

Abstract	i
Acknowledgment.....	ii
Abbreviations	iii
1 Introduction.....	1
1.1 Background	1
1.2 Aim	1
1.2.1 Objectives	1
1.3 Limitations	2
2 Literature review	3
2.1 Earlier retrofitting options – in Sweden	3
2.2 Environmental impact	4
2.3 Profitability	5
2.4 Thermal comfort	6
2.5 Conclusion	6
3 Theoretical framework	9
3.1 Building & systems	9
3.1.1 Envelope & moisture safety	9
3.1.2 Ventilation	10
3.1.3 Heating	12
3.2 Life cycle cost	14
3.3 Life cycle assessment	15
3.4 Thermal comfort	16
4 Method	17
4.1 Investigation & selection of buildings	17
4.1.1 Data	17
4.1.2 Two buildings	18
4.2 Base cases	18
4.2.1 Building A	18
4.2.2 Building B	22
4.3 Energy use & thermal comfort	24
4.3.1 Input values	24
4.3.2 Thermal comfort	26
4.4 Retrofitting	28
4.4.1 Envelope & air infiltration	28
4.4.2 Ventilation system	30
4.4.3 Heating system	30
4.4.4 Parametric analysis	32
4.4.5 Energy	32
4.5 LCC	32
4.5.1 Net present value	32
4.5.2 Saved Operational Cost	32
4.5.3 Investment and maintenance costs	33
4.5.4 Sensitivity analysis	34
4.6 LCA	34
4.6.1 Goal, scope, and system boundaries	34
4.6.2 Embodied impact	34
4.6.3 Operational impact	35
5 Results & discussion	37
5.1 Building A	37
5.1.1 Base case - simulation	37
5.1.2 Envelope & systems	39
5.1.3 Energy	42
5.1.4 LCC	43
5.1.5 LCA	48
5.1.6 Thermal comfort	50

5.1.7 Summary	52
5.2 Building B	53
5.2.1 Base case - simulation	53
5.2.2 Envelope & systems	55
5.2.3 Energy	57
5.2.4 LCC	58
5.2.5 LCA	63
5.2.6 Thermal comfort	64
5.2.7 Summary	66
6 Conclusions	68
6.1 Further studies	69
References	70

1 Introduction

1.1 Background

As the living standard in countries continues to grow, energy demand worldwide increases as well. In the latest report by the International Energy Agency, the total energy usage of buildings reached a level of 37 TWh during the year 2022, a level which has been increasing on average by 1 % the last decade, and accounts for approximately 30 % of the total (123 TWh) energy use when compared with industry, buildings, transport, and other end-users in total (International Energy Agency, 2023). The building sector in Europe and Sweden is also responsible for approximately 40 % and 34 % of the total energy use respectively (European Commission, 2024). In Sweden the building sector's energy use has grown in the past decades, leading to a higher environmental impact due to increased energy use. The building sector in Europe stands for approximately 36 % of greenhouse gas emissions which stem from the construction, operation, maintenance, and demolition of the buildings (European Commission, 2020; Naturvårdsverket, 2023).

To combat the negative climate changes caused by the environmental impact of the building sector and promote sustainable development, climate goals have been introduced by the EU. The European union has a long-term goal of reaching climate neutrality by the year 2050 and another goal to reduce the net emissions by the year 2030, by at least 55 % compared to the year 1990 (European Commission, 2024). The European countries are obliged to introduce legislation to help achieve these goals and since the building sector is responsible for a big part of the emissions, improvements need to be made to reduce the environmental impact. In the quest for sustainable development, building retrofitting is a crucial strategy, offering a pathway towards mitigating the environmental impact, improving energy efficiency, and enhancing the overall performance of existing buildings. Since 75 % of European buildings have very poor energy performance, renovating the building stock is, therefore, the key to energy efficiency and sustainable development (European Commission, 2020). Traditionally, the assessment of retrofitting measures has mainly focused on energy efficiency to reduce operational costs (Santamouris et al., 2000). However, as buildings become more airtight, they retain the heat in the building, increasing the risk of thermal discomfort due to higher indoor temperatures (Zou et al., 2023). Consequently, the need for the integration of thermal comfort in the decision-making process is growing. Therefore, it is important to consider broader perspectives when assessing various retrofitting measures.

The growing interest and effort in improving energy efficiency and reducing the climate impact of the building industry have led to many questions regarding the types of retrofitting, and how they affect the building. This study strives to contribute to the growing knowledge surrounding retrofitting buildings in pursuit of sustainable development, by comparing them within categories.

1.2 Aim

This study aims to analyze potential retrofitting options for buildings with the lowest energy performance and similar characteristics in Skåne, Sweden, selected from a database consisting of energy declarations.

1.2.1 Objectives

To achieve the aim of this study the following objectives were used to analyze the retrofitting options.

- Identifying retrofitting options with the lowest energy use.
- Identifying the most profitable retrofitting options in terms of NPV.
- Identifying retrofitting options with the lowest environmental impact in terms of LCA.
- Identifying retrofitting options with the best thermal comfort, in terms of overheating hours.

1.3 Limitations

The database used for selecting the base cases included only buildings with an energy declaration performed between 2019 and 2022, which is fairly limited in number. It was deduced that some buildings had an incorrectly declared performance, resulting in lower energy performance.

Daylighting was not included in the study, and it should be advised that adding insulation to the façade will negatively impact the amount of daylight, resulting in effects not considered in this study. Furthermore, the design of the ventilation ducting did not consider the reduced living area. Even though the installation of vertical ducts was focused on the stair area and the wardrobes in the apartments, some ducting had to be installed in other spaces of the apartments. This could likely have a negative effect on the profitability of this measure but was not considered.

Additionally, software used to design heating systems such as IDA ICE and HoneyBee usually uses a DDY file to consider hours of peak load. This study did not utilize this type of file format, which could lead to an undersized peak load. Furthermore, an HP is usually combined with an additional heat source such as an electric cartridge to cover the peak demand during peak hours, since it is not economically feasible to cover the whole demand only with an HP. However, similar to photovoltaic panels, this was not included in the study. The inclusion of photovoltaic panels could have provided more options for these buildings, thereby improving the decision-making process for selecting suitable options, but was not selected due to the lack of time.

Due to the lack of information regarding the repair and maintenance of the base case, only costs and environmental impact of operational energy were included for LCC and LCA assessment of the base case. If repair and maintenance had been included, one could expect higher costs and carbon impact. Thus, resulting in different recommendations than currently stated. Furthermore, in the calculations regarding environmental impact, stages A1- A5 (production, transport, and installation), B2 (maintenance), and B4 (replacement) are included. Stage B4 is represented by the environmental impact of product replacements. During this stage, the used products are replaced with new ones, meaning that environmental impact from stages A1-A5 is used to account for the impact of the new product. However, stages C1-C4 (end of life) representing the disposal and waste processing of the old product, are not included in the study. This is due to a lack of information about the environmental impact of stages C1-C4 for some products. Thus, including the impact of only some of the products will not create grounds for a fair comparison. Therefore, it is decided to only include impacts from stages A1-A5 in the B4 stage.

Additionally, there was no inclusion of electric components in either of the heating- or ventilation systems. This was mainly due to the lack of knowledge of which components to include, but also due to the lack of EPDs in the current market for electronics. Nonetheless, an inclusion could have increased the accuracy of the results and increased the impacts of these systems.

2 Literature review

This chapter aims to illustrate which EEMs previous studies have researched and what to consider when retrofitting existing buildings.

2.1 Earlier retrofitting options – in Sweden

In the literature review published by Abdul Hamid et al. (2018) 234 references were analyzed regarding retrofitting measures and retrofitting strategies. The most researched topic was energy, and the most implemented retrofitting involved envelope, airtightness, ventilation-, and heating systems.

When retrofitting a building into an energy-efficient building it is important to implement a holistic approach to illustrate which retrofitting might be the most efficient, by analyzing peak loads and energy demand. Factors that can and should be considered when creating an energy-efficient building are window size, energy-efficient frames- and glazing, thick insulation, favorable orientation relative to irradiation, low thermal bridges, airtightness, MVHR, solar control, an efficient heating system, and cool colors (Bastian et al., 2022; Janson, 2008). However, the implementation of such measures will not be as effective in existing buildings, mainly due to ineffective compact building shape, orientation, and thermal bridges (Ekström & Blomsterberg, 2016).

In the extensive publication made by Bournas et al. (2016), a holistic approach was used to improve the energy demand of a building named Maria Park, located in Sweden, into an office building using building performance simulations. The method of the study consisted of first reducing peak and energy demand, by decreasing the heat loss from the envelope by installing new energy-efficient windows and improving the facades by adding insulation on the inside with account to its heritage value. The roof and façade were also improved by the addition of insulation, which was analyzed concerning moisture safety using WUFI. The floor plan was optimized with regards to the type of room and required daylighting, shading was implemented to reduce the amount of overheating, and night-time natural ventilation was used to cool down the building during summer. Furthermore, daylighting was analyzed to reduce the use of lighting equipment and decrease the risk of glare. Two HVAC systems were analyzed and evaluated in terms of operational energy, the first was an all-air system that provided hygienic fresh air and heating from a heating coil in the AHU. The second was a combination of an air system providing hygienic fresh air and a hydronic system with heating supplied by radiators. Both systems utilized a heat exchanger with DH. The energy required for heating was decreased by approximately 80 % when using either all-air or the hydronic system, and the previously mentioned measures.

In the conclusions made by Bolliger et al. (2015), it is stated that there is a great synergy between renovating the envelope before replacing the heating system since it reduces the peak load and thereby improves the conditions of a heating system. Another article related to HVAC and peak load is the article published by Q. Wang et al. (2016), in which an HVAC system with ventilation heat recovery jointed heating was evaluated regarding energy performance, environmental impact, and indoor air quality (IAQ), in a multi-family building, located in Sweden, using the software IDA ICE. Three types of radiators, conventional radiators, ventilation radiators, and baseboard radiators, with the same surface area, were investigated in combination with an MVHR-system. It was concluded that the reduction of the heating peak load is a crucial part of installing an effective low-temperature heating system since it reduces the energy demand and, thus the required supply temperature, which in turn improves the COP of the HP. Compared with conventional radiators, it was possible to increase the COP of the air-to-water HP between 12 % and 18 %, for ventilation radiators and baseboard radiators respectively, using the same surface area.

In the article published by Ekström & Blomsterberg (2016) four single-family houses built during the Million programs, located in Sweden, were analyzed using IDA ICE. The study involved a step-by-step implementation starting with the envelope and ending with the heating system, a method which is appropriate when reducing the energy demand effectively. The measures included adding insulation to the façade, roof, and foundation, new windows and doors, improved airtightness, ventilation with heat recovery, and new and improved circulation pumps. Energy-efficient controllers for heating were also installed, which reduced indoor temperature from 21 degrees to 18 degrees when tenants were not at home and asleep, which proved to have a large impact on the energy demand. Similar findings were deduced in a study made by Avelin et al. (2017). The results indicated a potential to decrease the heating demand by approximately 75 % to 80 %. A similar reduction

was achieved in the article published by Bastian et al. (2022), where a high-rise building in Gothenburg, Sweden, built during the Million program, was renovated using Passive house concepts. The measures involved, replacing the windows with new and more energy-efficient windows, installing a thick layer of insulation on the façade, blowing 500 mm of cellulose on the attic floor which had a low environmental impact, and utilizing the already existing ducts to install a MVHR-system. Since the drainage around the building was going to be replaced, the existing ground material was replaced with foam glass gravel, which was chosen due to its drainage and insulation capabilities. The final energy demand was approximated to decrease by 75 %.

2.2 Environmental impact

In the comprehensive literature review published by Bahramian & Yetilmezsoy (2020), more than 230 articles between the period of 1997 to 2018 were identified and analyzed to summarize two decades' worth of research to describe the current state of the subject. The authors concluded that low-rise buildings (1-5 floors) were significantly more often researched than high-rise buildings (≥ 5 floors), with approximately two times the number of articles. Furthermore, when analyzing low-rise buildings, residential was the most common, and when analyzing high-rise buildings commercial buildings gained more attention. The most frequent indicator used was GWP. The most frequently analyzed stages were the use and construction phases, with a census in the industry that the use phase had the largest impact on the life cycle stage, followed by the construction phase. Lastly, it was stated that the definition of the functional unit varied from article to article, while most articles used “m²” as a functional unit (60 %), some used “whole building” (20 %). This led the authors to conclude that the definition of the functional unit lacks a standardized definition.

In the publication made by Jaemoon et al. (2023), the authors stated that the impact from the operational stage has the largest impact considering a life cycle perspective, but that many options are being implemented country-wide to install renewable energy as well as improve the energy performance of buildings. However, there are still improvements to be made in the material production stage, due to it being the second largest impact during a building's life cycle. The study focused on evaluating 29 school facilities from the earliest stages (production) to the end of the building's life (cradle-to-grave), in South Korea, using a self-developed life cycle evaluation tool. The authors started by setting up each case and implementing environmental product declarations (EPDs) on five materials with high environmental impact. The results indicated a relevant reduction on each impact: GWP, ODP, ADP, AP, EP, and POCP, illustrating the importance of choosing environmentally friendly materials early in the construction phase.

In the article published by Ramírez-Villegas et al. (2019), the authors focused on analyzing four refurbishment-packages on a residential multi-family building located in Borlänge, Sweden, using primarily EPDs as an impact-factor. The analysis was performed using the indicators: GWP, AP, ADP, and EP, on all stages of the building's life cycle (cradle-to-grave). The packages consisted of installing HR in the existing MV-system, adding insulation to the façade and the unheated attic, and replacing the windows. The operational stage, including construction and installation, proved to have the largest environmental impact on all scenarios. The results could be explained by the cold climate and low irradiation during the cold months, which allowed for a large amount of saved operational energy, which in turn led to a large reduction of the environmental impact, relative to the base case. Additionally, the authors noted a significant impact from the material and construction stages, excluding transportation.

According to Decorte et al. (2024), many studies simplify the process when calculating the LCA of a technical system, such as ventilation and heating systems, mainly due to the high number of components, and if the construction is in at an early design phase and lacks a bill of materials. The article analyzed the difference between such simplified calculations compared to more detailed ones. A total of six heating and four ventilation scenarios were carried out. The reference building was a newly built, three-story residential building, and was located in Flanders, Belgium. The functional unit was defined as a “single-family dwelling with a gross floor area of 154 m²”, analyzing the effects of GWP, for 60 years, in the stages of production (A1-A3), construction (A4-A5), operation energy use (B6), replacement (B4), and end of life (C1-C4). The results indicate that simplifications can decrease the accuracy of the LCA up to 12 % of the embodied impact, and it should be considered simultaneously that a technical system could contribute between 5 % to 20 % of the entire life cycle impact and that the contribution increases with more energy-efficient systems. A large amount of the embodied impact was due to production and replacements. Furthermore, emphasis was put on not neglecting materials

with low weight relative to the total building, since the impact per kg could be higher and thus relevant for the assessment.

2.3 Profitability

In the article published by Ban & Bungâu (2022), three different HPs were analyzed, air, ground, and water, with a COP set to 4, 4.6, and 4.7 respectively, assuming it would be possible to implement both water and ground source HP. The analysis was based on the profitability using LCC, of the three options, with a fixed electricity price equal to approximately 2.7 SEK/kWh (exchange rate based on currency of 2024), and a lifespan of 20 years for the HPs, and a calculation period of equal time. The systems were analyzed on an energy-efficient two-story single-family building, located in Romania. The results illustrated that the air-source HP was the most profitable 10 years into the calculation period, after which the ground source HP became more profitable. Looking at the perspective of 20 years the ground source should be prioritized, followed by the water source, and lastly, the air source. The analysis included a sensitivity analysis using different levels of both electricity price and interest rate separately and partially confirmed the results of the LCC.

Potential HVAC and envelope solutions were analyzed for two detached houses in Norway by Heide et al. (2022). The authors provided a comprehensive analysis consisting of nine HVAC combinations, including HPs (exhaust, ground, air-to-air, air-to-water), solar collectors, electric boilers, and balanced- and extract ventilation. All heating systems had an auxiliary electric resistance heater for the peak load, reducing the risk of oversizing. The article concluded that most investments with large investments cost-effectively reduced the operational energy but drastically increased the cost beyond the lifespan of the installation and that the investment of certain HPs can be effective if no hydronic distribution is required. Additionally, it was concluded that there were no optimal solutions for both reducing energy use and LCC.

The aim of the article published by La Fleur et al. (2019) was to identify cost-optimal EEMs using LCC for a commonly built multi-family building located in Linköping, Sweden. Several measures were implemented and analyzed including adding insulation to the façade, roof, and attic, replacing the windows, and installing a MVHR and a ground source HP. The study concluded that the saved operational energy represents a small part of the LCC for the specific building and that the assumed energy price directly affects the profitability, additionally that the capital required to retrofit is too large relative to the savings. However, there is a great potential in retrofitting the façade due to the large area, but since the initial U -value of the facades was relatively low, the results were poor. For buildings in need of retrofitting and having a higher U -value the profitability should increase. The MVHR system was not preferred when aiming for the lowest LCC, and the ground source HP had a lower LCC compared to district heating. Additionally, the capital costs will vary depending on the building type, contractor, and the building location. The article highlights that the results could be used for similar buildings in similar climates, but that building types differ and that a comprehensive analysis is required to determine which EEMs are the most optimal for a specific building.

In the comprehensive article published by Milić et al. (2019), the authors evaluated the LCC for refurbishment strategies for 12 historic buildings that represent the historical building stock in Visby, Sweden. The EEMs included three types of new windows, weatherstripping, and insulation on the façade, roof, and floor. The heating systems included a wood boiler, district heating, a groundwater HP, and electric radiators. The results indicated that it is profitable in most cases to decrease the energy use by 50 %, but that the profitability of the EEMs depends on the transmission losses before the retrofitting. The results indicated that the most cost-effective EEMs are weatherstripping and added insulation in the roof and floor. Furthermore, the article concluded that the building characteristics will affect the choice of a cost-optimal heating system, specifically its construction properties and running costs. In general, district heating was more suitable for single-family housing, and wood boilers in apartment buildings.

In the article published by Niemelä et al. (2017), a Finnish brick-building, typical to most brick buildings built in Finland during the first half of the 1960s, was used as a reference case to analyze cost-effective HVAC systems and refurbishments to the envelope. Four heating systems were analyzed including ground source HP, exhaust air HP, air-to-water HP, and DH. With a scenario where the current radiator system was renovated to fit a new low-temperature heating system. The ventilation system was also retrofitted to an MVHR. The measures applied to the envelope were additional insulation on the walls, in the roof, and new windows. The authors concluded that the installation of an MVHR is not economically feasible even though the building has

a current exhaust system. This is mainly due to the large initial cost of the system, and the outcome did not change even if the saved energy would increase. It was, however, noted that thermal comfort typically improves when refurbishing a ventilation system into an MVHR and that this cannot directly be measured using economic calculations. Additionally, it was stated that adding insulation to the roof and/or replacing the windows were economically feasible while adding insulation to the facades was not. Lastly, it was stated that the HPs delivered the best results in terms of energy efficiency and cost-effectiveness and that from these the ground source HP performed the best, followed by air-to-water and exhaust air HP.

2.4 Thermal comfort

As previously mentioned in the article published by Bournas et al. (2016), the authors presented a holistic approach to retrofitting an office building using software to suggest an energy-efficient retrofitting. The authors used GH to evaluate the risk of overheating in the building and were able to reduce the overheating substantially by analyzing optimal shading while still maintaining a good amount of daylight. Furthermore, natural ventilation was also analyzed to further reduce overheating and the demand for active cooling. It was concluded that the combination of these measures reduced the overheating by approximately 20 % to 50 %, depending on the type of room.

Li et al. (2024) concluded that passive cooling techniques such as natural ventilation, exterior shading, thermal mass, and cool roofs could improve the indoor thermal environment effectively, while simultaneously reducing the cooling demand. It was further concluded that the mean air temperature was reduced by 2.8 °C for the specific building when using natural ventilation, external shading, and cool roofs. The study was conducted using a building with two identical rooms, referred to as chambers, in Tongling a cooling-dominated region of China. The measures were implemented in one of the chambers while the other chamber was used as a reference and was set as free-floating with no measures applied to it, thus allowing for a comparison between the two rooms. The study aimed to analyze the short- and long-term performance of the measures, both individually and in combination.

In the article published by Liu et al. (2015), the study aimed to evaluate both the indoor environment and energy use of a multi-family building from the 1970s located in Linköping, Sweden. The building had previously undergone retrofits and was used in comparison to a similar building that did not have the same installations, thus allowing for a comparison of the effects before and after retrofitting. The building went from an exhaust air system to an MVHR-system and had EPS added to the exterior part of the façade, including an air barrier to reduce infiltration and moisture. The existing windows were replaced from double-glazed to triple-glazed, reducing the U -value from 2.9 W/(m²·K) to 1.2 W/(m²·K), additionally, the roof had 50 cm insulation added to it. Furthermore, the article investigated the placement of different blinds to accommodate a better indoor environment during summer. The study included factors such as indoor air quality, air temperature, PPD, and PMV, using both measurements, questionnaires, and simulations using IDA ICE. It was concluded that the energy demand could be decreased by approximately 39 % and that the indoor environment could be further improved by adding blinds, with interior blinds reducing overheating by approximately 4 % and exterior blinds by 10 %.

2.5 Conclusion

From the literature review, it can be stated that among the most commonly researched topics energy is at the lead, and usually involves EEMs such as improving the envelope with better windows and added insulation, improving the airtightness, and installing MVHR-, and heating systems, usually involving the use of HP or the use of existing DH. Other common topics include environmental impact, profitability, and thermal comfort; however, these topics are rarely studied together. Additionally, the researched literature usually focused on typical buildings, or buildings which can represent a somewhat larger amount of the building stock, thereby enabling the application of the results in a broader context. Reference buildings are also used to illustrate the effect of retrofitting methods, in which the building does not necessarily represent a part of the building stock.

This study, similar to the reviewed literature, will include the previously mentioned EEMs. However, these measures will be investigated in different categories and the results will be presented separately in terms of

energy use, profitability, environmental impact, and thermal comfort, while considering moisture-safe constructions, thus separating this study from most articles.

A large quantity of the analyzed research has included the previously mentioned EEMs, with a resulting reduction of heating demand by up to 80 %, indicating a large potential when aiming for a lower operational energy use. This usually affects the environmental impact positively when analyzing the environmental impact from the life cycle of the building, due to the operational stage having an important part in the impact of the building. A common approach for retrofitting is to reduce the peak loads first to avoid oversizing the heating system, however, in this study, the heating systems were designed for the case with the highest peak load, since the measures are not implemented in a specific order. Parametric analysis has been implemented in many studies to analyze the best combination of the chosen EEMs. However, the information is limited on how the airtightness is calculated when implementing one measure relative to several, and in this study the authors implemented an airtightness that will depend on the specific combination of EEMs since it was assumed that the reduction of airtightness should not be equal for all applied measures.

The researched literature highlights the need to address thermal comfort and reduce overheating during summer, and that it can be reduced by using passive cooling techniques such as night-time natural ventilation, natural ventilation, solar shading, lower g-value, and cool roofs. It is stated that a combination of two or more of these measures can effectively improve thermal comfort by reducing overheating, with some cases reducing overheating as much up to 50 %, with a higher reduction of overheating using external blinds compared with internal.

While many studies have researched similar retrofitting measures presented in this study, this study aims to present comprehensive results with aspects relevant to energy efficiency, environmental impact, profitability, and thermal comfort, while still considering the moisture safety of any proposed retrofitting. These results can be used to retrofit similar buildings and thus, increase the energy efficiency of the building stock.

3 Theoretical framework

This chapter provides a theoretical overview of relevant building parts, systems, costs, environmental impacts, and thermal comfort, related to this study. Understanding these aspects will help the reader understand why the specific subjects were included in the study.

3.1 Building & systems

3.1.1 Envelope & moisture safety

The building envelope is usually a significant source of heat losses. These losses are defined as transmission losses and include thermal bridges. It is imperative to consider the potential of making it as energy-efficient as possible since it will decrease the operational energy and the peak power demand (Björklund & Ohlsson, 2018; Hagentoft & Sandin, 2017; Warfvinge & Dahlblom, 2010).

If a building does not fulfill the requirements set on the primary energy number after retrofitting, the constructions should have the following heat loss coefficients presented in Table 1, (Boverket, 2021a).

Table 1. Maximum U -value for envelope construction, according to BBR29.

Envelope constructions	U -value / (W/(m ² ·K))
Windows	1.2
Facade	0.18
Roof	0.13

Windows, façade, and roof

When retrofitting the envelope of a building, windows can have a significant impact on both the indoor environment and the technical installations (Poirazis et al., 2008). Compared to the surrounding walls, windows usually have a higher U -value due to the frame. The g -value of the glazing affects the solar gains and thus, the degree of overheating (Dubois et al., 2019; Hagentoft & Sandin, 2017). By installing new and more airtight windows, while also addressing the potential cracks around the installation module, the airtightness can be improved drastically and thus, improve thermal comfort by reducing the risk of draft. By reducing the air leakage, both operational energy and peak power demand will decrease, and also improve the heat recovery of a potentially installed ventilation system (Hagentoft & Sandin, 2017; Rønneseth et al., 2019). Modern windows are usually more energy-effective compared to traditional windows, which use two panes glazing, no inert gas, and low-E coating (Grynning et al., 2013; Jelle et al., 2012). Energy-efficient modern windows are usually constructed with three panes glazing, an inert gas between them, and a low-E coating to reduce the rate of heat loss (Hagentoft & Sandin, 2017). Similar to windows, the exterior wall configuration plays an important role in improving thermal comfort and minimizing heat losses, especially since the façade-area can be quite extensive. With a low U -value, benefits can be gained both in operative temperature and operational energy (Gustafsson et al., 2016; La Fleur et al., 2019; Terés-Zubiaga et al., 2015). By reducing cracks and other defects on the façade, the airtightness can be further improved, reducing the operational energy and peak power demand of heating, while also improving the thermal comfort (Hagentoft & Sandin, 2017; Warfvinge & Dahlblom, 2010).

Retrofitting the attic or the roof can significantly decrease operational energy usage, but the savings will vary depending on the area and the U -value (Gustafsson et al., 2016; Jradi et al., 2017; Terés-Zubiaga et al., 2015). By reducing cracks, and potential damage on membranes, the airtightness can be improved and thus, leading to a further reduction in operational energy (Hagentoft & Sandin, 2017; Warfvinge & Dahlblom, 2010)).

Moisture safety

When renovating a building it is important to consider the hygrothermal conditions of the constructions of interest, because a faulty renovated construction may create more problems than it started with. Conducting a thorough moisture safety analysis before retrofitting could prevent the wrong constructions from being built, consequently reducing the risks directly associated with mold (Arfvidsson et al., 2017; Hagentoft & Sandin, 2017).

Physical or chemical changes in a product caused by moisture are called moisture-related damages. Moisture-related damages can be in different forms, such as mold (microbiological growth), biodegradation (rot), fogging and staining, and frost damage. Moisture damage can lead to esthetical changes, physical, chemical, and biological degradation, as well as odors and health risks (Arfvidsson et al., 2017). Organic materials such as pine and spruce are sensitive to high levels of moisture and, hence, require a higher level of attention during an analysis. While inorganic materials are less susceptible to moisture-related damage, they still require attention (Arfvidsson et al., 2017).

One of the moisture damages that is dangerous for building materials and human health is mold growth. At a temperature above 0 °C and relative humidity above 75 % mold could start to grow in materials such as spruce and pine (Hukka & Viitanen, 1999), which in turn can lead to issues such as tiredness, headache, coughing, dry skin, and deterioration of the material. The relative humidity at which mold starts to grow is called critical relative humidity. The high water content of inorganic materials can also lead to moisture damage. The water content can increase to a level that negatively affects the properties of the material, and creates potential risks including frost damage, and increased thermal conductivity (Arfvidsson et al., 2017). Mold growth on wooden materials can be calculated using a mathematical model, developed by Hukka & Viitanen (1999). This model describes how mold growth happens as a function of temperature, relative humidity, and time. The amount of mold growth in the model is based on the mold index, which is a standard index based on the visual appearance of the studied surface, it scales from 0 to 6 and each scale is described further in Table 2.

Table 2. Mold index, developed by Hukka & Viitanen (1999).

Index	Growth rate	Description
0	No growth	Mold spores not activated
1	Some growth detectable only with a microscope	Initial stages of mold growth
2	< 10 % mold coverage of the surface	Detectable with microscope
3	Some mold growth on the surface	Detected visually
4	> 10 % mold coverage on the surface	Detected visually, moderate growth
5	> 50 % mold coverage on the surface	Detected visually, plenty of growth
6	Mold coverage around 100 %	Very heavy and tight growth

3.1.2 Ventilation

Ventilation is a crucial part of a building, providing fresh air and thereby mitigating the accumulation of CO₂ and moisture, thus, resulting in a more favorable environment to interact continuously in. The peak power demand is also a factor related to the ventilation, because of the losses from the ventilation and the heat recovery. It has the potential to affect the required capacity of the heating system due to the size of the losses and is thus an important part of the amount of operational energy required of a building (Björklund & Ohlsson, 2018; Warfvinge & Dahlblom, 2010).

Passive stack ventilation

Passive stack ventilation is driven by the difference in air density between the indoors and outdoors, but also the wind which can force air into the building. Typically, the air enters the building through supply air valves positioned on the façade, and usually located in the bedrooms and living areas, while the air exits the building through valves commonly placed on the chimney, located in the kitchen, bathroom, and laundry rooms. This ventilation method has benefits such as low maintenance requirements, long lifespan, and no operational cost. However, the drawbacks include a lack of control over air distribution, insufficient air change during summer due to low-temperature differentials, and a risk of excessive air changes during the colder months which leads to unnecessarily large heat loss. Passive stack ventilation was the most common type in residential buildings before 1970 and is still very common in older buildings to this day (Awbi, 2003; Björklund & Ohlsson, 2018; Hagentoft & Sandin, 2017; Warfvinge & Dahlblom, 2010).

Mechanical ventilation with heat recovery

MV is a system that utilizes fans to regulate the airflows, with separate fans for the supply and extraction of air. The air is supplied and extracted to and from the zones through diffusers connected to the ducting, following a similar principle for placement as passive stack ventilation. The ducting is connected to an AHU, usually consisting of filters, coils, fans, and heat recovery. Filters clean the air, both improving the air quality and protecting the heat recovery unit, while coils are powered by electricity or liquid and can be used to either heat

or cool the supply air depending on user requirements. The fans are used to supply and extract the air from the zones, while the heat exchanger is used to recover the heating energy, from the air leaving the building. Unlike passive stack ventilation, mechanical ventilation systems require balancing to correctly distribute the airflow, otherwise, it might not perform as intended (Awbi, 2003; Warfvinge & Dahlblom, 2010).

Mechanical ventilation systems, such as MVHR systems can be designed as a CAV or a VAV system. A constant airflow is used in a CAV system with the possibility to adjust the air temperature, often requiring fewer controls and less space for ducting, making it more cost-effective. In contrast, the VAV system initially is more expensive but has a lower operational cost due to adjustable air flows, while demanding more controls and larger space for ducting and AHU due to higher air flows. MVHR is the most common type in today's newly built buildings. The advantages of this system are the possibility to use heat which otherwise would be lost, control over airflow and its temperature, and cleaner air. However, the drawbacks include a higher operational cost, more maintenance, and that it requires space for both ducts and the fan room (Björklund & Ohlsson, 2018; Warfvinge & Dahlblom, 2010).

Designing an MVHR system

The minimum supplied airflow requirement for residential buildings is set to $0.35 \text{ l}/(\text{s}\cdot\text{m}^2)$, with an additional $7 \text{ l}/(\text{s}\cdot\text{person})$ for office spaces. However, it is a common practice in some cases to allocate a supply airflow of 4 (l/s) per bedroom and bed space, and a return airflow of 10 l/s per bathroom, this practice should however be neglected if the airflow falls below $0.35 \text{ l}/(\text{s}\cdot\text{m}^2)$ (Awbi, 2003; Boverket, 2021a; Warfvinge & Dahlblom, 2010).

The AHU is an important part of a mechanical ventilation system and can be designed using software such as Acon. Input data for the design includes critical paths of all ducting systems and the required air flows. Ideally, the fan room should be centrally placed on the roof or in an attic, creating better conditions for the supply and extraction of air, which also allows for a more symmetrical system and thus, reducing the pressure drop. Moreover, the fans create noise and therefore it should be considered when installing a ventilation system (Awbi, 2003; Warfvinge & Dahlblom, 2010). Furthermore, when placing diffusers, it is important to consider how the air will be distributed, with the number of diffusers depending on the airflow. Good air distribution will ensure that the air is not crashing and creating drafts, promoting better indoor quality through adequate air change rates. Furthermore, to improve comfort, the air velocity is usually designed at a level below 0.15 m/s during winter and 0.25 m/s during summer (Boverket, 2021a; Warfvinge & Dahlblom, 2010).

During the design stage, it is important to design the ducting with minimal bends and a symmetrical layout to minimize the pressure drop and simplify balancing. A balanced system ensures a correct airflow from each diffuser and is usually performed by locating the critical path and then adjusting the airflow in the remaining diffusers. The distance between two bends should be designed approximately with a minimum distance equal to $6\cdot D$, D being the diameter of the duct, to avoid unnecessary pressure drops and noise. The extracted air from polluted sources like kitchens should be separated. Furthermore, the ducting should be planned, to facilitate proper workspace for the installer (Boverket, 2021a; Warfvinge & Dahlblom, 2010).

The supply air temperature should be designed with consideration for thermal comfort, ensuring that it should be within a reasonable range to avoid discomfort. A coil is usually installed to regulate the temperature and can be powered by either a liquid or electricity. The size of the coil is dependent on factors such as airflow, specific heat capacity, density, and temperature. In cases where a heat exchanger is not installed or is malfunctioning, the DVUT can be used to ensure that the air is heated to a comfortable level (Awbi, 2003; Björklund & Ohlsson, 2018; Warfvinge & Dahlblom, 2010).

When selecting ducts, designers need to consider both space constraints and airflow requirements. While rectangular ducting may be necessary for a shortage of space, circular ducts utilize their area more efficiently compared to rectangular due to their corners, the products are also thinner since the geometry makes them stiffer, resulting in a cheaper, lighter, and more airtight product compared to the rectangular alternatives (Awbi, 2003; Warfvinge & Dahlblom, 2010). A common method for sizing the duct system is called equal friction, where the objective is to maintain an equal pressure drop across each part of the ducting. A pressure drop of 1 Pa/m is usually used, though variations may occur depending on the strategy. A friction chart or pressure drop diagram is used to determine the size of the ducts relative to the airflow, while still considering the velocity and the type of duct, see Table 3 (Awbi, 2003; Warfvinge & Dahlblom, 2010).

Table 3. Air velocities for different duct types, according to Warfvinge & Dahlblom (2010).

Duct-type	Air velocity /(m/s)
Main duct	6 – 9
Stem duct	4 – 6
Branch duct	2 – 4
Connecting duct	2

The choice of heat exchanger varies depending on the situation, with two typical heat exchangers being rotary- and plate heat exchangers. Rotary heat exchangers use a wheel that transfers the energy from the extracted air to the supply air. While they usually have a larger temperature efficiency, there is a risk of unintentionally transferring gas, particles, and moisture between airflows. On the contrary, the plate heat exchanger usually has a lower temperature efficiency but separates the supply air from the extract air, eliminating the risk of transferring unintentional gases, particles, and moisture between the airflows (Svensk Ventilation, 2024; Warfvinge & Dahlblom, 2010).

The efficiency of the fan is also crucial for the energy efficiency of the whole system. The SFP quantifies the efficiency of the fan system and depends on factors such as pressure drop reduction, the size of airflows, the efficiency of the ducting design, and efficient components. When installing a new ventilation system, or renovating an existing one, the SFP should be below $1.5 \text{ kW}/(\text{m}^3 \cdot \text{s})$ (Boverket, 2021a; Warfvinge & Dahlblom, 2010).

3.1.3 Heating

Heating plays a crucial role in improving the performance of the building, affecting factors such as comfort, moisture safety, and energy use, where a poorly designed system can lead to an increase in energy use (Siegenthaler, 2023; Warfvinge & Dahlblom, 2010). Understanding the different types of heating systems is essential to choosing and designing the correct system for a building.

District heating

The DH system consists of three parts; 1) a plant producing heat from various sources, 2) a distribution net transferring the heat, and 3) a heating center in the building responsible for exchanging the heat from the plant into the building's distribution system. These systems generally keep a relatively high temperature compared to other systems, between $70 \text{ }^\circ\text{C}$ and $120 \text{ }^\circ\text{C}$, using a very high pressure to reduce the risk of boiling (Björklund & Ohlsson, 2018; Warfvinge & Dahlblom, 2010). The user pays for the heating energy it uses from the distribution net, using a fixed energy price which can be altered one time each year by the owners of the district heating net (Energimarknadsbyrå, 2023). A DH system cannot utilize heat the same way as an HP, its COP can be said to equal 1 in the best cases (Warfvinge & Dahlblom, 2010). The disadvantages of this system include a relatively low COP and low flexibility in terms of choosing the energy supplier since each district can only buy from a specific supplier. The advantages include the possibility of a high supply temperature to the user and a steady energy price which can only be changed once every year.

Heat pump

An HP uses the concept of converting energy from a relatively low-temperature source to energy from a higher-temperature source. Depending on the type of HP, different energy sources can be used, such as air, water, or soil. An HP usually consists of four main components, an evaporator in which the temperature of the circulating liquid is lower than the energy source's, causing heat to be transferred into the circulating liquid as it evaporates. The second component is a compressor which compresses the vaporized liquid, creating a larger pressure and increasing the temperature even further. The third component is a condenser, in which the temperature of the circulating vaporized liquid releases heat and condensates to a highly pressurized liquid, the liquid then flows to a thermal expansion valve which reduces the pressure and thus the temperature before beginning its path in the evaporator again. The heat gained from the evaporator and compressor determines the COP, and the smaller the temperature difference is between the evaporator and condenser, the less heat will be added by the compressor, resulting in a higher COP. Compared to a DH system, an HP supplies a much lower temperature (Siegenthaler, 2023; Warfvinge & Dahlblom, 2010). Advantages of the system include a relatively high COP which can decrease the purchased operational energy substantially, and their ability to provide both heating and cooling. However, the drawbacks include low performance during peak demand periods and the requirement for larger and/or more radiators due to the relatively low supply temperature.

Designing a heat pump system

The required peak power is determined by calculating the transmission, leakage, and ventilation losses for each space of the building while considering thermal bridges, no internal load, and no solar gains, using the DVUT for the specific building (Warfvinge & Dahlblom, 2010). The peak power demand will determine the capacity of the HP, and its placement can depend on many factors, such as incoming cold water, access to the connection point of the heating net, and noise levels. It is usually located in the basement of residential buildings (Siegenthaler, 2023).

Determining the type of system depends on the available capital and desired efficiency, the most common are the one- and two-pipe systems, three-pipe systems also occur but are usually not considered since they require more capital. In a one-pipe system the radiators are connected to the supply piping with both the supply- and return, resulting in less needed piping but requiring larger radiators, and since both supply and return are connected to the same supply piping the temperature in the piping will decrease after each radiator, and thus affecting the possible size of the system. In a two-pipe system the supply and return are separated, creating a larger cost for piping but requiring a small cost for radiators. It is also possible to supply each radiator with the same supply temperature, which in turn makes the system easier to size. Typical materials used for piping are steel, copper, and plastic (Siegenthaler, 2023; Warfvinge & Dahlblom, 2010).

In residential buildings, there are usually section- or panel radiators connected to the hydronic heating system and are usually placed below the windows to reduce the cold draft. The radiators are usually sized with a width 200 mm smaller than the window width, with an adequate height that enables good air circulation, usually with a free space of 100 mm below and above the radiator. The size of radiators depends on factors like peak power, supply/return temperature, and the temperature setpoint of the space. During operation, solar irradiation and internal loads will affect the temperature of the zone, and thus, a thermostat connected to the radiators can be used to detect the temperature and adjust the power delivered to the radiator by decreasing/increasing the water flow (Warfvinge & Dahlblom, 2010).

When determining the size of the pipes, the velocity and pressure drop should be constantly considered. A larger pipe diameter results in a low pressure drop and a low velocity but on the other hand, requires more capital investment. The optimal velocity for small and medium-sized systems ranges between 0.5 m/s and 0.7 m/s to reduce the risk of noise and allow air bubbles to be released from the system thus reducing the risk of corrosion. A constant friction approach with the pressure drop set between 100 Pa/m and 400 Pa/m, can be used when sizing the pipes, while most systems use 250 Pa/m (Siegenthaler, 2023; Warfvinge & Dahlblom, 2010).

To facilitate the water circulation in the system a circulation pump is required. The choice of a circulation pump depends on the mass flow rate of the water and the maximum pressure drop in the system, which can be calculated. The path from the heating system to a radiator with the highest pressure drop is called the critical path, which provides information for the required mass flow rate and the maximum pressure drop in the system. The design and actual installation of a circulation pump can differ, therefore a safety factor of 10 % can be used to consider the differences between design and installation, accounting for additional fittings, valves, or pipes. The number of circulation pumps depends on the system, but in most cases, it will consist of two pumps in the heating loop. Installing two pumps parallel will work as a safety factor; if one pump fails the remaining will take its place. Additionally, there are also pumps with two in-built wheels, increasing cost- and energy efficiency compared with purchasing two separate pumps (Siegenthaler, 2023; Warfvinge & Dahlblom, 2010). Hydronic heating systems usually contain components such as expansion vessels, control systems, and a variety of valves like safety valves, check valves, and regulation valves (Siegenthaler, 2023).

Due to the risk of legionella, it is important to prevent the freshwater in the system from becoming too cold and stagnant. The supplied freshwater to the tenants needs to be accommodated at a minimum temperature of 50 °C. In a potential accumulator tank, the required minimum temperature is 60 °C, allowing for potential mixing with cold water before supplying it to the tenants. The temperature of cold water supplied to a building varies in the South of Sweden and typically ranges between 4 °C and 15 °C (Boverket, 2016, 2021a; Warfvinge & Dahlblom, 2010).

3.2 Life cycle cost

The profitability of an investment is an important factor in the decision-making process regarding the choice of investment measures. Therefore, a life cycle cost calculation can be conducted to help with the decision-making, while focusing on economic efficiency. The life cycle cost analysis serves as a tool to evaluate the total cost of a product or investment throughout its entire lifespan, including initial investment cost, maintenance cost, and operational costs (Flodin et al., 2021; Kansal & Kadambari, 2010).

One of the methods used to calculate the LCC of an investment is the Net Present Value (NPV) method (Menassa, 2011). Using this method, all costs are presented as a present value, factoring in the time value of money, meaning that all future cash flows are discounted and presented as a present value together with the initial investment costs (Park, 2018).

Depending on the type of cost different formulas are used to calculate the NPV. When dealing with a single future cash flow, the value for the future payment is calculated first and then discounted to a present value using Equation 3.1.

$$NPV_1 = P(1 + g)^N(1 + i)^{-N} \quad [SEK] \text{ (Equation 3.1)}$$

Where NPV_1 is the net present value of the payment, P is the current value for the payment, i is the interest rate, g is the price change rate of the investment, and N is the number of years in the future when the payment is done.

If a series of cash flows is increasing or decreasing by a fixed percentage at regular intervals, the geometric gradient formula shown in Equation 3.2 can be used to calculate the net present value, with the condition that the interest rate and price change rate are not equal. If the interest rate is equal to the price change rate, then Equation 3.3 is used instead.

$$NPV_2 = A_1 \left(\frac{1 - (1+g)^N (1+i)^{-N}}{i-g} \right) \quad [SEK] \text{ (Equation 3.2)}$$

$$NPV_2 = A_1 \left(\frac{N}{1+i} \right) \quad [SEK] \text{ (Equation 3.3)}$$

A_1 is the future value of the initial cost at year one and is calculated using Equation 3.4.

$$A_1 = A_0(1 + g)^1 \quad [SEK] \text{ (Equation 3.4)}$$

Where NPV_2 is the net present value of a series of payments, A_1 is the cost at year one in a series of years, g is the price change rate, i is the interest rate, N is the calculation period, and A_0 is the initial cost at the beginning (year zero).

Factors that affect the total life cycle cost for retrofitting and need to be considered are the calculation period, product lifespan, and replacement costs (Lavy & Shohet, 2007). One of the main elements of an LCC analysis is the interest rate, it is a percentage that is applied periodically to a sum of money, representing the amount of interest added to that sum (Park, 2018). Interest rates are divided into real and nominal interest rates. The real interest rate is the real growth of money, excluding the effects of inflation which is the decrease in the purchasing power of money. While the nominal interest rate considers the effects of inflation and the real growth of money (ECB, 2024). Another significant element in the LCC calculations for construction is the price growth rate, meaning that the cash flow increases or decreases over time by a certain percentage, such as price changes due to inflation (Park, 2018). The impact of these input variables on the total cost can be investigated by performing a sensitivity analysis. This allows uncertainty and risks during the long-term operation stage of the building to be included in the calculations (N. Wang et al., 2012).

3.3 Life cycle assessment

To better understand the environmental impact of a product throughout its life cycle, a life cycle assessment can be conducted. This approach helps the decision-making process and mitigating the environmental impacts (Swedish Standard Institute, 2006). An LCA study can be divided into four phases:

1. The goal and scope definition phase: In this phase, the aim of the study is established. Depending on the use of the study, the functional unit and system boundaries are defined. The calculation period, lifespan of the products, life cycle stages, and environmental impact categories included in the study are also defined here.
2. The life cycle inventory analysis (LCI) phase: Here the data necessary to calculate and meet the goals of the defined study are collected. It involves gathering information on inputs and outputs related to a product's life cycle.
3. The life cycle impact assessment (LCIA) phase: Additional information is provided in this phase to help with the assessment of the environmental impact of a product and understanding of the LCI results. This information aids in evaluating the significance of different environmental impacts.
4. The interpretation phase: In this phase, the results of the study are interpreted, and the results from LCI and LCIA are analyzed to conclude the goal and scope of the study.

These steps can be applied to evaluate the environmental impact of construction projects. The life cycle of construction projects is divided into four stages, each containing several information modules describing the entire product system of any construction project. The LCA results of a construction product are presented in an EPD, organized according to the life cycle stages and their information modules, which are presented in Figure 1. To develop an EPD a company must follow the standards set by SS-EN 15804:2012 + A2:2019 (Swedish standard) or/and the equivalent international standard EN 21930:2017, thus ensuring that the product has been independently verified (Swedish Institute for Standards, 2021).

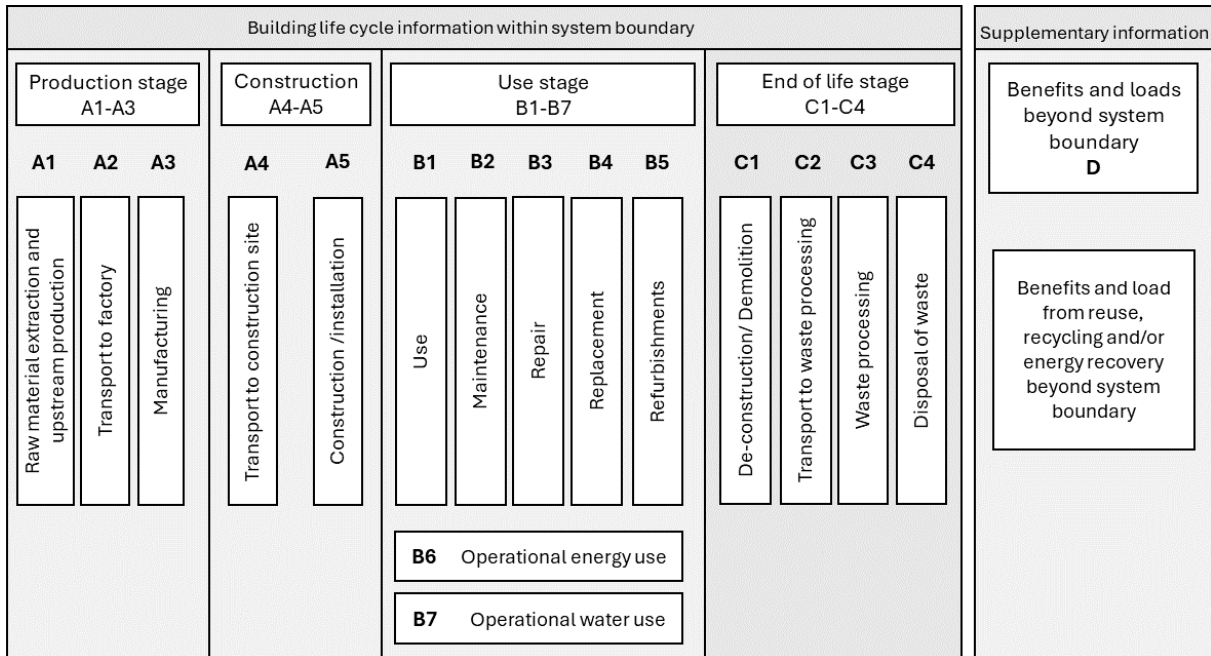


Figure 1. An illustration of the life cycle stages, what each stage contains, and supplementary information (Swedish Standard Institute, 2020).

An EPD The environmental impact of a product is presented in different categories in an EPD. These categories are determined depending on the type of emissions associated with the product. The mandatory impact categories to be included in an EPD are as follows (Swedish Standard Institute, 2020):

- Global warming potential (GWP): This category is a measure of greenhouse gas emissions released into the atmosphere, including gases such as carbon monoxide (CO), carbon dioxide (CO₂), methane (CO₄),

nitrous oxide (N₂O), methyl bromide (CH₃Br), chlorofluorocarbons (CFCs), and hydrofluorocarbons (HFCs), and is measured using kg CO₂ eq. per functional unit (IPCC, 2007). These gases contribute to the greenhouse effect, absorbing thermal radiation and trapping heat within the atmosphere, leading to climate change (Circular Ecology, 2024).

- Ozone depletion potential (ODP): This impact describes the effect of various substances on the depletion of the ozone layer in the stratosphere and is measured using kg CFC-11-eq. per functional unit (Baumann & Tillman, 2004).
- Eutrophication potential (EP): This category describes the effect of added nutrients in soil or water, which can cause an overgrowth of certain species such as algae and plants, leading to less oxygen production and death of aquatic animals. This category is measured using kg P eq. per functional unit (Farinha et al., 2021).
- Acidification potential (AP): Represents pollutants that transform into acids, leading to acidification of ground and water, and damaging or corrosion of building materials. The effect is measured using a mole of H⁺ eq. per functional unit (Farinha et al., 2021).
- Photochemical oxidant creation potential (POCP): This is an environmental impact produced due to photochemical oxidation of gases, creating ground-level ozone which is toxic and can affect human health. This impact is measured using kg Ethene eq. per functional unit (Farinha et al., 2021).

The integration of regulations and certifications with LCA promotes sustainable building practices. For instance, the Swedish National Board of Housing, Building, and Planning has introduced requirements for climate declaration of new buildings, effective from January 2022, with a focus on minimizing the environmental impact of the constructions. A climate declaration should include an assessment of the environmental impact from the construction phase, covering information modules A1-A5, during a calculation period of 50 years. Moreover, GWP-GHG should be used to measure the environmental impact on a building, the absorption and emission of biogenic carbon dioxide should not be included due to the lack of evidence on how to correctly present the data (Boverket, 2021b). Furthermore, certification systems such as Miljöbyggnad, BREEAM, and Noll-CO₂ also dedicate a part to LCA, ensuring more sustainable buildings. Adhering to Boverket's rules regarding climate declaration, the calculation period for the assessment in certification systems is 50 years and the assessed impact category is GWP-GHG.

3.4 Thermal comfort

Thermal comfort is defined as the state where a human being is satisfied with the experienced temperature of a space and does not desire any hotter or colder environment. The effects of poor thermal comfort can include, trouble concentrating due to high concentrations of CO₂, development of bacteria, and fungus, as well as asthma because of too high/low relative humidity. Additionally, discomfort can be a result of overheating and large temperature differences between the floor and ceiling (Warfvinge & Dahlblom, 2010).

When designing or retrofitting a residential building, attention should be paid to the risk of overheating, especially from April to September when the risk of overheating is at its highest. Excessive overheating can lead to discomfort among the occupants and may also have other adverse effects. According to Feby18 guidelines, the degree of overheating should remain below 10 % from April to September (FEBY18, 2024).

4 Method

4.1 Investigation & selection of buildings

In this chapter, the method of locating two buildings with the lowest energy performance is described. The located buildings would later be used as a base case when analyzing and proposing retrofitting measures.

4.1.1 Data

Approximately 5 500 buildings with the lowest energy performance were examined using Excel, to identify the most common group of buildings. These buildings exhibit an energy class of G, according to the Swedish National Boards of Housing, Building, and Planning. The dataset consisted of all buildings in Skåne that had performed an energy declaration between the years of 2019 to 2022 and had a low energy performance. The analysis involved the categorization of buildings across different parameters: type code, building type, No. of stories, A_{temp} , ventilation type, heating type, and built year. This analysis aimed to identify the most common building types among those with the lowest energy performance, to determine the most typical retrofitting measures that would be appropriate for most of the buildings.

The building type code was determined by the tax office and was based on the building's designated use. Building type refers to whether the building's structure was detached, semi-detached, or intermediate (connected from both sides). No. of stories was the number of floors above ground excluding the attic. A_{temp} referred to heated floor area, while ventilation type included either natural, MEV-system, MV-system, or MVHR-system. The year built refers to the year the construction was finished (Skatteverket, 2029).

The selection process for these buildings involved analyzing and filtering data to determine the most common types and systems within each category. The categories and resulting characteristics of the buildings are illustrated in Figure 2.

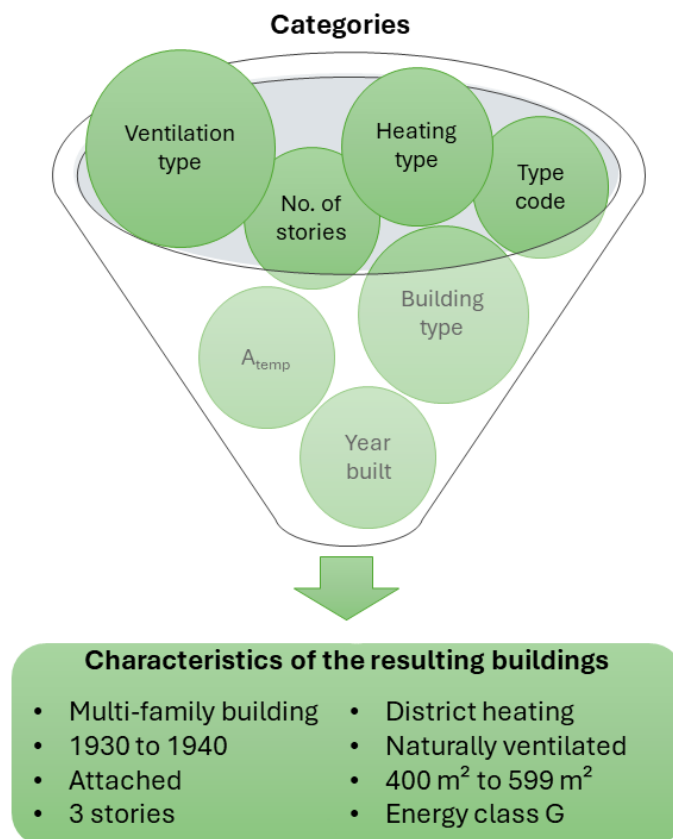


Figure 2. An illustration of the included categories and the characteristics of the resulting buildings.

4.1.2 Two buildings

After filtering the data 15 buildings were left of the initial 5 500 buildings, with the resulting characteristics illustrated in Figure 2. Each building was investigated to determine if there were any drawings available on the respective municipality website, and if a building had any drawings the building was favored as a better option compared to a building without. Finally, two buildings with the best available drawings were chosen and modeled in both Rhino and Revit. After this, contact was established with the property owners to determine if it was possible to inspect the buildings and collect any necessary information. The chosen buildings were named *building A* and *building B* and are described further in chapter 4.2.

4.2 Base cases

This chapter presents an overview of the two buildings, containing illustrations of the actual buildings, their floor layout, constructions, and systems. The information was used as a basis to determine which retrofitting should be performed.

4.2.1 Building A

The first building was situated on Rasmusgatan 24, in Malmö. It was built in 1937 and is currently owned by a housing cooperative named Sofielund. It is a three-story building with a heated floor area of 529 m².

Site visit

The site visit was used to verify the accuracy of the drawings from the City Planning Office by measuring the floor area and performing an ocular inspection of the building constructions.

All spaces were investigated during the site visit, including four apartments, in which information was gathered regarding heating, ventilation, and windows, which is described further in *Constructions & systems*. Below is an illustration of the building today, see Figure 3.



Figure 3. An illustration of Building A, from three perspectives.

Floor layout

The building consisted of three stories, excluding a basement and a cold attic which currently was not in use. The three intermediate levels each accommodated four residential units, and two staircases enabling access from the basement level to the attic. Figure 4 illustrates the floor layout of the building, except the layout for the attic which was an empty space.



Figure 4. Floor plans of building A.

Constructions & systems

Most construction details were verified by using the collected drawings for each building part during the site visit. Constructions that were lacking details or which were not possible to inspect were determined using relevant literature (Björk et al., 2021). The U -value and area of each building part are illustrated in Table 4.

Table 4. Area and U -values of each building part of Building A.

Name	Area /m ²	U -value /(W/(m ² ·K))
Roof	270	1.8
Façade	250	1.4
Basement walls	48	2.5
Ground slab	230	2.9
Slab	230	0.4
Windows X ¹	18	2.5
Windows Y ²	66	1.2
Window office	4	3.5

¹ Window in the basement, and staircase.

² Windows in the apartments.

The roof was uninsulated and consisted of wooden beams carrying the load of the roof, with spruce installed on top, upon which the external layer was installed. The roof tilted towards north and south with different external layers, one with roof felt and one with roof tiles. The roof construction is illustrated in Figure 5.

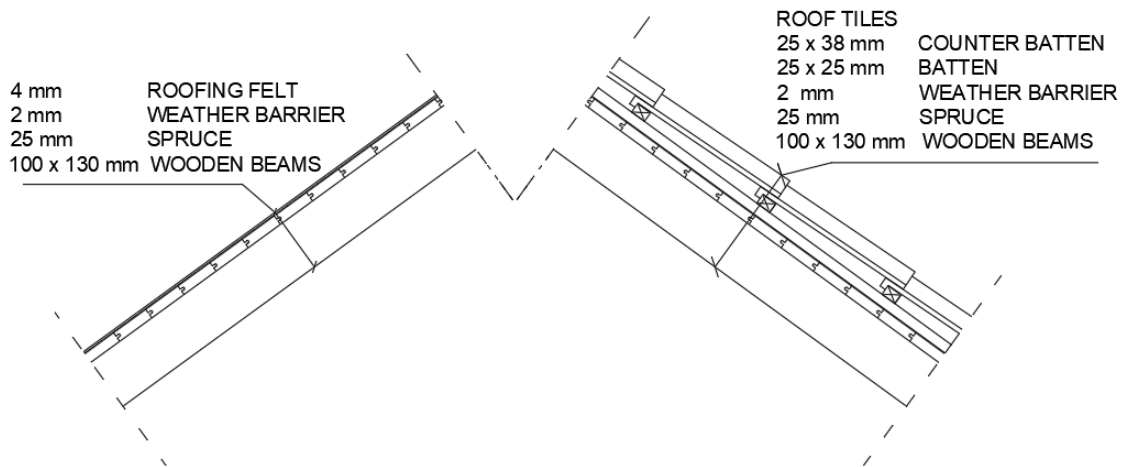


Figure 5. Roof construction of building A.

The facade consists mainly of bricks covered with lime plaster both internally and externally. The basement walls consisted of concrete with a layer of lime plaster applied externally. The wall constructions are illustrated in Figure 6.

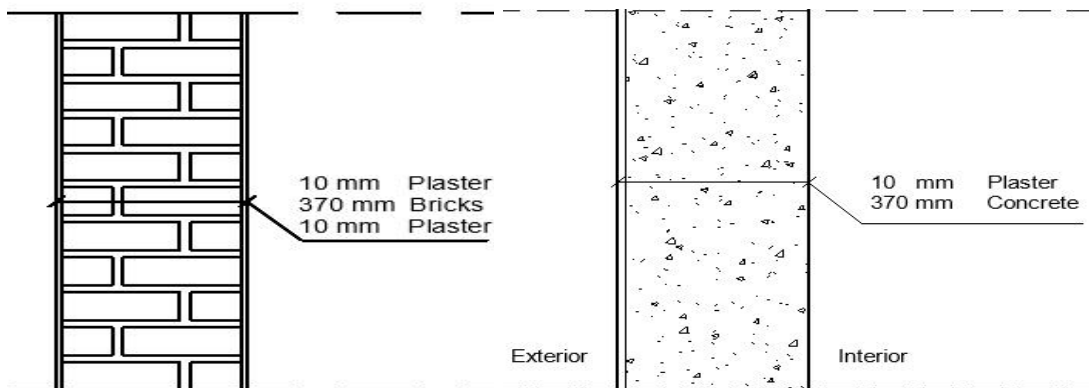


Figure 6. Illustration of basement walls and façade constructions of building A.

The ground slab was assumed to consist of gravel and concrete, while the intermediate slabs were of lightweight construction, consisting of load-bearing steel beams supporting wooden beams arranged between them, along with filling made of ash. Both slab constructions are illustrated in Figure 7.

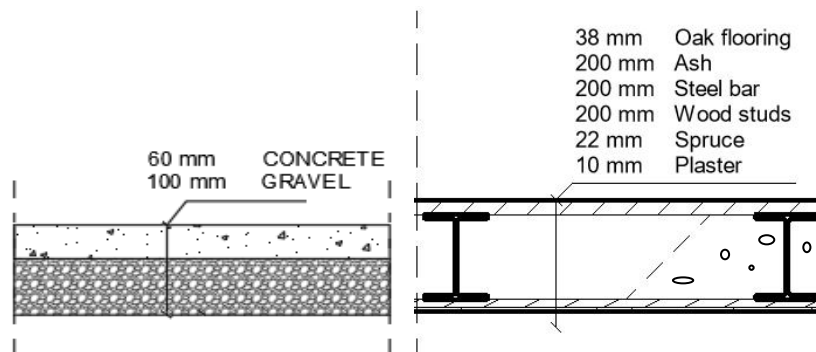


Figure 7. Ground slab and intermediate slab constructions of building A.

The apartment windows named “Y” had already been replaced a couple of years ago with triple-glazed windows, and their U -value was approximated, see Table 4. The highlighted windows named “X”, in Figure 8 had not yet been replaced and were deemed well past its lifespan. The office window was not a standard window, but a window frame with an installed “plexi-glazing”, its U -value was also approximated, see Table 4.

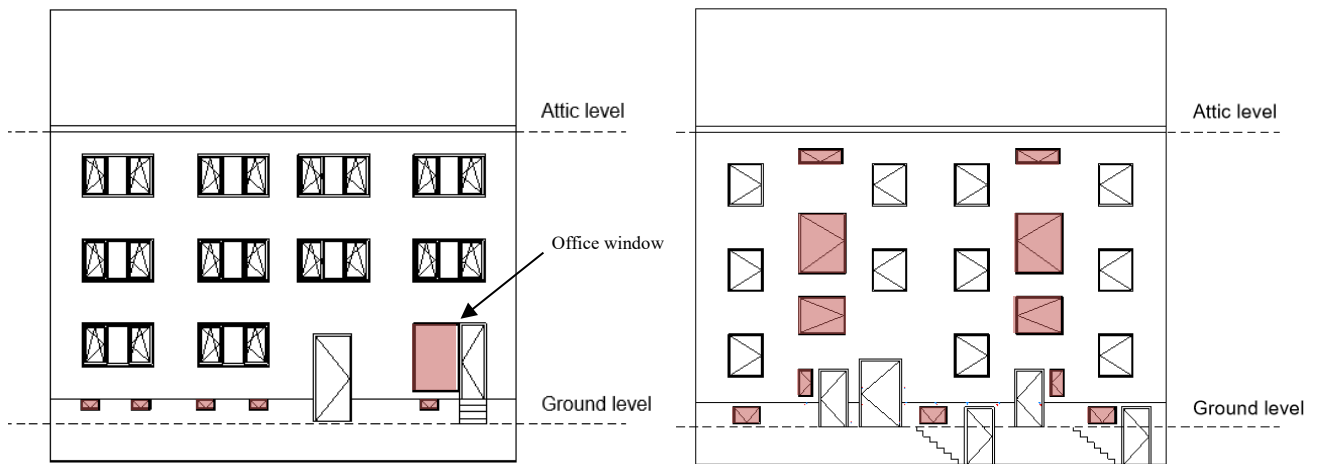


Figure 8. Façade-view of Building A, the highlighted windows illustrate window “X” in need of replacement, the unmarked windows are referred to “Y”.

The building was naturally ventilated with supply air valves on the façade and extract air valves on the chimney. The property’s heating was delivered through district heating. The heat from district heating (primary side) was transferred with a heat exchanger to both the building’s space heating system and domestic hot water system (secondary side), the heating was further distributed to radiators.

4.2.2 Building B

The second building was located on Timmermansgatan 33, in Landskrona. It was built in 1942, consisted of three stories with a heated floor area of 436 m², and is currently owned and managed by HSB.

Site visit

The site visit was used to gather additional information about the building which was missing from the drawings. Contrary to Building A this building lacked accurate and detailed drawings, thus the models for this building were based more on the ocular inspection, measurements, data provided by HSB, and relevant literature.

All the spaces were not investigated during the site visit, only the staircase, basement, and one apartment were available for inspection. Below is an illustration of the building, see Figure 9.



Figure 9. An illustration of building B, from three perspectives.

Floor layout

The building consisted of five floors, including a non-heated basement, three floors with apartments, one staircase, and a recently renovated attic converted into one apartment. There was a total of seven apartments in the building, with two apartments on each of the three intermediate floors and one in the attic. The floor plans for each level are presented in Figure 10.

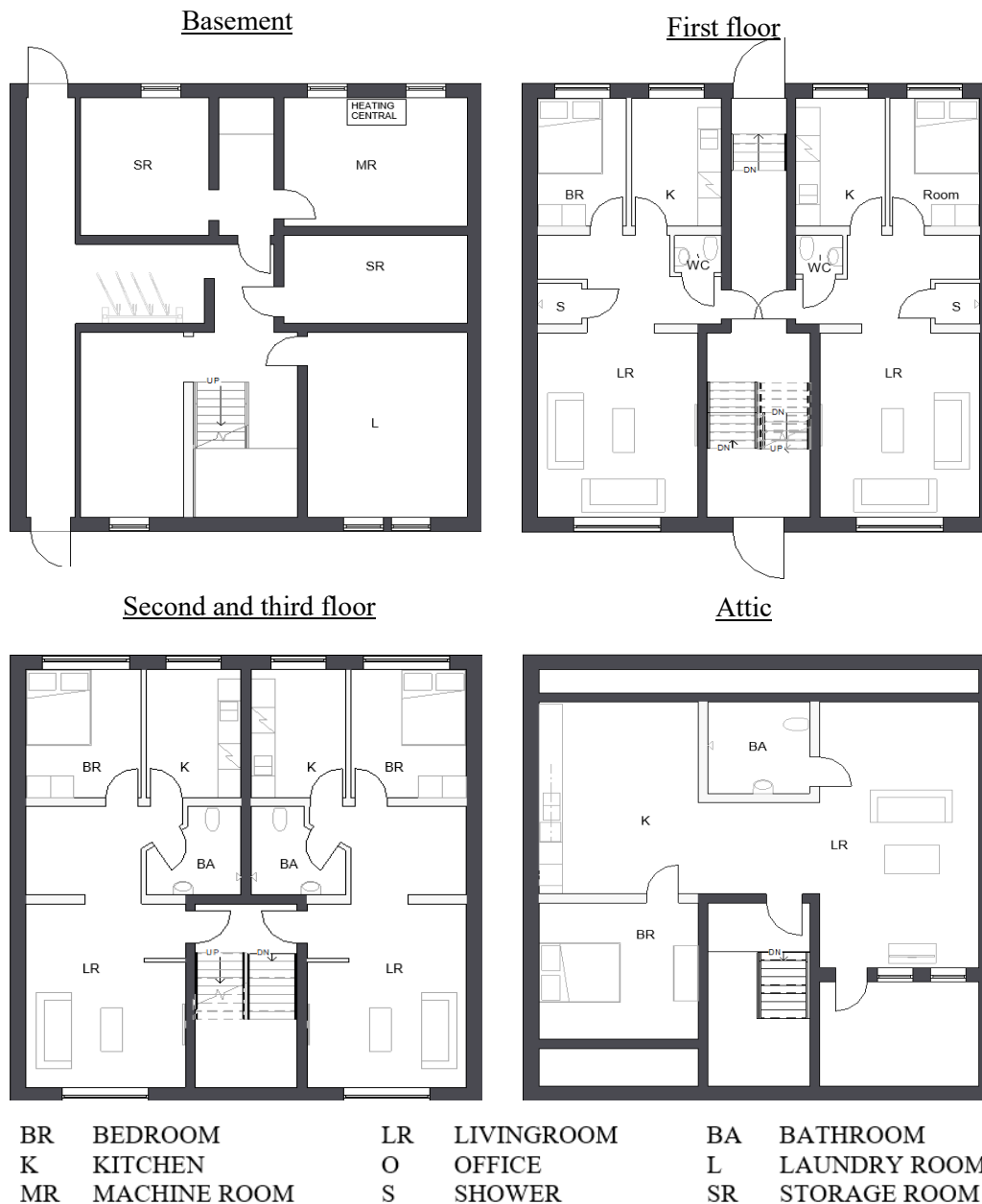


Figure 10. Floor plans of building B.

Constructions & systems

Most of the building envelope constructions were decided during the site visit, where it was observed that all constructions resembled those of building A, except for the windows, façade, and roof. This conclusion was based on a closer inspection and measurements of the building constructions. The U -value and area of each building part are presented in Table 5.

Table 5. Area and U -values of each building part, for building B.

Name	Area /m ²	U -value //(W/(m ² ·K))
Roof	153	1.9
Façade	185	1.5
Ground-walls	46	2.5
Ground-slab	149	2.9
Slab	149	0.4
Windows	54	2.5
Windows top floor	7	1.2

The load-bearing structure of the façade and roof was similar for both buildings. However, building B had a brick façade with no additional plaster on the exterior and the wooden beams in the roof had a larger dimension compared to the beams in building A, and the whole roof was covered with brick tiles externally. The roof and external wall constructions are illustrated in Figure 11.

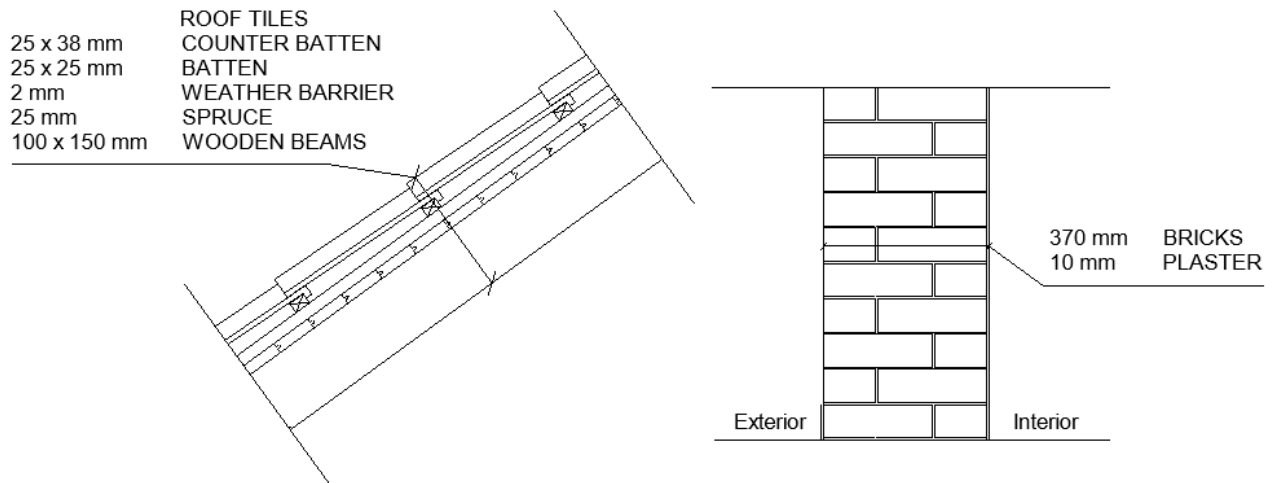


Figure 11. Roof and façade construction, for building B.

According to the maintenance plan received by HSB, none of the windows in building B had been changed since 1981, except for those in the attic which recently had been refurbished into an apartment. The highlighted windows in Figure 12 illustrate the windows that need to be changed.

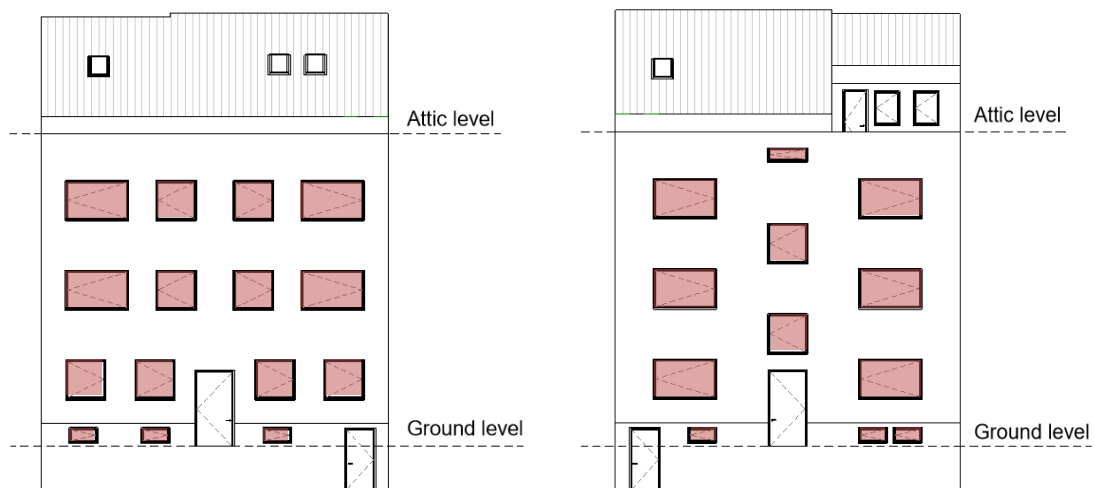


Figure 12. Façade-view of building B, highlighting the windows in need of replacement.

4.3 Energy use & thermal comfort

This chapter describes the setup of the energy model in CS, how the energy use and thermal comfort were simulated, and illustrations of the zones.

4.3.1 Input values

An EPW file was incorporated into CS for both locations, representing a typical meteorological year (TMY_x), covering the years 2007 to 2021 (ClimateOneBuilding, 2024). Building A was assigned an EPW file based on Malmö while building B was assigned to Helsingborg due to the lack of specific EPW files for Landskrona, and Helsingborg was the closest city.

Envelope

The envelope of the building was based on the constructions previously mentioned in chapters 4.3.1 and 4.3.2, thermal bridges were accounted for by adding 30 % to the UA (SGBC, 2022). The U -values used in CS are illustrated in Table 6.

Table 6. Input values used to simulate the base case in CS for both buildings.

Name	Building A U -value $/(W/(m^2 \cdot K))$	Building B U -value $/(W/(m^2 \cdot K))$
Facade ¹	1.8	1.9
Ground wall	2.5	2.5
Roof	2.4	2.5
Foundation	2.9	2.9
Intermediate slabs	0.4	0.4
Windows X ²	2.5	(-)
Windows Y ²	1.2	(-)
Office window ²	3.5	(-)
Windows ³	(-)	2.5
Windows attic ³	(-)	1.2

¹ The exterior walls connected to the surrounding buildings were set as adiabatic.

² See Figure 8 for illustration.

³ See Figure 12 for illustration.

Heating

To create an energy model that can represent the actual building, the annual and monthly heating bill was collected from the property owners. These were later normalized using normalization factors obtained from SMHI to represent the energy demand for a typical year. The resulting values were used as a reference when creating the energy model for the base case. To further increase the resemblance between the model and the actual building, the inefficiency of the current heating system was considered. Any potential heat loss from piping and the heating system was accounted for by manually adding 5 % to the annual heating use and is based on experience from practice in the field of energy simulations.

The software uses an ideal air load system that supplies energy based on the requirements of the zone, supplying energy until the requirements are met. The heating was constantly on, with a setpoint of 21 °C in the apartments, and 18 °C in the staircase. The rest of the zones did not have any heating (Sveby, 2012).

Ventilation

The ventilation was set to constantly on, with an assumed airflow of 0.35 l/(s·m²), based on the requirement set by BBR29 (Boverket, 2021a). While natural ventilation was accounted for by adding 4 kWh/m² A_{temp} on the annual heating use, due to the uncertainty of tenants' use of natural ventilation (Sveby, 2012).

People, equipment, and lighting

The people load (PL) was calculated using Equation 4.1, and the equipment load (EL) using Equation 4.2, both were implemented as a sum: total load (TL) into CS as equipment.

$$PL = \frac{p \cdot L}{A} \quad [W/m^2] \text{ (Equation 4.1)}$$

p is the number of people based on the number of rooms according to BEN 2, L is the heat load of an average person 80 W/m², and A is the area of the apartment which varies from apartment to apartment (Boverket, 2017).

$$EL = f \cdot \frac{E_q \cdot 1\,000}{8760} \quad [W/m^2] \text{ (Equation 4.2)}$$

f is the fraction of useable heat emitted from a person 0.7, E_q is the annual household electricity set to 30 kWh/m², set to be on 14 hours/day (Sveby, 2012). The lighting load was assumed and used the same schedule as the equipment.

The total load (TL) of *Basement High Eq.* was assumed since it had a large heating system creating a large amount of internal heat, but also due to the laundry room. The laundry room for building B was in the adjacent building, and the heating central was much smaller compared to that of building A, thus the TL in the Basement was assumed to equal 50 %. The internal loads are illustrated below in Table 7.

Table 7. Loads used for simulating both buildings in CS.

Building A			Building B		
Zone type	TL /(W/m ²)	Lighting load /(W/m ²)	Zone Type	TL /(W/m ²)	Lighting load /(W/m ²)
Apartments 1 ROK	7.6	4	Apartments 2 ROK	4.5	4
Apartments 2 ROK	5.9	4	Basement	2.4	0
Basement	0	0	Corridor	1	4
Basements High Eq.	4.8	4			
Local	7.6	4			
Corridor	1	4			

Infiltration

It was assumed that the heat loss from the ventilation should be larger relative to the infiltration. Thus, the ventilation was set last to ensure that the infiltration did not reach unrealistically high levels. The infiltration was calculated using an easy-to-use Excel sheet constructed by Agnieszka Czachura, which converts infiltration rates from 50 Pa to 4 Pa. The infiltration was set to 0.194 ACH, and 0.161 at 4 Pa, for building A and building B respectively.

4.3.2 Thermal comfort

Each apartment including the kitchen, bedroom, and living rooms was modeled into one zone. The shading of surrounding buildings was included, due to its effect on thermal comfort by heat load. But were downsized into vertices to reduce the simulation (Dubois et al., 2019).

The highest located apartment with a South orientation was chosen as the study object for thermal comfort. In both buildings, the living room faced the South and was thus chosen as the zone of interest (FEBY18, 2024). The degree of overheating would decrease if the entire apartment were simulated as one zone, thus, the apartments were divided into four zones, living room, bathroom, kitchen, and bedroom, with an air wall between the rooms which had an opening instead of a door. The separated zones used the same settings as *Apartment 2 ROK*, illustrated in Table 7. The models are illustrated in Figure 13 and Figure 14. Furthermore, the thermal comfort was analyzed only with regards to overheating from April to September, if the operative temperature reached 26 °C more than 10 % of the duration, the zone would be deemed uncomfortable (FEBY18, 2024).

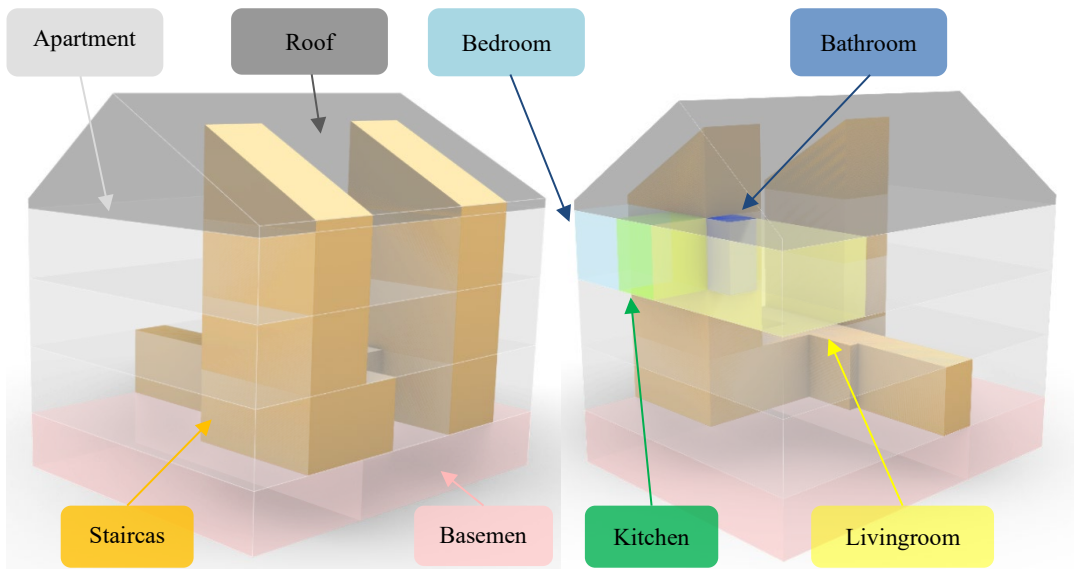


Figure 13. An illustration of the zones in building A.

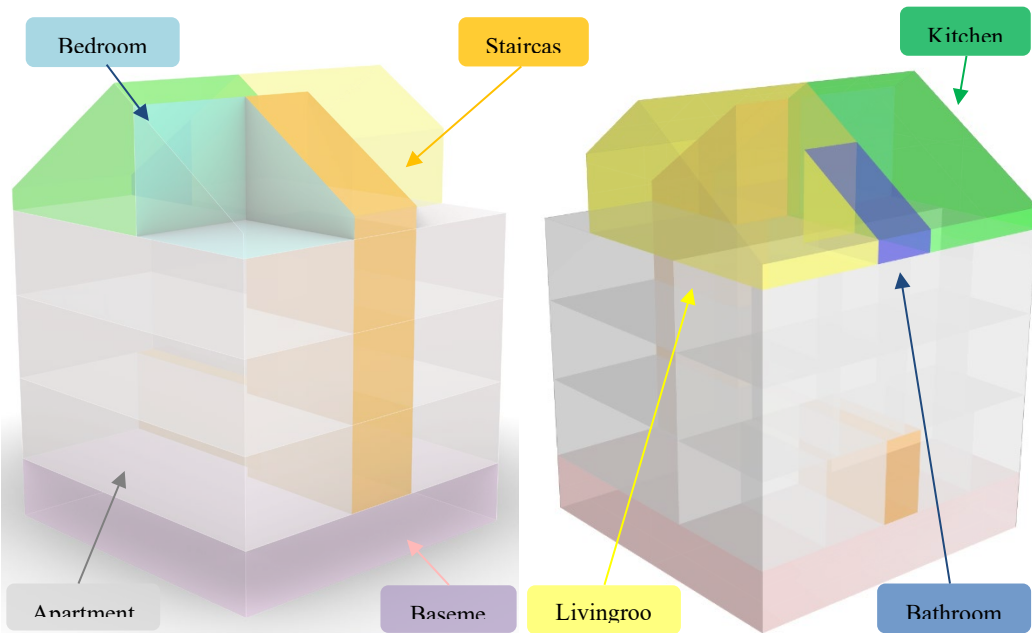


Figure 14. An illustration of the zones in building B.

4.4 Retrofitting

In this chapter, the applied retrofitting measures, the parametric analysis, and the calculation of the total energy use were described. Figure 15 illustrates the included measures for both buildings.

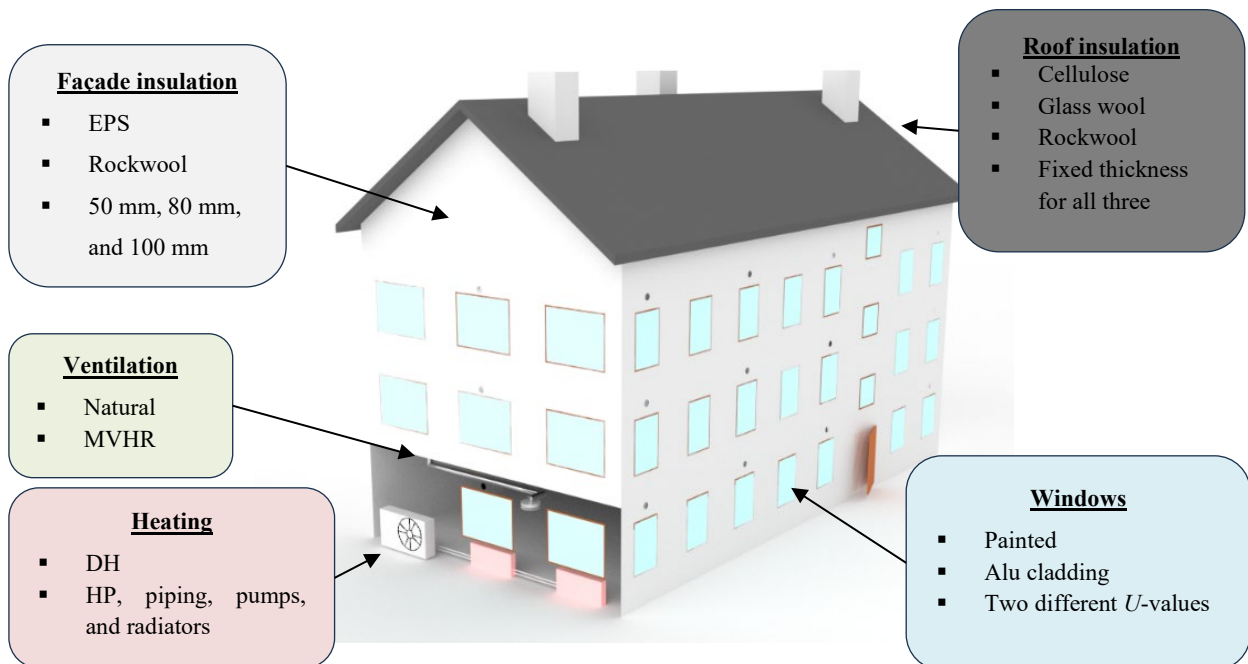


Figure 15. Illustration of which measures were included in the parametric analysis for both buildings.

4.4.1 Envelope & air infiltration

Facade

It was decided that the insulation material would be applied directly on the exterior part of the façade since it is a well-tested installation with good results from previous objects, and the fact that the façade was not heritage-protected. By mounting the insulation on the exterior, the temperature of the wall should increase and thus improve the hygrothermal conditions of the wall (Arfvidsson et al., 2017).

Both rockwool and EPS were used with varying thicknesses of 50 mm, 80 mm, and 100 mm. The constructions were analyzed with 100 mm insulation regarding their water content. Settings are illustrated in Appendix A. The principle of the constructions is illustrated in Figure 16.

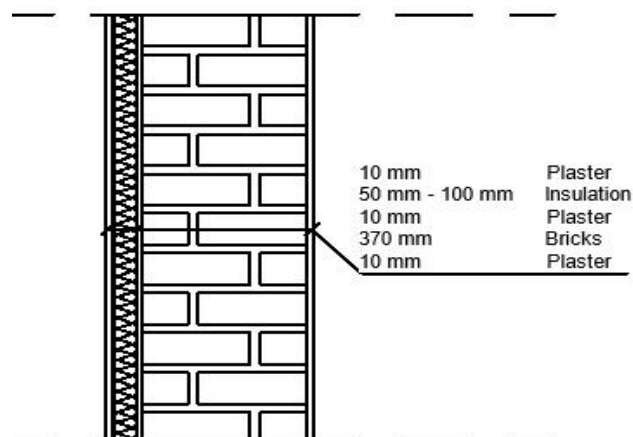


Figure 16. Principle construction when adding insulation and plaster.

Roof

It was decided that insulation should be installed between the wooden beams on the roof. Three types of insulations were simulated, rockwool, mineral wool, and cellulose, which mated the thickness of the wooden beams, followed by a PE-membrane and a gypsum board, see Figure 17. Both constructions were analyzed concerning the risk of mold, using the mold index as an indicator. Settings are illustrated in Appendix A.

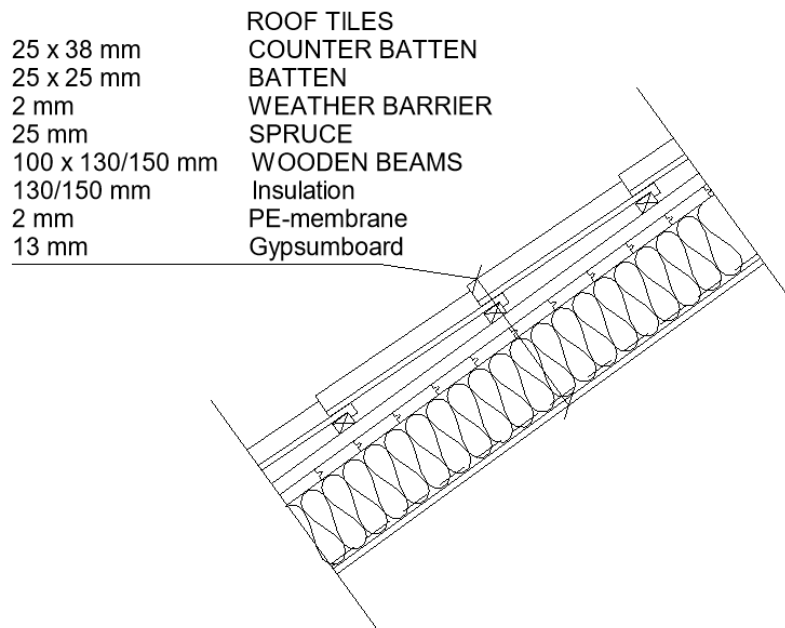


Figure 17. Roof construction when adding insulation, PE membrane, and gypsum board.

Windows

In building A, only a small amount of the existing windows was assumed to create a relevant improvement in terms of saved energy, namely the windows in the staircase and basement, the rest of the existing windows had recently been changed and were thus not replaced. In contrast to building A, building B had all windows replaced except in the attic, where the windows had been replaced during the retrofit from the attic to an apartment.

Both operable and fixed windows were included since it was assumed that the windows in the basement did not need to be openable since they were too small to act as a fire escape. All windows were made from wood with the same solar heat gain (0.50) and visual transmittance (0.60), and each type of window had two different U -values. The windows are described further in Table 8.

Table 8. Description of the windows implemented in retrofitting both buildings.

Name	Average total U -value $/(W/(m^2 \cdot K))$	Frame U -value $/(W/(m^2 \cdot K))$	Frame width /mm	Exterior finish
Windows used in the Apartments/Staircases				
VRIDFÖNSTER TRÄ 3-GLAS RUND PROFIL	0.91/1.2	1.43	97	Paint
VRIDFÖNSTER TRÄ 3-GLAS RUND PROFIL ALU	0.91/1.2	1.43	97	Aluminium
Windows used in the Basement				
3-GLAS FÖNSTER FAST KARM TRÄ	0.91/1.2	1.43	97	Paint
3-GLAS FÖNSTER FAST KARM TRÄ/ALU	0.91/1.2	1.43	97	Aluminium

Air infiltration

The maximum reduction of air leakage was set to 33 % and was based on research of a similar retrofitting, the building of interest had its air leakage reduced up to 50 % for a standard retrofitting, this was deemed too optimistic for the chosen buildings in this report since the buildings would reach passive house standard. The

second type of retrofitting reduced the air leakage by approximately 33 % when improving the entire envelope and was deemed more fitting to the buildings in this study (Rønneseth et al., 2019).

Each measure, both respectively and in combination, reduced the infiltration depending on whether the specific zone was affected by the retrofitting. Each measure, and combination, is illustrated below in Table 9.

Table 9. Specified reduction of air leakage, for both buildings.

Measure	Reduction of air leakage /%
Windows	17
Façade	8
Roof	8
Windows + Façade + Roof	33
Windows + Façade	25
Façade + Roof	16
Roof + Windows	25

4.4.2 Ventilation system

The ventilation was simulated using two different types, the first was the passive stack effect, which was simulated using a constant ventilation of 0.35 l/(s·m²) for both buildings. The second type of ventilation was an MVHR system using CAV, the design is described further below.

The airflow was calculated using BBR29's earlier requirements of 4 l/s supply air per bed space, and 10 l/s exhaust air per bathroom and kitchen, this sufficed a supply air flow higher than the required flow of 0.35 l/(s·m²) (Boverket, 2021a), with an assumed supply/return airflow ratio of 1/1.

The duct layout was based on designing the ducts as symmetrical as possible, using circular ducts, and that the space between two fittings should be six times the duct diameter. The stairs and hallways were utilized as much as possible, and the ducts were installed to minimize crossings to ensure a smoother installation. According to recommendations from BBR29 it is not recommended to include the air from the kitchen hoods in the ventilation system. Therefore, the kitchen hoods were not connected to the MVHR system, instead, the existing extract diffusers on the chimney were used to extract the air while cooking. The duct-sizing was performed using equal friction, set to a constant of 1 Pa/m. The minimum and maximum pressure drop for the selected diffusers was inserted into the software, after which the software used this information to throttle the diffusers until a correct airflow. The placement of the diffuser was based on distributing the air without reaching noise levels of 35 dB, and a maximum air speed of 0.15 m/s during winter, and 0.25 m/s during summer.

The AHU was placed in the attic of building A to minimize the disturbance to the tenants, and to keep the branches as symmetrical as possible. However, in building B, the AHU was placed in the basement since the attic had been refurbished into an apartment, and thus, it was the only available space for the installation. The AHU consisted of a plate heat exchanger, heating coil, filters, damper, and fans. The plate heat exchanger was chosen to ensure that the return and supply air were not mixed, to ensure that smell and particles from the bathrooms did not mix with the supply air. The heating coil was assumed to be powered by electricity. Furthermore, the distance between the outlet and the inlet was decided by considering the risk of mixing exhaust air with supply air (ASHRAE, 2021; Boverket, 2021a; Warfvinge & Dahlblom, 2010).

4.4.3 Heating system

Two types of heating systems were simulated, the first was DH which was initially installed in both buildings, and the second used air-to-water HP described further below and conceptually illustrated in Figure 18.

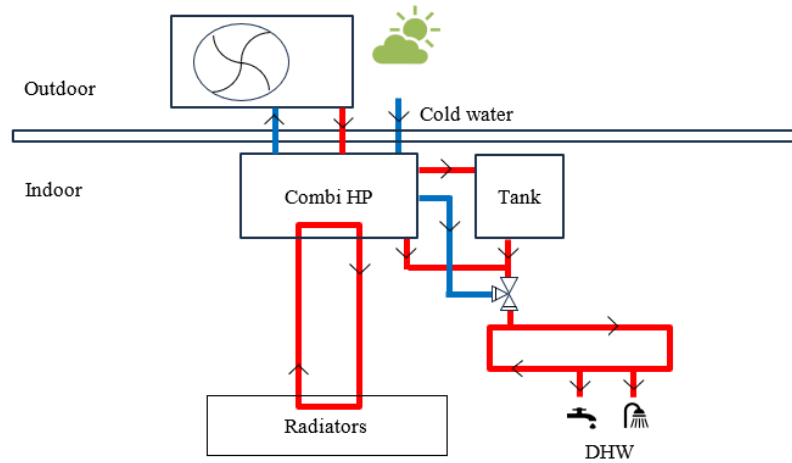


Figure 18. Illustration of the new HP-system.

It is common practice not to include solar radiation and internal loads when sizing the heating system, and only consider losses by transmission, ventilation, and leakage, thus, during the heating peak load simulation the internal loads were turned off, and the global radiation was removed from the weather file using Elements. To simulate the heating peak load the DVUT was set to $-10\text{ }^{\circ}\text{C}$ and $-8\text{ }^{\circ}\text{C}$ for Malmö and Landskrona respectively (Sveby, 2022). The results of the simulation were used to size the HPs using 70 % of the load, and an additional load for the DHW set to 0.5 kW per apartment. An accumulator tank was added to cover the hot water volume required during peak hours (Boverket, 2016; Warfvinge & Dahlblom, 2010).

The tank was chosen by its calculated water volume size (m_{pw}), see Equation 4.3.

$$m_{pw} = \frac{(T_S - T_{CW})}{(T_T - T_{CW})} \cdot \dot{m} \cdot n_{people} \quad [m^3] \text{ (Equation 4. 3)}$$

Where T_S is the supplied water temperature to the tenant set to $50\text{ }^{\circ}\text{C}$, T_{CW} is the temperature of the incoming cold water assumed to be $8\text{ }^{\circ}\text{C}$, T_T is the temperature of the water in the tank set to $60\text{ }^{\circ}\text{C}$, \dot{m} was the product of the assumed hot water use of 60 liters per person, n_{people} was the number of people residing in the building based on BEN 2, and was set to 20 people for building A, and 11 people for building B (Boverket, 2017).

Since an HP cannot supply an equally high supply temperature to the radiators compared to the existing DH system, it was assumed that the existing radiators and piping had to be replaced when installing an HP. This is due to the new heating system performing low-temperature heating and the supply of water with lower temperature required bigger radiators to provide sufficient heat to the rooms. The sizing of radiators was determined in MagiCAD by considering the peak load in combination with the specified supply/return temperature of $49/43\text{ }^{\circ}\text{C}$. The radiators were mainly placed below the windows, to reduce the risk of draught. Additional radiators were also placed in the hallways in cases with high peak loads to cover the building's heating demand. Thermostats were included, with a minimum limit set to 3 Pa, during the balancing process. Copper pipes were chosen due to the material's long lifespan and high conductivity, the pipe-sizing was done using the equal friction method, with a constant pressure drop of 250 Pa/m (Warfvinge & Dahlblom, 2010). The piping was also renewed, due to changes in water flow resulting from the installation of new radiators, which would have caused incorrect pipe sizes and higher pump pressure, making the system inefficient. Thus, renewal of the system was necessary concerning its efficiency and old age.

After calculating the critical path in MagiCAD, it was used as an input value together with the mass flow rate of the system, in the web-based software Grundfos. The software presented specific pumps matching the heating systems' requirements. Subsequently, two pumps were selected for the heating system.

4.4.4 Parametric analysis

In the GH environment, Colibri was used to iterate through all possible combinations of the retrofitting measures. A total of 560 iterations were simulated for each building and the input parameters are presented in Table 10.

Table 10. Each type of measure for each respective building part and system.

Façade insulation	Roof insulation type	Window type – /(W/(m ² ·K))	Ventilation type	Heating type
No insulation (existing)	No insulation (existing)	Existing	Passive stack ventilation (existing)	District heating (existing)
50 mm – EPS	Mineral wool	Painted – 1.2	MVHR	Hydronic system with HP
80 mm – EPS	Rockwool	Alu-clad – 1.2		
100 mm – EPS	Cellulose	Painted – 0.91		
50 mm – Rockwool		Alu-clad – 0.91		
80 mm – Rockwool				
100 mm – Rockwool				

Several IF functions were used in the script, and the infiltration varied depending on which measure was in use and if it was running in combination with another measure, furthermore, the airflow rate created by the ventilation also changed if the specific case had an MVHR-system or not.

4.4.5 Energy

The total operational energy (E_{op}) for each simulation was calculated using Equation 4.4.

$$E_{op} = \left(\sum_{k=1}^{8760} \left(\frac{E_{k,heat} \cdot E_{k,loss} + E_{k,NV}}{SCOP} \right) \right) + E_{vent} + \frac{E_{DHW}}{SCOP} \quad [kWh/(m^2 A_{temp} \cdot y)] \quad (\text{Equation 4. 4})$$

Where k represents each hour of the year, $E_{k,heat}$ is the simulated hourly energy required to heat the building, $E_{k,loss}$ is the assumed heat losses from the piping and heating system set to 1.05, $E_{k,NV}$ is the heat loss from natural ventilation set to $\frac{4}{8760}$ kWh/(m²·h), E_{vent} is the ventilation energy per m² (A_{temp}) gathered from ACON and consisting of fans and a heating coil, SCOP is the seasonal coefficient of performance of the heating system set to 1 for the existing DH and 3.8 for the HP, E_{DHW} is the annual assumed domestic hot water of 25 kWh/(m²·y).

4.5 LCC

This chapter describes the method of calculating the LCC, the data was processed and finalized using Excel.

4.5.1 Net present value

Equation 4.5 was used to calculate the total net present value (NPV_{total}) for each of the 560 cases.

$$NPV_{total} = NPV_{SOC} - NPV_I \quad [SEK/m^2 A_{temp}] \quad (\text{Equation 4. 5})$$

Where NPV_{SOC} is the present value of the saved operational cost calculated using Equation 4.8 and is described further in chapter 4.6.2. NPV_I is the NPV of the total investment costs calculated using Equation 4.10 and is described further in chapter 4.6.3.

4.5.2 Saved Operational Cost

SOC is defined as the saved operational cost of a case relative to the base case. The calculation is described below.

DH and electricity were used as energy sources in the two investigated heating systems, DH-central and HPs respectively. The price of electricity was based on the year 2022 and consisted of an hourly spot price with an added VAT of 25 %, energy tax of 45 Öre/kWh, and a transmission fee of 17.15 Öre/kWh (BjäreKraMV, 2022; Konsumenternas Energimarknadsbyrå, 2024; Vattenfall, 2024). The DH had a fixed annual price of 0.94 SEK/kWh (Energiföretagen, 2023), and the energy needed for the ventilation system was always delivered at a fixed annual electricity price of 2.6 SEK/kWh based on the year 2022.

Equations 4.6 and 4.7 describe the annual operational cost per m² (A_{temp}) if an HP or a DH-central was used respectively.

$$C_{HP} = \frac{(\sum_{k=1}^{8760} (\frac{E_{k,heat} + E_{k,loss} + E_{k,NV}}{SCOP}) \cdot EP_{k,el}) + (E_{vent} + \frac{E_{DHW}}{SCOP}) \cdot EP_{el}}{A_{temp}} \quad [SEK/(m^2 A_{temp} y)] \quad (Equation 4. 6)$$

Where C_{HP} is the annual operational cost of a case using HP, k represents each hour of the year, $E_{k,heat}$ is the simulated hourly energy required to heat the building, $E_{k,loss}$ is heat losses from the piping and heating system set to 5 %, $E_{k,NV}$ is the hourly heat loss from natural ventilation set to $\frac{4}{8760}$ kWh/(m²·h), $SCOP$ is the seasonal coefficient of performance of the HP, $EP_{k,el}$ is the hourly electricity spot price of 2022 including VAT, energy tax, and transmission fees. E_{vent} is the used annual energy by the ventilation system, E_{DHW} is the assumed energy use for domestic hot water of 25 kWh/(m²·y), A_{temp} is the heated floor area of the respective building, and EP_{el} was set to 2.6 SEK/kWh and is a fixed annual average annual electricity price based on the year 2022.

$$C_{DH} = \frac{(\sum_{k=1}^{8760} (E_{k,heat} \cdot E_{k,loss} + E_{k,NV}) \cdot EP_{DH}) + E_{DHW} \cdot EP_{DH} + E_{vent} \cdot EP_{el}}{A_{temp}} \quad [SEK/(m^2 A_{temp} y)] \quad (Equation 4. 7)$$

Where k represents each hour of the year, $E_{k,heat}$ is the simulated hourly energy required to heat the building, $E_{k,loss}$ set to 5 %, $E_{k,NV}$ set to $\frac{4}{8760}$ kWh/(m²·h), E_{DHW} set to 25 kWh/(m²·y), EP_{DH} is a fixed energy price for DH set to 0.94 SEK/kWh, E_{vent} is the used annual energy by the ventilation, EP_{el} was set to 2.6 SEK/kWh and A_{temp} is the heated floor area of the respective building.

Following the geometrical gradient formula in Equation 3.2, Equation 4.8 was developed and used to calculate the net present value of saved operational cost per m² (A_{temp}), abbreviated NPV_{SOC}.

$$NPV_{SOC} = \frac{((C_{opBC} - C_{op}) \cdot (1+g)) \cdot (\frac{1-(1+g)^N \cdot (1+i_n)^{-N}}{i-g})}{A_{temp}} \quad [SEK/m^2 A_{temp}] \quad (Equation 4. 8)$$

Where NPV_{SOC} is the present value of the saved operational cost, C_{opBC} is the annual operational cost of the base case, which was calculated using Equation 4.7, C_{op} is the annual operational cost for a retrofitting, calculated using Equation 4.6 or 4.7 depending on the case, g is the price change rate set to 2 %, N is the calculation period set to 50 years, i_n is the nominal interest rate set to 4 %, and A_{temp} is the heated floor area of the respective building.

4.5.3 Investment and maintenance costs

The NPV of the maintenance costs was calculated using Equation 4.9 and is abbreviated NPV_M .

$$NPV_M = m_0 \cdot (1+g)^n \cdot (1+i_n)^{-n} \quad [SEK/m^2 A_{temp}] \quad (Equation 4. 9)$$

Where m_0 is the maintenance cost per m² A_{temp} at year zero, and g is the nominal price change rate set to 2 %, n is the number of years in the future when the maintenance was done, and i_n is the nominal interest rate set to 4 %.

The NPV for the total investment costs was calculated with Equation 4.10.

$$NPV_I = i_0 + NPV_M \quad [SEK/m^2 A_{temp}] \text{ (Equation 4. 10)}$$

Where NPV_I is the NPV of total investment costs per $m^2 A_{temp}$ for a retrofitting. i_0 is the initial investment cost per $m^2 A_{temp}$ at year zero, and NPV_M is the NPV of maintenance calculated for the specific year the product was replaced/refurbished.

4.5.4 Sensitivity analysis

A sensitivity analysis was performed using Excel to analyze the performance of all 560 cases, with different interest rates and electricity prices. This analysis is conducted to check the sensitivity of the results, based on different input parameters. Thus, an interest rate of 1 % and 7 % were investigated, in addition to the base scenario of 4 %. Two different energy prices were also chosen, where the prices were predicted to increase by 50 % and decrease by 50 % compared to the energy prices for the base scenario from the year 2022. The nominal price change rate of 2 % was always the same in these scenarios and when one parameter was changed all the other variables were held constant. This resulted in a total of five scenarios, including the base scenario with a nominal interest rate of 4 % and energy prices for the year 2022.

4.6 LCA

A LCA was conducted to assess the environmental impact of each retrofitting option, the calculations were performed using Excel. The method is described below.

4.6.1 Goal, scope, and system boundaries

The objective was to assess the environmental impact of the retrofitting measures by calculating their carbon emissions, focusing on total GWP-GHG. The functional unit was determined as $m^2 A_{temp}$. Consequently, all functional units and impacts from the respective EPDs and impacts from the operational energy of all cases were converted to a chosen functional unit. The LCA results which contained the embodied and operational energy impacts, were presented as $kg CO_2 eq./m^2 A_{temp}$.

The life cycle stages considered were A1-A5 (production and installation), B2 (maintenance), B4 (replacement), and B6 (operational energy), and a calculation period set to 50 years, ensuring a comprehensive evaluation of the environmental impact caused by the retrofitting.

4.6.2 Embodied impact

The embodied impact involving lifecycle stages A1-A5 primarily concerned the production phase. Relevant EPDs were used to obtain the impact of GWP-GHG for most products in this report. For products lacking specific EPDs, the environmental impact data of general products were used from Boverket's climate database. But, in cases where the data regarding the impact of GWP-GHG of a specific product was unavailable, the impact was estimated by calculating the weight of the raw materials that the product consisted of and multiplying it with the respective impact from obtained Boverket's generic database.

A product and its impact source selection were done while giving priority to products that had an EPD and were produced locally to get a more accurate value for the impact from the A4 stage and mitigate its impact due to transportation. Figure 19 demonstrates the product and impact source selection and their prioritization.

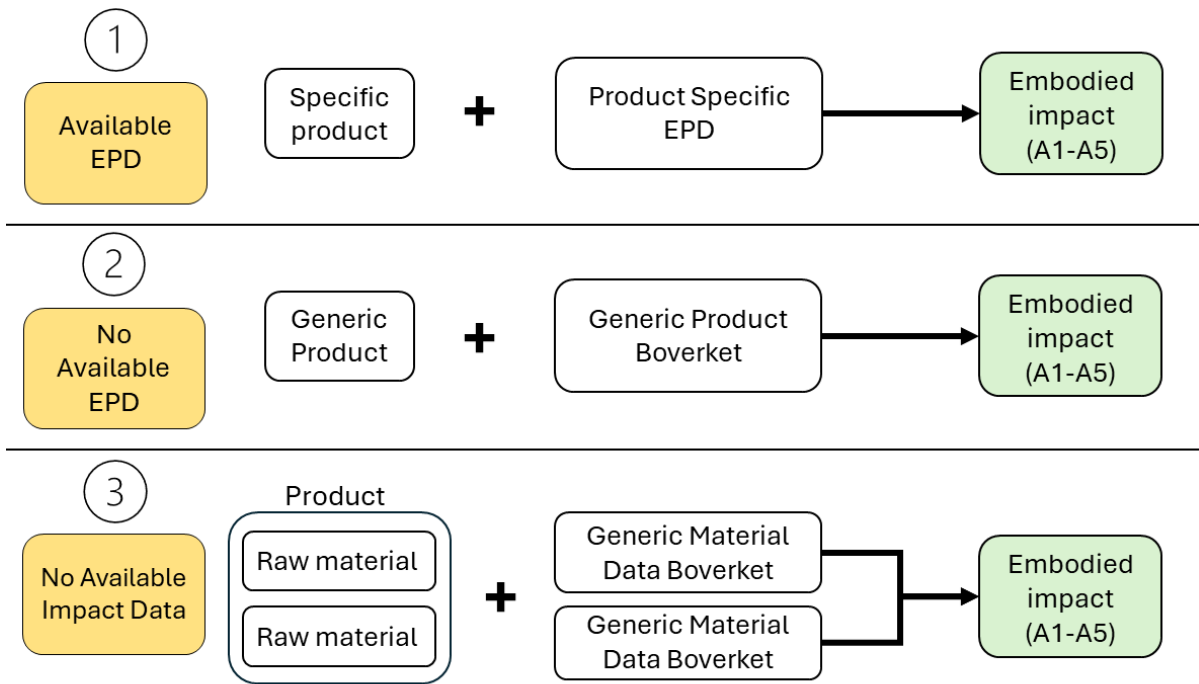


Figure 19. Product and impact source selection and their prioritization.

4.6.3 Operational impact

The operational impact in this study is represented by life cycle stages B2, B4, and B6. Appendix B provides an overview of all involved products, their lifespans, corresponding life cycle stages, and input values for the calculations from different sources.

Stage B2 represented the environmental impact caused by maintaining a measure or a product. Maintenance was done on wooden windows and the MVHR-system. The wooden windows required repainting after a period of 25 years which was considered as maintenance within stage B2, including the environmental impact of the paint. The MVHR-system underwent maintenance, where the filters in the AHU were renewed every year, thus included in stage B2. The impact for stage B2 was calculated by using information from stages A1-A5 and Equation 4.11.

$$B2 = A_{1-5} \cdot a \quad [kg \text{ CO}_2 \text{ eq./m}^2 A_{temp}] \text{ (Equation 4. 11)}$$

Where A_{1-5} is the impact for Stages A1- A5 and a is the number of maintenances during a period of 50 years.

The environmental impact of the replacement of a product (B4) is due to its shorter reference lifespan, compared to the 50-year calculation period. To determine the lifespan of different products, information was gathered from multiple sources. Primarily, the reference lifespan of different products was collected from EPDs. However, in cases where the lifespan was not stated in the EPDs, alternative methods were used such as field experience from professionals, estimates from manufacturers, and typical minimum service life for building parts according to EU: levels (European Commission, 2021).

The measures in need of future replacements included the new heating and ventilation system. Within the new heating system, products requiring replacements were circulator pumps, thermostats, HPs, and tanks, each with respective life spans of 10 years, 10 years, 25 years, and 25 years. The environmental impact for stage B4 was calculated by adding the impacts from stages A1-A5 and multiplying by the number of times the replacements were needed. See Equation 4.12.

$$B4 = A_{1-5} \cdot n \quad [kg \text{ CO}_2 \text{ eq./m}^2 A_{temp}] \text{ (Equation 4. 12)}$$

Where A_{1-5} is the impact for Stages A1- A5 and n is the number of replacements during a period of 50 years.

Stage B6 involved the environmental impact of each case resulting from operational energy use. The impact of the relevant energy source was taken from Boverket's climate database. The base cases of both buildings were heated using DH. However, upon implementing the measure of installing HPs, the heat source was changed to electricity. Representative average impacts for the Swedish DH and Swedish electricity mix were 0.056 kg CO₂ eq./kWh and 0.037 kg CO₂ eq./kWh respectively (Boverket, 2024). The following Equations 4.13 and 4.14 were used to calculate the environmental impact for stage B6 when the heat sources were DH and electricity respectively.

$$B6 = (E_{heat} + E_{DHW}) \cdot I_{DH} + E_{Vent} \cdot I_{El} \quad [kg \text{ CO}_2 \text{ eq./m}^2 A_{temp}] \text{ (Equation 4. 13)}$$

Where E_{heat} is the heating energy needed for a case, E_{DHW} is the energy needed for domestic hot water, E_{Vent} is the energy needed for the ventilation system, I_{DH} is the impact for 1 kWh of energy by district heating, and I_{El} is the impact for 1 kWh of energy by electricity.

$$B6 = (E_{heat} + E_{DHW} + E_{Vent}) \cdot I_{El} \quad [kg \text{ CO}_2 \text{ eq./m}^2 A_{temp}] \text{ (Equation 4. 14)}$$

Where E_{heat} is the heating energy needed for a case, E_{DHW} is the energy needed for domestic hot water, E_{Vent} is the energy needed for the ventilation system, and I_{El} is the impact of 1 kWh of energy by electricity.

The total environmental impact of a case is calculated by utilizing Equation 4.15.

$$LCA_{total} = A_{1-5} + B2 + B4 + B6 \quad [kg \text{ CO}_2 \text{ eq./m}^2 A_{temp}] \text{ (Equation 4. 15)}$$

Where A_{1-5} is the impact from stages A1- A5, $B2$ is the impact from stage B2, $B4$ is the impact during stage B4, and $B6$ is the impact during stage B6.

5 Results & discussion

5.1 Building A

5.1.1 Base case - simulation

The results of Brf. Sofielund showed that the heating use was relatively high compared to other buildings, Further analysis revealed that the heating, as stated in the energy declaration, included additional domestic hot water when in reality the performance of the building was better than initially assumed. This conclusion was drawn by using separate energy bills for heating and DHW and calculating the building's energy use.

The annual heating was simulated to 132 kWh/m²A_{temp} and differed approximately 7 % from the actual normalized heating demand of 142 kWh/m²A_{temp}. Figure 20 illustrates a comparison of the monthly heating demand. May is the only month with a large deviation between the simulated and normalized heating, while the rest of the year only differed by approximately 1 kWh/m². This minor deviation validated the accuracy of the energy model, and thus, it was assumed that the model could be used as a representation of the actual building.

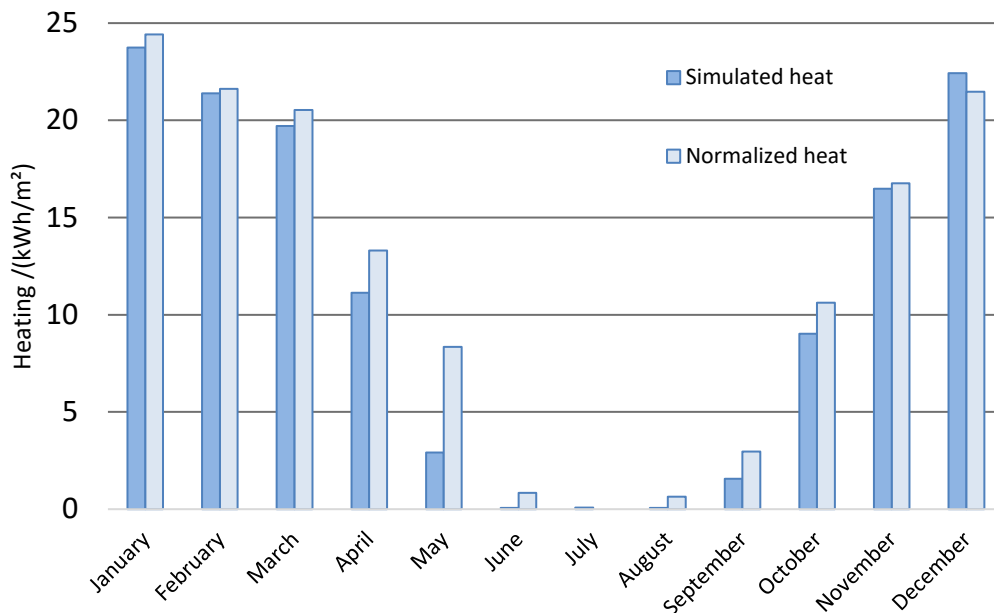


Figure 20. Monthly heating of the simulated model and the actual building A.

The distribution of energy losses in the simulated base case is illustrated in Figure 21. The results show that the heat losses occur mostly through the building envelope and ventilation system. This indicates that improving the envelope constructions and ventilation system holds the highest potential for achieving the most reduction in energy losses.

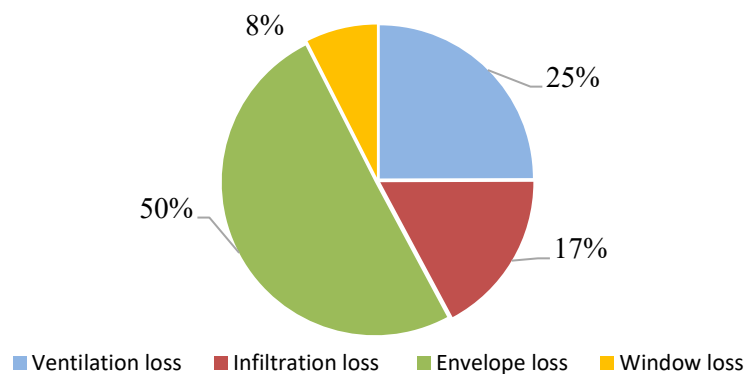


Figure 21. Distribution of heat losses from building A.

Moisture safety of current construction

The external wall of the building consists of inorganic materials such as bricks and plaster, meaning these materials are not vulnerable to mold. Figure 22 illustrates the water content of the façade, along with the temperature and relative humidity of the exterior surface. The amount of water increased initially over four years, after which it reached a state of equilibrium. The increase indicated that the facade does not dry out., As observed in Figure 22, there is a risk of frost damage to the external parts of the wall, leading to increased costs due to potential repairs.

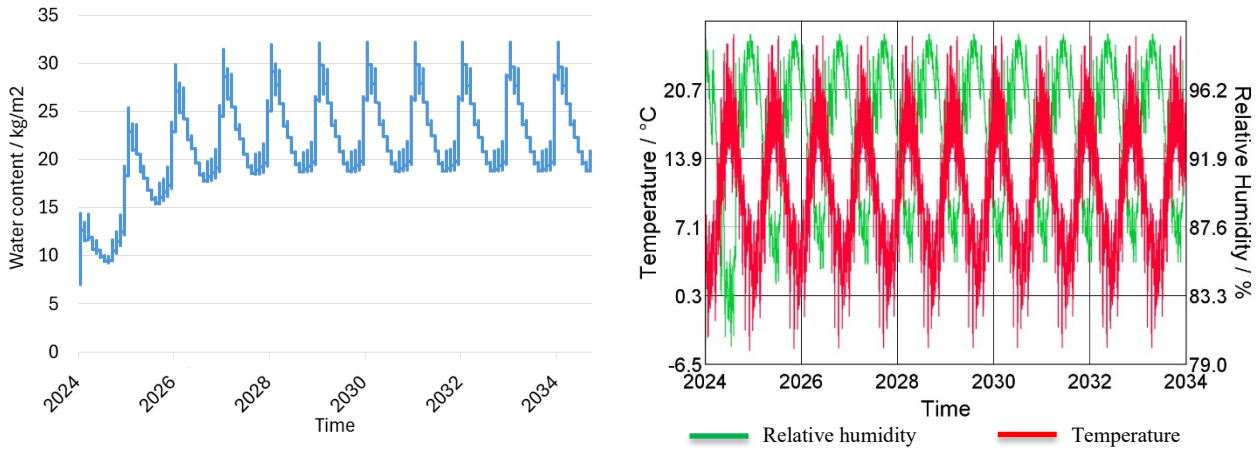


Figure 22. Water content, temperature, and relative humidity of the base case façade construction, building A.

The roof construction consisting of wooden beams is susceptible to mold growth and therefore a mold index analysis is done. Specifically, the external part of the wooden beam layer was chosen to be analyzed, due to its role as a load-bearing structure and any mold growth can lead to several problems, such as degradation of material and even health risk. The result of the mold index analysis is illustrated in Figure 23. Initially, the mold index reached a level of one and reduced over time. After approximately three years the index reached safe levels with an index of zero, indicating no mold on the surface.

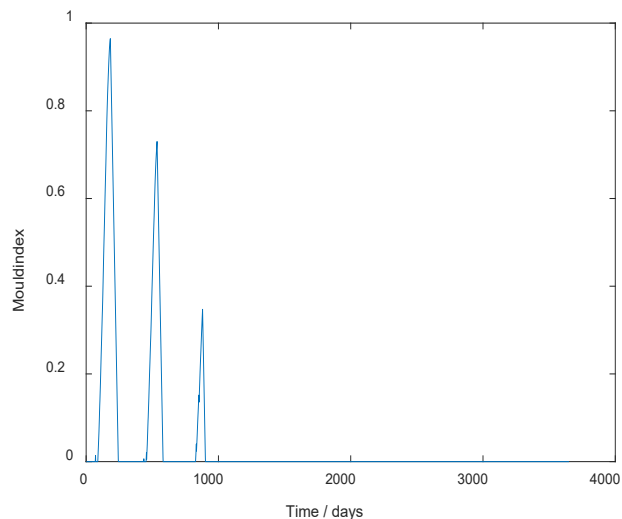


Figure 23. Mold index of the base case roof construction in building A.

5.1.2 Envelope & systems

Envelope - moisture safety

To enhance the energy performance of the wall construction, the façade was insulated externally with the inorganic insulation materials rockwool and EPS. Therefore, the risk of mold growth is significantly decreased. Analysis of the total water content within the constructions, shown in Figure 24, reveals that the construction is drying out over time, and the risk of moisture-related damage decreases. Initially, the water content decreases in both constructions but eventually stabilizes to a level that renders the wall drier compared to the base case. Notably, adding rockwool insulation to the facade resulted in a more rapid reduction in moisture content, compared to EPS insulation. Moreover, the external insulation also increases the temperature in the bricks, minimizing its vulnerability to frost-related damage. The result from WUFI simulations shows that the brick's exterior surface temperature stays within a safe range of 12 °C to 22 °C throughout the year, thus eliminating concerns of frost damage.

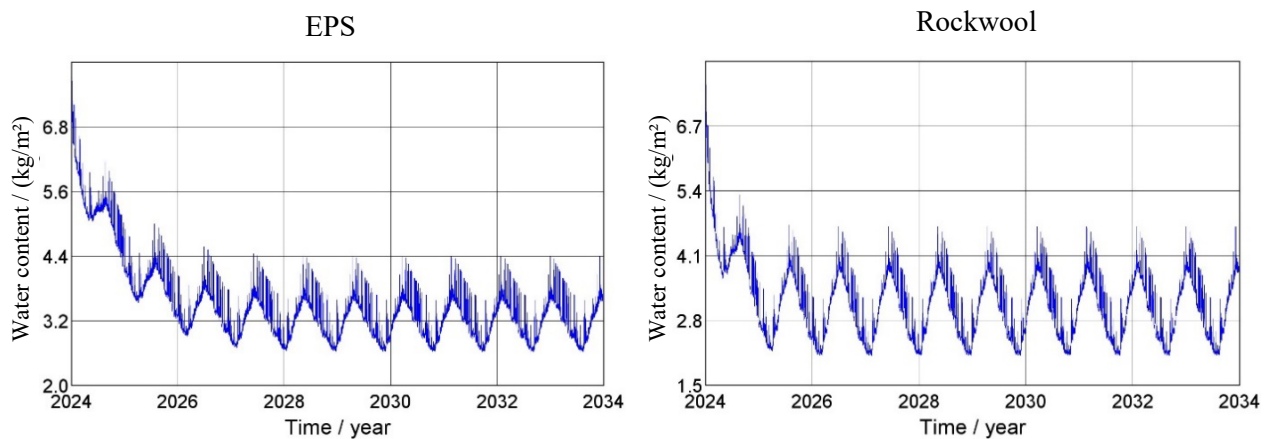


Figure 24. The total water content of facade constructions with added EPS or rockwool insulation, building A.

The three improvement options for the roof construction were analyzed regarding moisture safety, focusing on the wooden beam's sensitivity to mold. Figure 25 shows the mold index for the wooden beam layer throughout the analysis period. It is evident from the results that these constructions are moisture safe. It shows some small amounts of mold in the beginning with a mold index below 1, meaning that mold is only detectable with a microscope. However, the mold index decreases gradually over time which minimizes the risk of mold formation in the long term. Furthermore, the relative humidity in the layer is mostly below the critical relative humidity threshold across all options, further ensuring the moisture safety of the construction, see Appendix C.

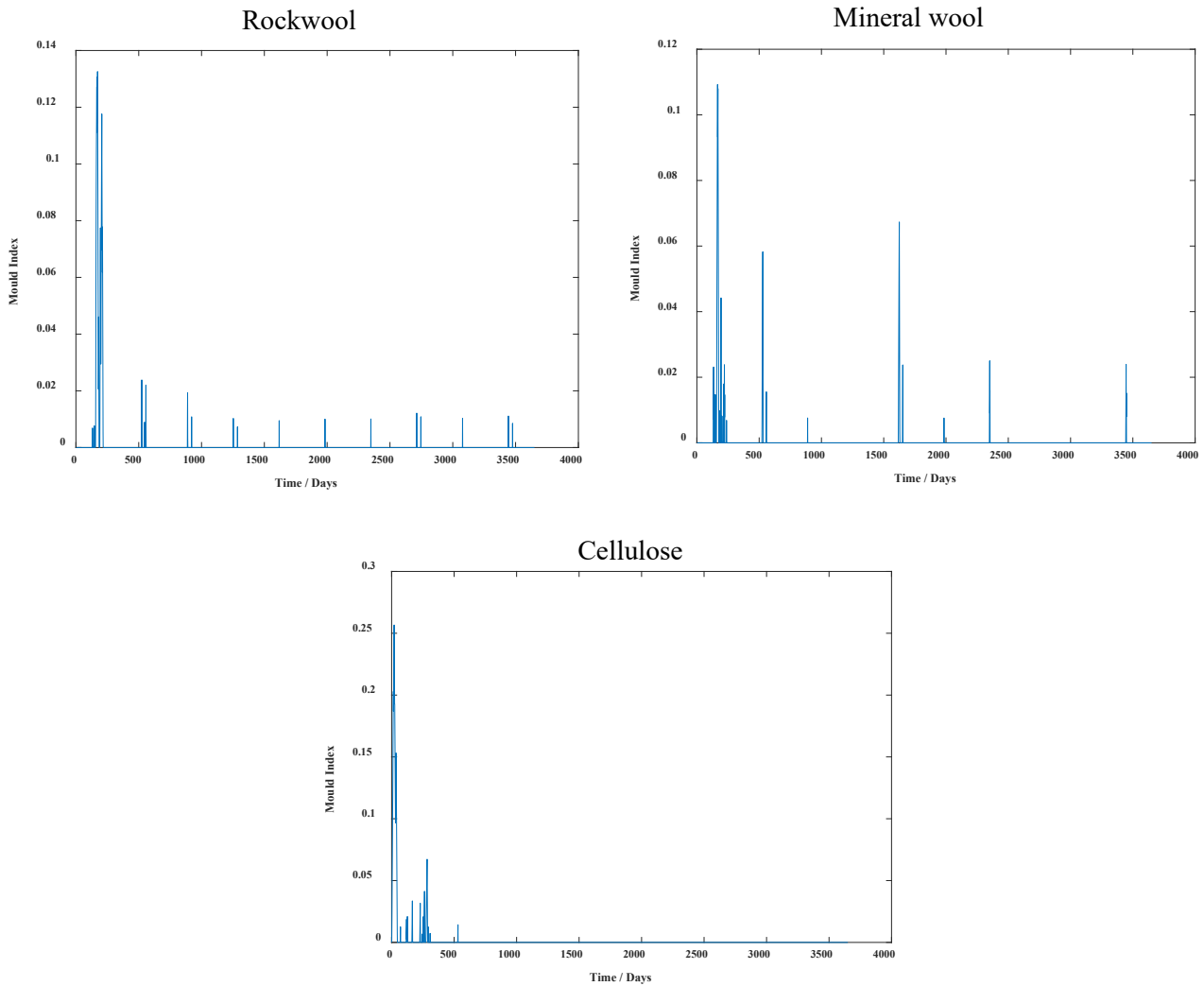


Figure 25. Mold index of the proposed roof constructions, building A.

Ventilation

Figure 26 shows the duct layout of the MVHR-system designed for building A, where the supply and return air ducts are represented by the colors blue and red respectively. The design of the system was done with both economic- and energy efficiency in mind. The total required airflow for the building was calculated to be 260 l/s, which equals 0.51 ($l/(s \cdot m^2)$). The supply to exhaust air system was designed using a ratio of 1:1. Strategically, the AHU was centrally placed in the attic floor to optimize access to fresh outdoor air, and easier design of the duct system for air distribution. The supply air system consists of 22 wall-mounted diffusers of the same size throughout the building. Wall-mounted diffusers were chosen, to reduce the amount of visible ductwork, making the system more aesthetically pleasing. Additionally, this design results in less ductwork and fewer holes in the walls or floors of the building, compared to if ceiling diffusers were utilized. Notably, the critical path for this system is located on floor 1, which is farthest away from the AHU, highlighted in Figure 26. Similar to the supply air system, the exhaust air system is comprised of 24 wall-mounted diffusers of identical size, with the critical path also located on floor 1, shown in Figure 26. An overview of the supply and exhaust system sizing and balancing is provided in Appendix D.

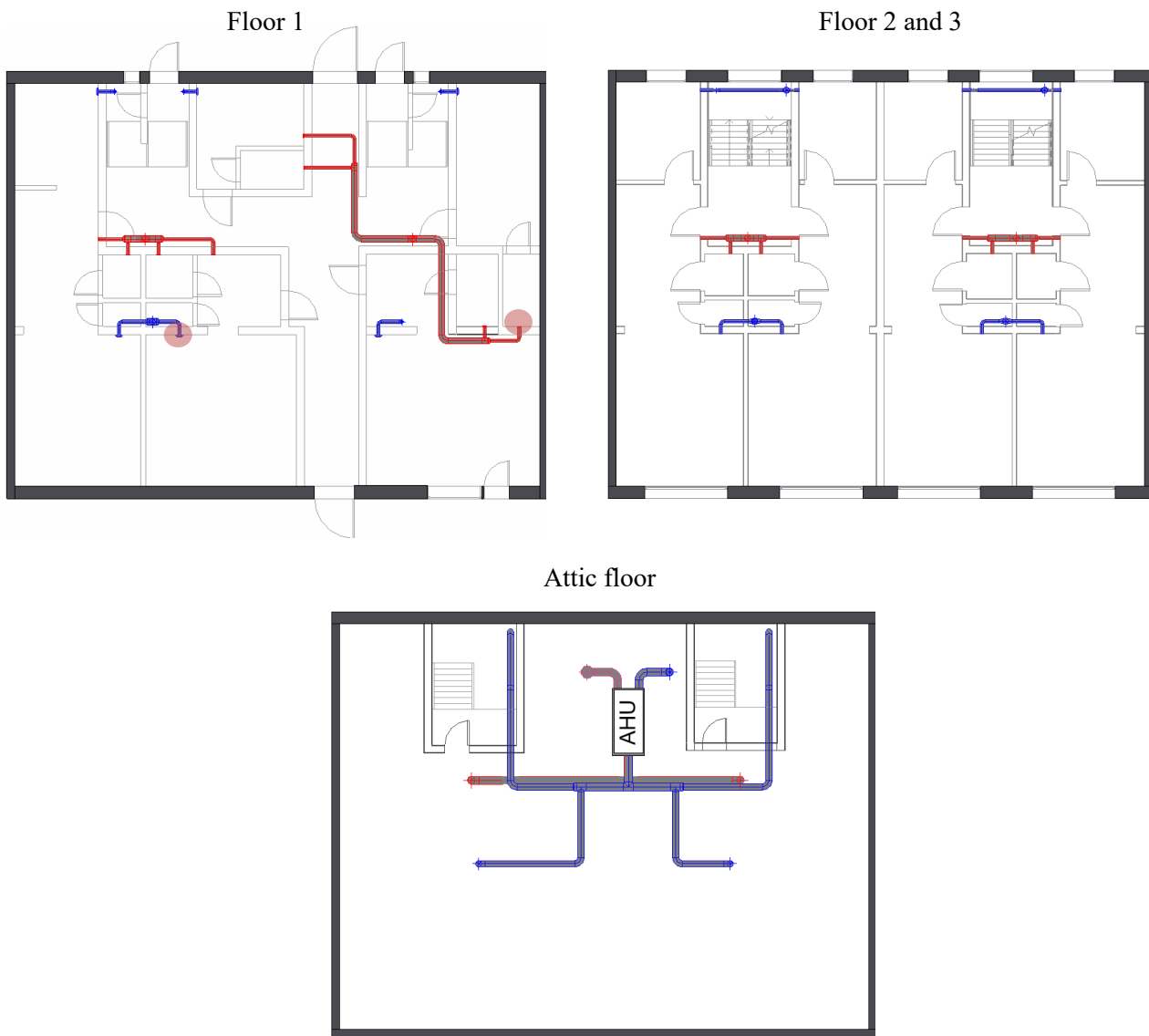


Figure 26. Plan view of the proposed ventilation system, building A.

The air inlet and outlet from the building are placed at a distance from each other to avoid the intake of polluted exhaust air. The pressure drop in exhaust and supply ducts was calculated to be 40 Pa and 71 Pa respectively, and the pressure drop in the critical paths of the supply and extract systems was measured at 73 Pa and 48 Pa respectively. Using this information and the total airflow, an AHU was designed utilizing the ACON designer tool. The AHU consists of different components such as a heating coil with a power output of 5 kW, a plate heat exchanger with an 85 % counterflow heat recovery efficiency, and fans with an SFP of 1.05 kW/(m³·s). Introducing the MVHR-system leads to additional energy use due to the operation of fans and the heating coil. The annual energy use of the ventilation system amounts to 4 000 kWh, where all the energy is supplied by electricity.

Heating system

The new heating system was designed to cover 70 % of the highest peak load scenario, which is the base case, requiring a heating peak load of 21 kW and an additional 6.5 kW for DHW. The corresponding peak volume of domestic hot water was calculated to be 950 liters when considering hot water usage for all tenants during the peak hours. This new system contained new radiators and pipe systems, circulators, air-to-water HPs, and an accumulator tank. Two circulation pumps were chosen to circulate the water (Grundfos Magna3 25-60), followed by three HPs (NIBE S2125) consisting of one with a size of 12 kW and two at 8 kW each, collectively satisfying the building's peak power demand of 28 kW. Each HP was connected to an indoor combi tank (NIBE VVM S325) with a volume capacity of 172 liters. Additionally, a storage tank (CTC 2 500L) was used to fulfill the remaining hot water needs.

When simulating all cases involving an HP, a COP of 3.8 was assumed for heating, which is an average SCOP for HPs in typical cold climates according to manufacturers. The heat distribution to the rooms was done through copper pipes connected to radiators which were strategically placed under the windows in rooms requiring heating, to mitigate cold draught. The new heating system was designed to reduce energy use by effectively performing low-temperature heating with a supply water temperature of 49° C and a return mean water temperature of 43° C. The size of the radiators was selected based on the simulated heating demand of each room. The radiator and piping layout adhered to the same layout and design as the existing DH system. Detailed information regarding radiator piping and balancing can be seen in Appendix E.

5.1.3 Energy

The retrofitting measures were implemented both separately and in combination with each other, the individual effect on purchased annual energy and peak load of each measure is presented in Figure 27. An analysis of the results indicates that the largest reduction in purchased energy while implementing an individual measure is achieved by installing an HP. The installation of a new heating system did not affect the losses or the total energy use of the building at all, however, it had the largest reduction of purchased energy which is a result of the COP of the HPs. On the other hand, the smallest reduction in energy use was achieved by installing new windows which reduced the peak load marginally. The reduced peak load when installing MVHR-system was a result of reduced ventilation losses and heat recovery. The largest impact on peak load was by adding insulation on the façade, which could be explained by the combining surface area and reduced U -value. The least reduction was achieved by installing windows, this could be explained by the fact that only some of the windows need to be changed, which leads to a small reduction in transmission losses.

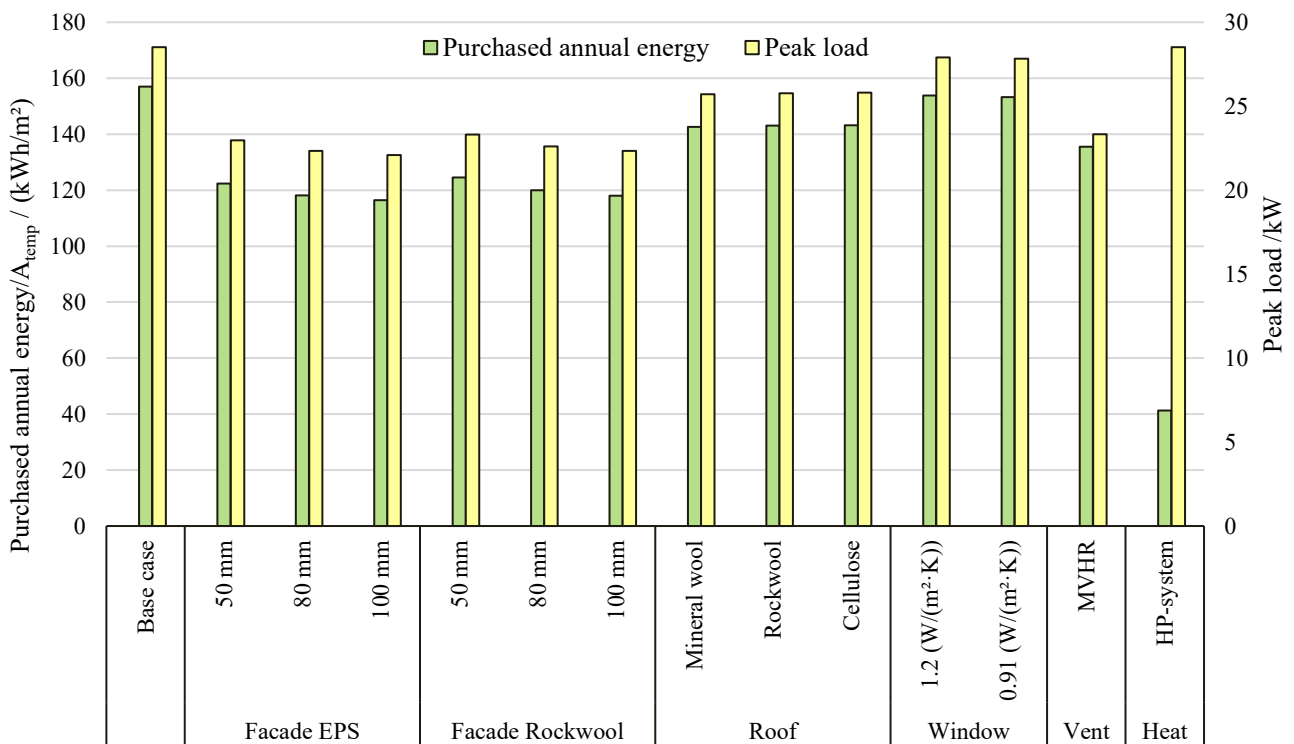


Figure 27. Purchased annual energy and peak load of each measure individually, for building A.

Figure 28 illustrates the annual energy use and peak load for all 560 cases. A clear pattern can be seen in the results, primarily due to the type of heating system and the type of ventilation system. Implementation of the HP-system decreases a case's purchased energy, yet the building's heating peak load remains unchanged. However, in cases where an MVHR system is integrated, both the heating peak load and annual energy use of the building are reduced. Similar conclusions can be drawn for other measures. Moreover, the effect of an improvement measure is much more visible if the DH-system was in use, while if the HP-system was used, then the impact of other improvement measures was less visible, in comparison to the effect of the HP-system itself on the purchased annual energy. The three cases with the lowest annual purchased energy are highlighted with the colors green, yellow, and orange, representing their performance as first, second, and third best, the base

case is also presented with the color red. These cases are further described in Table 11, in which the “-“ refers to no alteration being made.

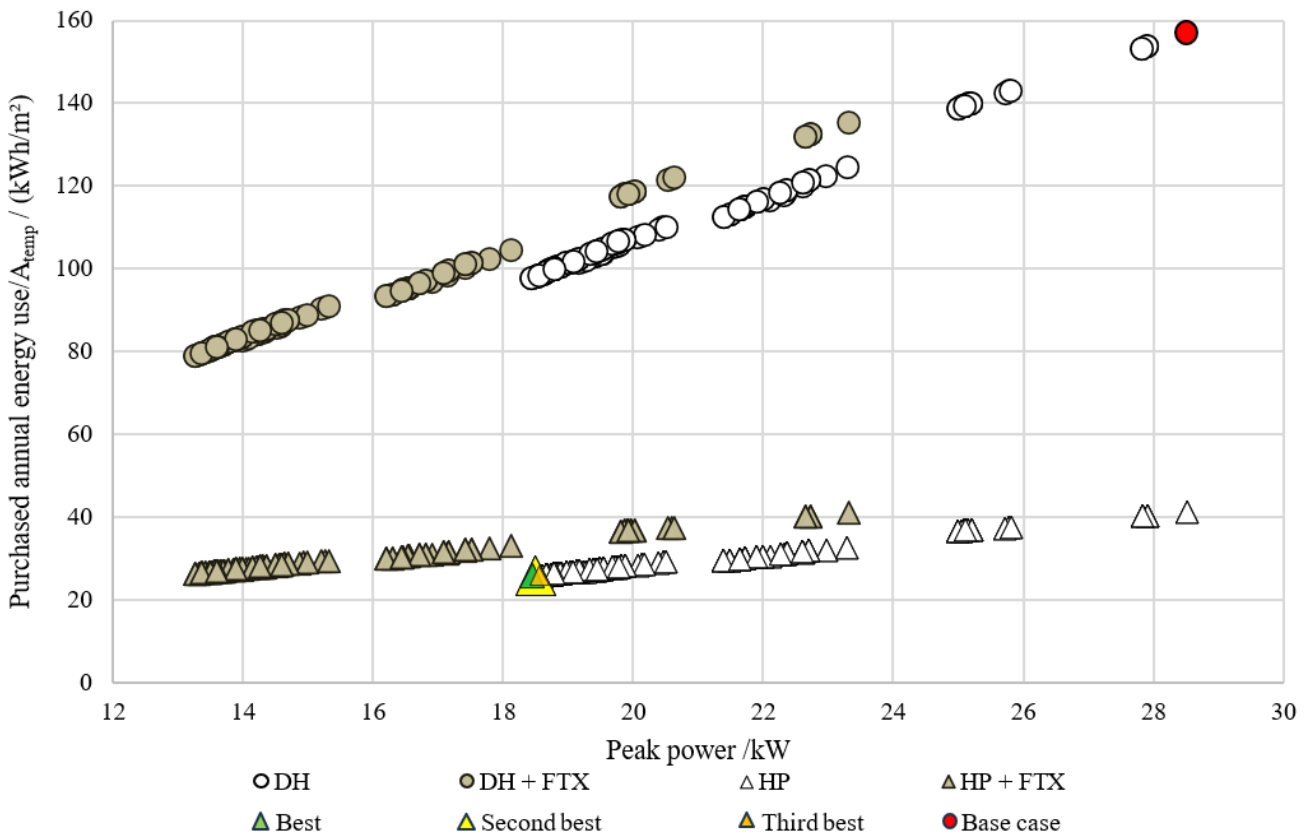


Figure 28. Purchased annual energy use and peak power for all 560 cases in building A.

Table 11. The three best combinations for building A, regarding energy use.

Rank	Façade insulation	Roof insulation	U-value window	Heating type	Ventilation type	Energy use / (kWh/(m²A _{temp} ·y))
Best	100 mm EPS	Mineral wool	0.91	HP-system	-	25.7
2 nd Best	100 mm EPS	Rockwool	0.91	HP-system	-	25.8
3 rd Best	100 mm EPS	Mineral wool	1.2	HP-system	-	25.9
Base case	-	-	-	-	-	157

The results highlight that the most effective approach for reducing purchased energy is a combination of roof insulation, 100 mm EPS facade insulation, new windows, and an HP-system. On the contrary, implementing an MVHR-system alongside an HP-system is not an optimal choice, due to the additional operating energy of the MVHR-system. However, implementing an MVHR-system together with the current DH-system can prove to reduce the annual purchased heating by approximately 19 %.

5.1.4 LCC

The cost of each measure is illustrated in Figure 29 below. However, certain measures have to be maintained during the calculation period, including refurbishment of the painted windows, change of AHU and balancing of the ventilation, and new circulation pumps and thermostats for the heating system.

Appendix F illustrates the costs in more detail, including its source. Based on the results, insulating the roof had the lowest cost, while installing a new heating system with HP had the highest cost, followed by the installation of a new MVHR-system. The high cost associated with a new heating system stems from the necessity to renew all system components for the HP installation. Additionally, the design of the new heating system is based on a worst-case scenario, having the highest heating peak load, resulting in an oversized heating system in most cases with a lower peak load.

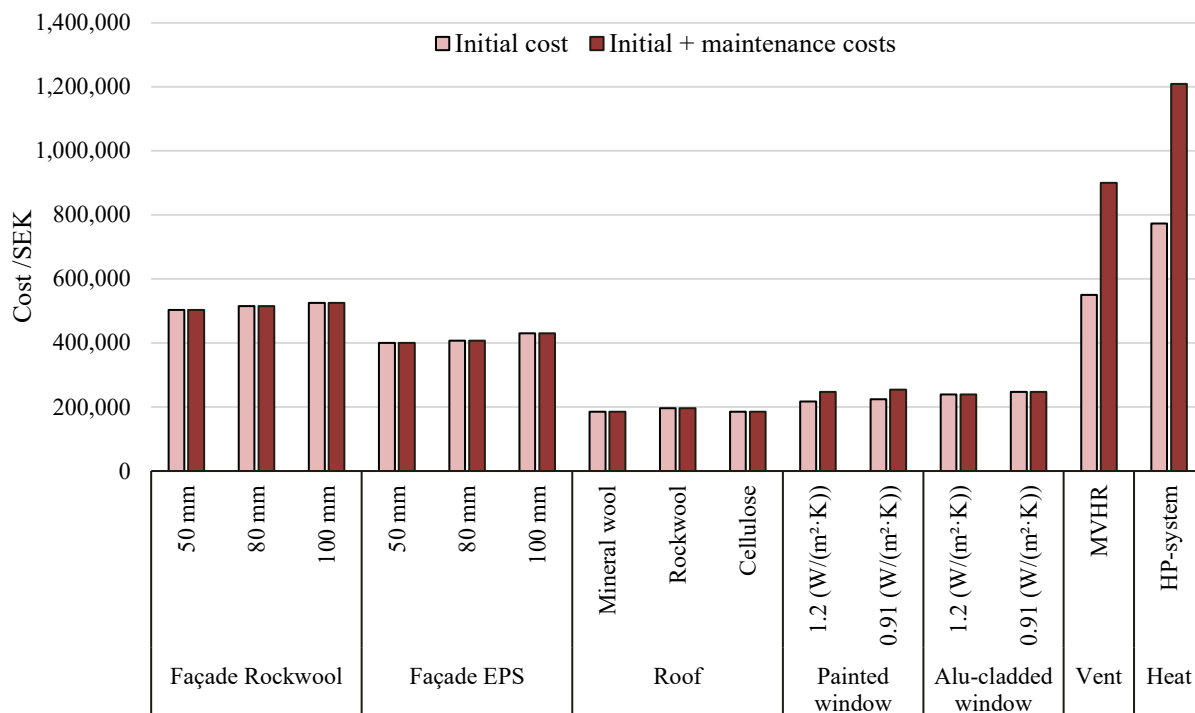


Figure 29. Cost for both initial and initial + maintenance for each measure individually.

Figure 30 presents the total NPV of all 560 combinations relative to their total investment costs. The NPV varies from -3 200 SEK/m²A_{temp} to 495 SEK/m²A_{temp}. The findings indicate that a higher investment cost does not necessarily increase the profitability of a measure within a 50-year calculation period. Among these combinations, a total of 63 cases show profitability, displaying a positive NPV. Interestingly, none of these combinations include MVHR-system or HP installations, while the majority of the profitable cases had additional façade and roof insulation. The three most profitable cases are highlighted in Figure 30 and described further in Table 12.

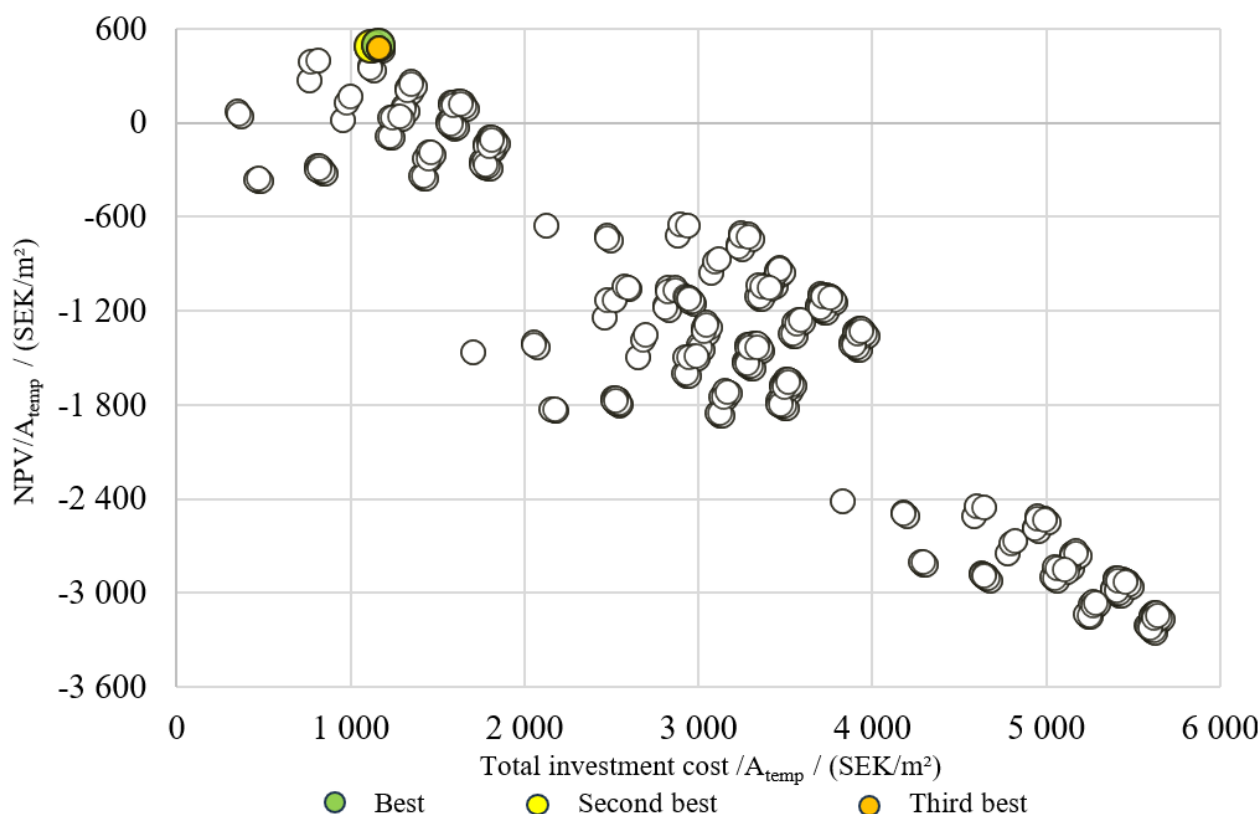


Figure 30. NPV and total investment cost for all 560 cases in building A.

Table 12. The three best combinations for building A, regarding NPV.

Rank	Façade insulation	Roof insulation	U-value window	Heat. type	Vent. type	Invest. cost /((SEK/m ² A _{temp}))	NPV /((SEK/m ² A _{temp}))
Best	100 mm EPS	Mineral wool	-	-	-	1 160	495
2 nd Best	80 mm EPS	Mineral wool	-	-	-	1 120	486
3 rd Best	100 mm EPS	Cellulose	-	-	-	1 160	477

As shown in Table 12 the best-performing cases from a LCC perspective have a combination of different insulation types on the roof and different thicknesses of EPS insulation on the façade. The profitability of these combinations is the result of the high amount of saved energy at a low cost. Despite the high energy savings from installing HPs, their high investment cost does not make it a feasible option within the 50-year calculation period under the base scenario inputs.

Sensitivity analysis – Interest rate

Scenarios 2 and 3 describe the 1 120 cases created, based on the condition of having a fixed nominal price change rate of 2 %, electricity price of the year 2022, but different interest rates of 1 % and 7 %. The results of the sensitivity analysis with different interest rates are shown in Figure 31 and Figure 32, where the NPV_{total} of these scenarios is presented with its investment cost. The best-performing cases from these scenarios are selected and marked with colors corresponding to Table 13.

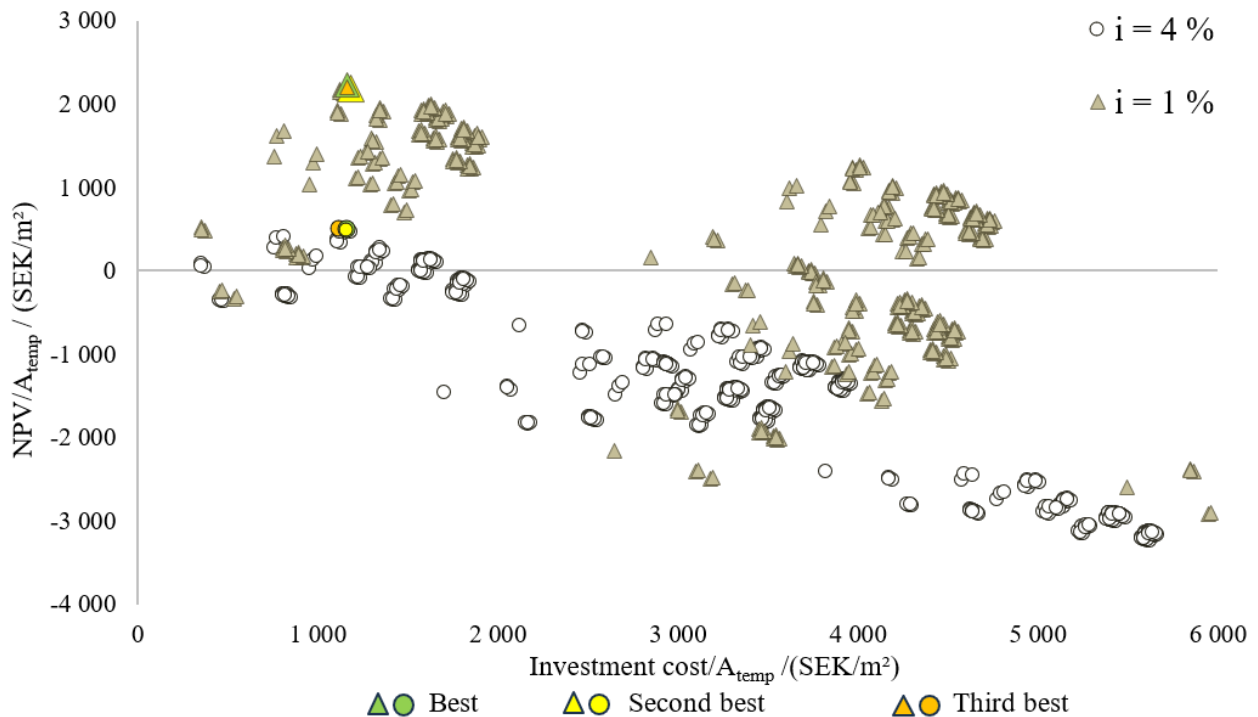


Figure 31. Scenario 2 - Sensitivity analysis with interest rates of 1 % and 4 %.

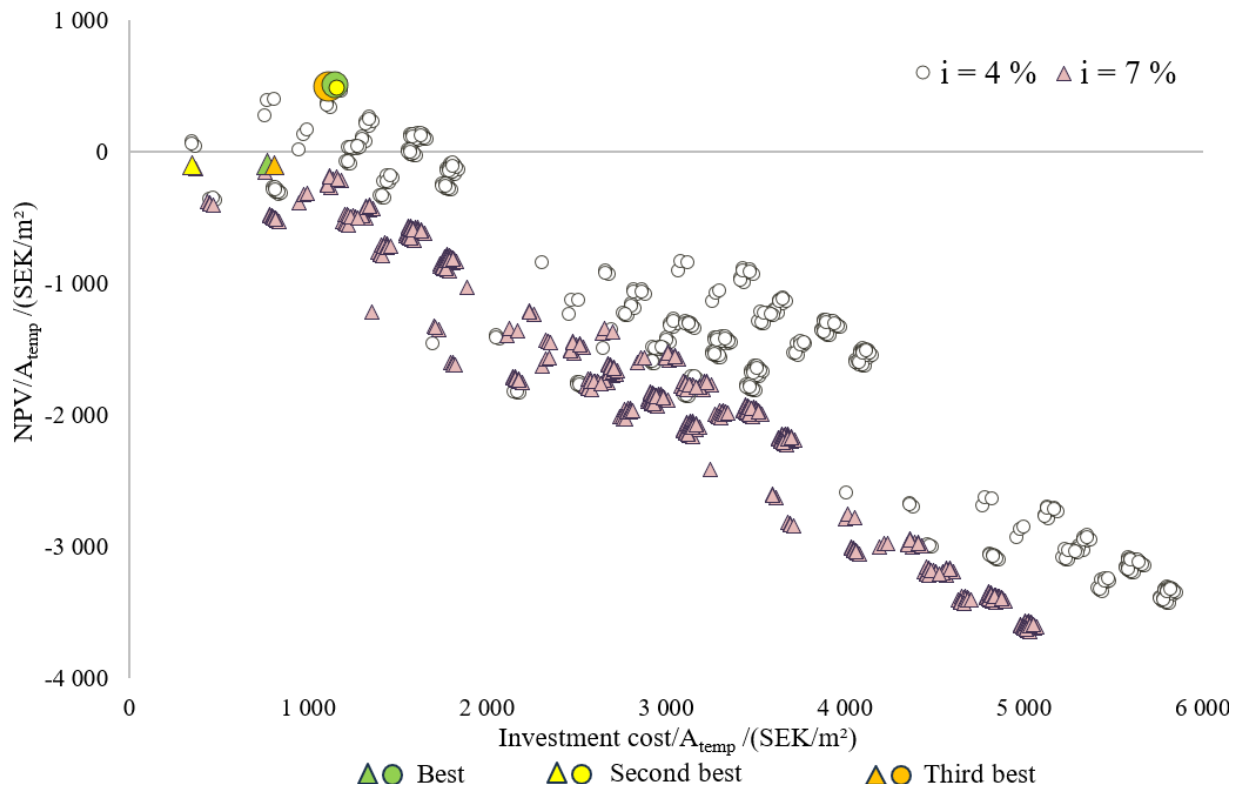


Figure 32. Scenario 3 - Sensitivity analysis with interest rates of 4 % and 7 %.

As illustrated in Figure 31 and Figure 32, the profitability of the cases increases when the nominal interest rate decreases and decreases when the nominal interest rate increases. The varying interest rate also affects the investment costs of different measures due to maintenance during its lifespan, where a rise in interest rate results in reduced investment costs and total NPV. The results imply that the profitability of an investment increases as interest rates decrease, leading to more cases being feasible.

Table 13. The three best combinations for building A of the base scenario and scenarios 2 & 3, regarding NPV.

Rank	Façade insulation	Roof insulation	U-value window	Heating type	Ventilation type	Invest. cost /((SEK/m ² A _{temp}))	NPV /((SEK/m ² A _{temp}))
Base scenario							
(Interest rate 4 %)							
Best	100 mm EPS	Mineral wool	-	-	-	1 160	495
2 nd Best	80 mm EPS	Mineral wool	-	-	-	1 120	486
3 rd Best	100 mm EPS	Cellulose	-	-	-	1 160	477
Scenario 2							
(Interest rate 1 %)							
Best	100 mm EPS	Mineral wool	-	-	-	1 160	2 240
2 nd Best	100 mm EPS	Cellulose	-	-	-	1 160	2 200
3 rd Best	100 mm EPS	Rockwool	-	-	-	1 190	2 190
Scenario 3							
(Interest rate 7 %)							
Best	80 mm EPS	-	-	-	-	771	-91
2 nd Best	-	Mineral wool	-	-	-	350	-99
3 rd Best	100 mm EPS	-	-	-	-	813	-104

Despite fluctuations in interest rates impacting investment costs and total NPV, the absence of HP-system, MVHR-system, and new windows in the best-performing cases remains consistent. In scenario 3, when the interest rate is 7 %, none of the cases are profitable over the 50 years. This is primarily because of high interest rates, making the NPV of the energy savings insufficient to cover the investment cost for the implemented measures.

Sensitivity analysis – energy prices

Scenarios 4 and 5 define the 1 120 cases formed, based on the condition of having a constant nominal price change rate of 2 %, and nominal interest rate of 4 %, but different prices for the energy compared to the year 2022 with a 30 % decrease and increase respectively. The results of the sensitivity analysis with different energy prices are shown in Figure 33 and Figure 34, where all cases in scenarios 4 and 5 are shown in comparison to the base scenario.

In the scenarios with higher energy prices, cases with higher energy savings will be more profitable, resulting in a higher NPV, while lower energy prices lead to a lower total NPV. The three cases with the highest profitability are highlighted in Figure 33 and Figure 34 and described further in Table 14.

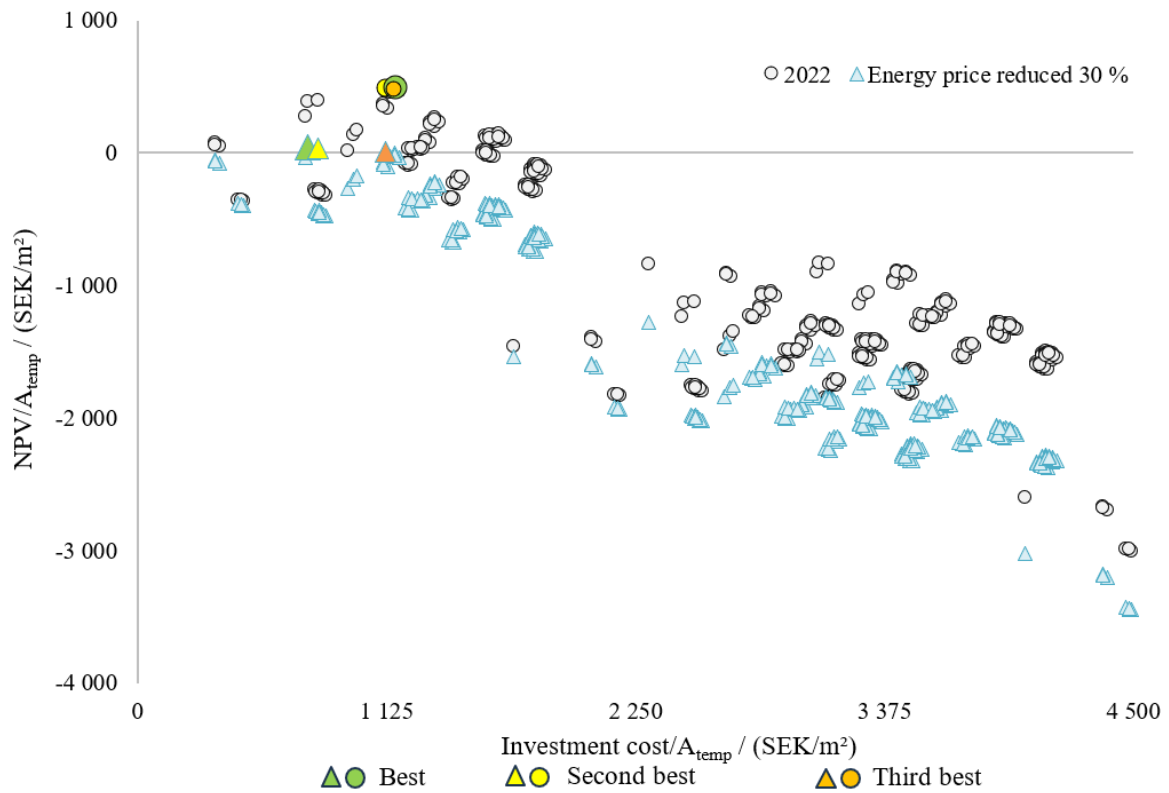


Figure 33. Scenario 4 - Sensitivity analysis with electricity price for 2022 and 30 % reduced prices.

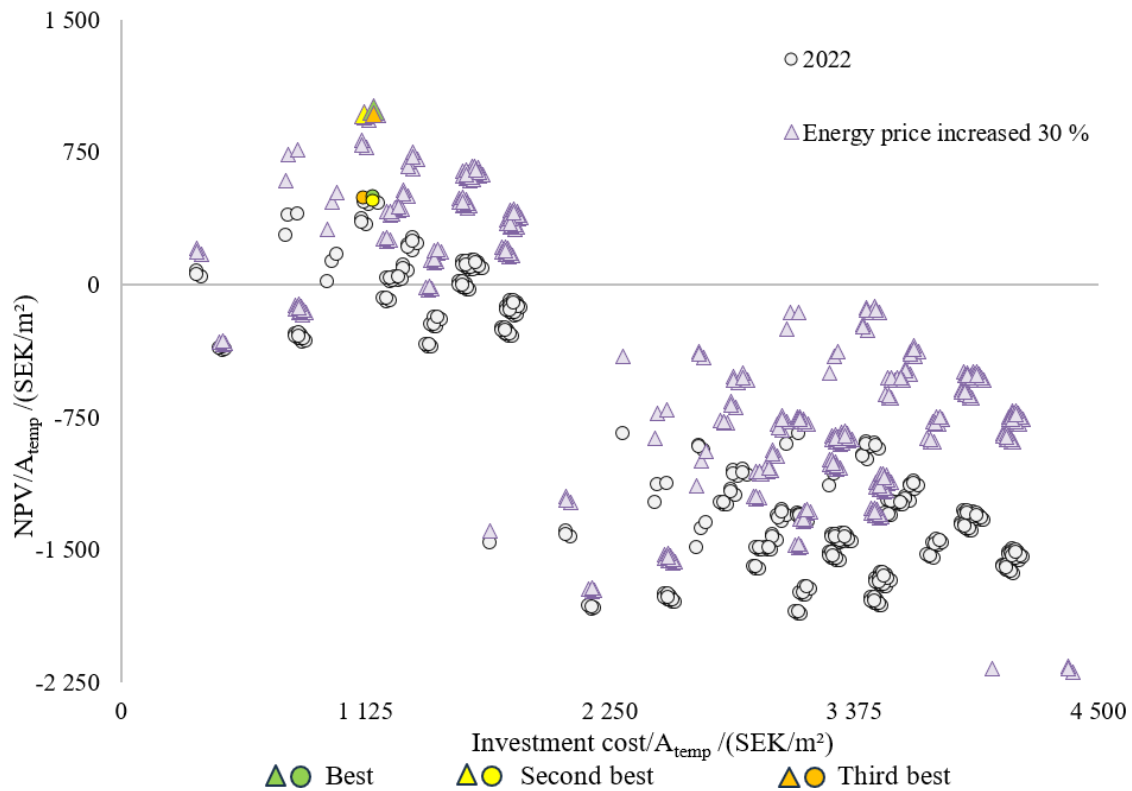


Figure 34. Scenario 5 - Sensitivity analysis with electricity price for 2022 and 30 % increased prices.

Table 14. The three best combinations for building A in the base scenario and scenarios 3 & 4, regarding NPV.

Rank	Façade insulation	Roof insulation	U-value window	Heating type	Ventilation type	Invest. cost /(SEK/m ²)	NPV /(SEK/m ²)
Base scenario (energy prices 2022)							
Best	100 mm EPS	Mineral wool	-	-	-	1 160	495
2 nd Best	80 mm EPS	Mineral wool	-	-	-	1 120	486
3 rd Best	100 mm EPS	Cellulose	-	-	-	1 160	477
Scenario 4 (30% reduced energy prices)							
Best	80 mm EPS	-	-	-	-	771	43
2 nd Best	100 mm EPS	-	-	-	-	813	36
3 rd Best	80 mm EPS	Mineral wool	-	-	-	1 120	4
Scenario 5 (30% increased energy prices)							
Best	100 mm EPS	Mineral wool	-	-	-	1 160	993
2 nd Best	80 mm EPS	Mineral wool	-	-	-	1 120	969
3 rd Best	100 mm EPS	Cellulose	-	-	-	1 340	969

These variations in energy prices do not affect the investment costs, therefore, the cases maintain the same investment costs across these scenarios. The best cases evaluated based on total NPV remain unchanged between scenario 5 and the base scenario. These involve combinations of different EPS insulation thicknesses for the façade paired with different roof insulation types, without incorporating other measures. However, in scenario 4, where the energy prices decrease, only three cases were profitable. This leads to the conclusion that only façade insulation using rockwool with thicknesses of 80 mm and 100 mm is a feasible measure.

5.1.5 LCA

The embodied GWP-GHG of all the investigated measures when implemented separately are presented in Figure 35. The HP-system demonstrates the highest individual impact, followed by the ventilation system. However, it is worth noting that the size of the HP-system is overestimated in most cases since the system is designed to cover the demand of the case with the highest peak load. This results in an overestimated environmental impact in most cases. Furthermore, changing windows, and adding cellulose insulation on the roof had the lowest individual impact. The low impact of cellulose can be explained by its high degree

composition of recycled waste material. Thus, drastically reducing the extraction of new raw materials leading to less embodied impact. Furthermore, replacing the windows also had a low environmental impact, mainly due to the few number of windows being replaced in building A. Among the insulation options categories, rockwool insulation registered the highest individual impact for both façade and roof construction. This could be explained by its large impact per functional unit, relative to mineral wool and cellulose.

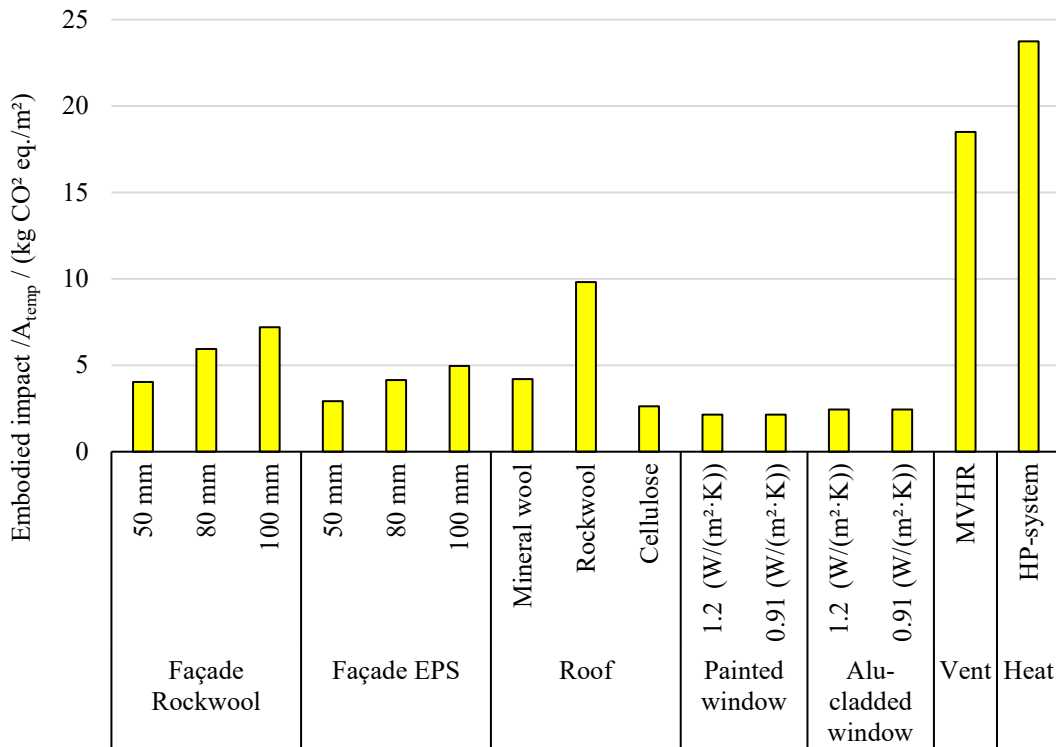


Figure 35. Embodied impact of each separate measure, building A.

Figure 36 shows all the analyzed combinations on building A and their corresponding environmental impacts relative to their purchased operational energy. The cases with the highest environmental impact also require a lot of purchased energy. The high total impact from these cases is explained by the high operational impacts from the operation phase. This means that measures or combinations of measures that reduce the operational energy the most also yield the greatest reduction in total environmental impact because the total environmental impact is mostly dominated by the operational impact of a case. Consequently, all the retrofitting options lead to a lower environmental impact compared to the base case, since the base case demonstrates the highest energy use.

Figure 36 also indicates that even though the embodied impact is increased by the implementation of measures such as the heating system, the total impact from the whole life cycle decreases due to reductions in the operational energy impacts. The cases with the lowest environmental impact can effectively reduce the operational energy to a greater extent than the size of its embodied impact. Cases with the lowest environmental impact are highlighted in Figure 36 and described further in Table 15. These low-impact cases also demonstrate the highest reduction in operational energy.

It is worth noting that the impact data used for the LCA-calculations are primarily sourced from Boverket's climate database, which could have a higher impact value compared to some EPDs. Consequently, better results could be achieved by using EPDs with more favorable impact data. The environmental impact of all cases could also be reduced by using more environmentally friendly materials. However, in this building, the material choices were limited to those compatible with the already existing structure.

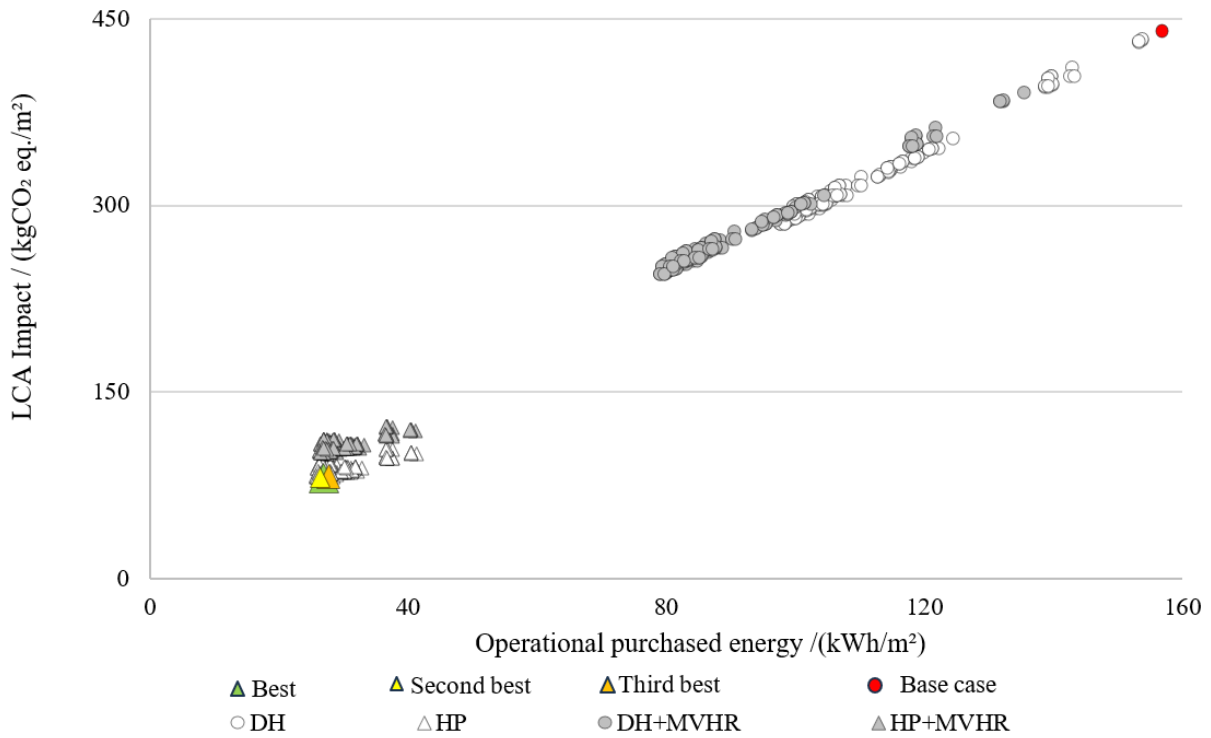


Figure 36. Total environmental impact and annual purchased operational energy of different cases in building A.

Table 15. The base case & the three best combinations for building A, regarding environmental impact.

Rank	Façade insulation	Roof insulation	U-value window	Heating type	Ventilation type	LCA-impact / (kg CO ₂ eq. /m ² A _{temp})
Best	100 mm EPS	Cellulose	-	HP-system	-	81.04
2 nd Best	80 mm EPS	Cellulose	-	HP-system	-	81.06
3 rd Best	100 mm EPS	Cellulose	0.91	HP-system	-	81.34
Base case	-	-	-	-	-	440

Analyzing the results, a trend can be seen where all the cases consisting of a combination of measures such as EPS insulation on the façade with cellulose insulation on the roof and an HP-system have a lower environmental impact than other cases. These cases consist of combinations, where the reduction in the operational energy impacts outweighs the embodied energy impact. Consequently, reducing the total environmental impact of the cases.

5.1.6 Thermal comfort

Each measure generates an overheating below the limit of 10 % and is illustrated in Figure 37, where the base case is illustrated as a red line for easier comparison. This can be explained by the implementation of natural ventilation and interior blinds in all cases. While the MVHR-system illustrated the most significant decrease in overheating of the analyzed measures, likely due to its increased airflow rate, which effectively extracted more hot air from the zone compared to before. On the contrary, insulating the façade illustrated the worst performance regarding overheating, which could be due to the insulation preventing heat transfer to the outdoor. When comparing the two insulation materials, EPS had the largest effect, possibly due to its smaller thermal conductivity. The HP-system had no impact on this metric, as it only affects the purchased energy, not the energy usage. Additionally, the effect from windows illustrated a small increase in overheating, similar to the façade insulation. This measure also reduces the transmission losses, thus less heat transferring from the zone. Similar to the façade insulation and replacing windows, the added roof insulation reduces the transmission losses. However, this measure also decreases overheating which could be due to the insulation preventing excess heating into the building.

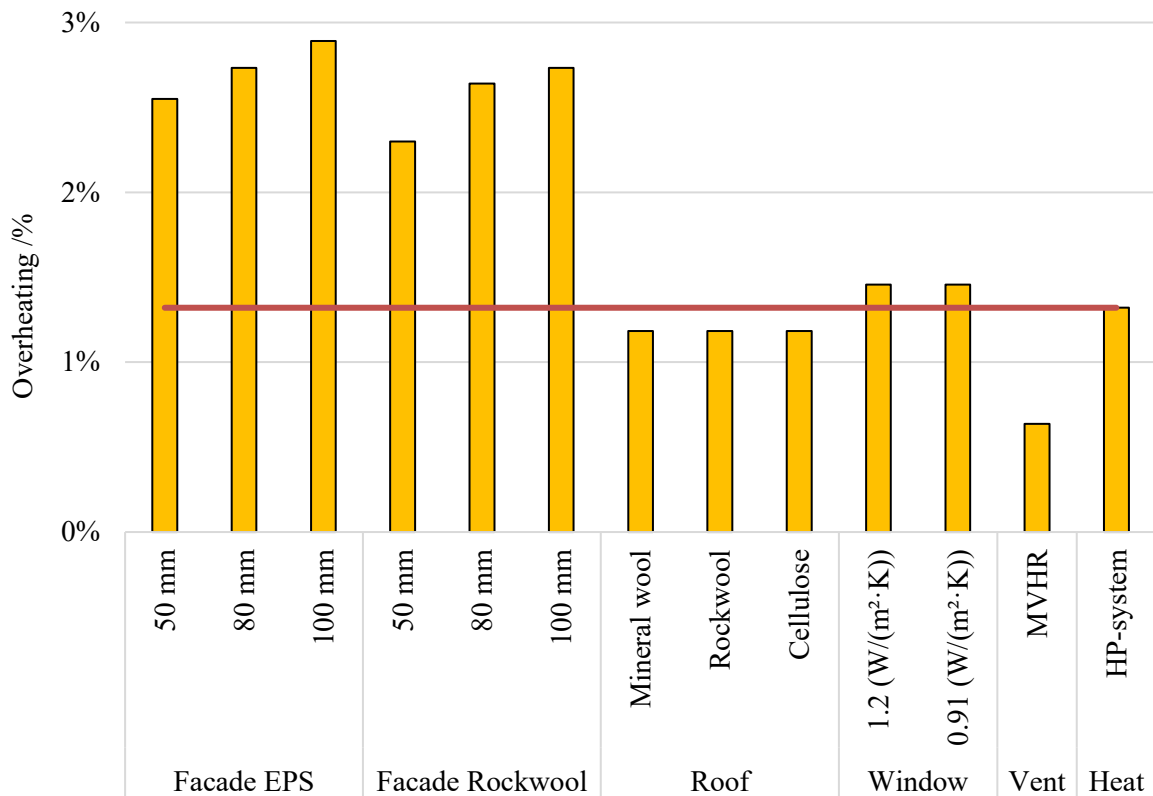


Figure 37. Overheating percentage of cases when a measure is applied individually compared to the base case.

Figure 38 illustrates the impact of all measures individually and in combination on the thermal comfort relative to the heat loss of the building in all 560 cases. The base case is illustrated as a line of reference considering the overheating. All cases exceeding the base case overheating consist of added façade insulation. This measure negatively affects the performance rendering the zone much hotter. However, the cases that only include an MVHR system and/or added roof insulation perform the best. Additionally, the results illustrate the possibility of decreasing heat loss in the building while still improving thermal comfort simultaneously. The three cases with the lowest overheating are highlighted in Figure 38, these cases are described further in Table 16.

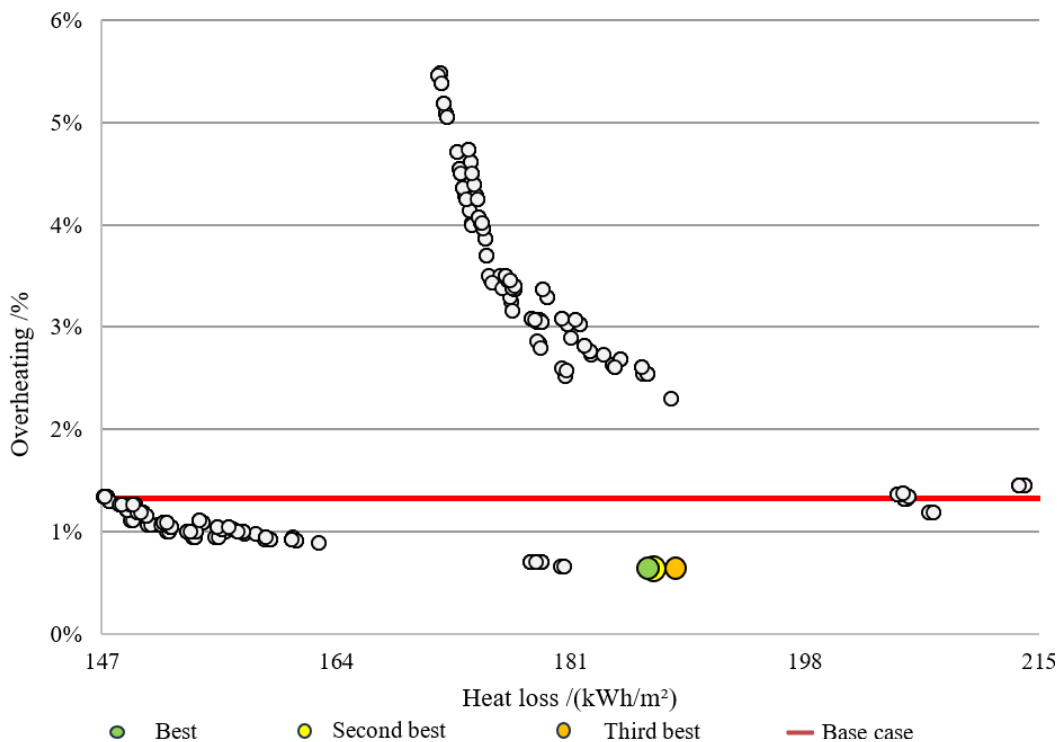


Figure 38. The overheating percentages of all cases in building A.

Table 16. The three best combinations of building A, regarding thermal comfort.

Rank	Façade insulation	Roof insulation	U-value window	Heating type	Ventilation type	Heat loss /(kWh/m ²)	Overheating /%
Best	-	-	-	-	MVHR	189	0.64
2 nd Best	-	-	1.2	-	MVHR	187	0.64
3 rd Best	-	-	0.91	-	MVHR	186	0.64

5.1.7 Summary

The best-performing cases across all analysis categories are presented in Table 17 to be further analyzed. Notably, the best-performing cases vary across categories, due to prioritization of different factors being analyzed in the categories. While analyzing LCA and operational energy, optimal cases emerged with the combination of cellulose insulation in the roof and 100 mm EPS insulation on the wall in addition to the utilization of HPs as a heat source. Moreover, cases with the highest energy reduction are the best performing cases within the analyzed category of LCA and operational energy. The roof insulation has proved to be very effective in all analysis categories since the best-performing cases in all categories have some type of roof insulation. Another measure proving to be effective in many categories is façade insulation where EPS is the preferred insulation type, due to its low environmental impact and cost. However, insulating the façade is not the best measure when thermal comfort is the main focus, the overheating in those cases is approximately 4 %, which is still below the requirement of 10 %, but higher than the base case, due to more heat getting trapped inside the building. Moreover, the MVHR system is a very good retrofitting option regarding thermal comfort, but it is not preferred in other categories, due to its high environmental impact and costs. An HP-system is also very beneficial due to its ability to reduce the purchased operational energy. Thus being a good option for energy efficiency and LCA, but when other factors are considered, it is not an optimal choice, due to high initial costs.

Table 17. Results summary for building A.

Rank	Façade insulation	Roof insulation	U-value window	Heat type	Vent type	Energy /(kWh/m ²)	NPV /(SEK/m ²)	LCA /(kg CO ₂ eq./m ²)	Overheating/ %
Annual purchased energy									
Best	100 mm EPS	Mineral wool	0.91	HP-syst	-	25.7	-1 280	82.6	5.5
2 nd Best	100 mm EPS	Rockwool	0.91	HP-syst	-	25.8	-1 310	88.4	5.5
3 rd Best	100 mm EPS	Mineral wool	1.2	HP-syst	-	25.9	-1 280	82.9	5.2
LCC									
Best	100 mm EPS	Mineral wool	-	-	-	102	495	293	4.1
2 nd Best	80 mm EPS	Mineral wool	-	-	-	103	486	297	3.5
3 rd Best	100 mm EPS	Cellulose	-	-	-	102	477	294	4
LCA									
Best	100 mm EPS	Cellulose	-	HP-system	-	26.9	-885	81.04	4
2 nd Best	80 mm EPS	Cellulose	-	HP-system	-	27.3	-877	81.06	3.4
3 rd Best	100 mm EPS	Cellulose	0.91	HP-system	-	25.9	-1 290	81.34	5.4
Overheating									
Best	-	-	-	-	MVHR	121	-1 394	391	0.64
2 nd Best	-	-	1.2	-	MVHR	122	-1 430	384	0.65
3 rd Best	-	-	0.91	-	MVHR	122	-1 410	383	0.66

5.2 Building B

5.2.1 Base case - simulation

Similar to building A, the heating for this building was relatively high in energy declaration. Further analysis of the energy bills revealed that the heating in the energy declaration included additional domestic hot water, and thus, that the performance of the building was better than stated in the declaration. Thus, separate energy bills were used for heating and DHW, when calculating the buildings' energy use.

The annual heating demand was simulated to $142 \text{ kWh/m}^2 A_{\text{temp}}$ which differentiated 13 % from the normalized annual heating demand of $164 \text{ kWh/m}^2 A_{\text{temp}}$. The comparison of monthly demand is illustrated in Figure 39, where December was the month with the highest difference between the simulated and actual normalized values, varying with approximately 5 kWh/m^2 , in general the rest of the months varied in a range of one to four kWh/m^2 .

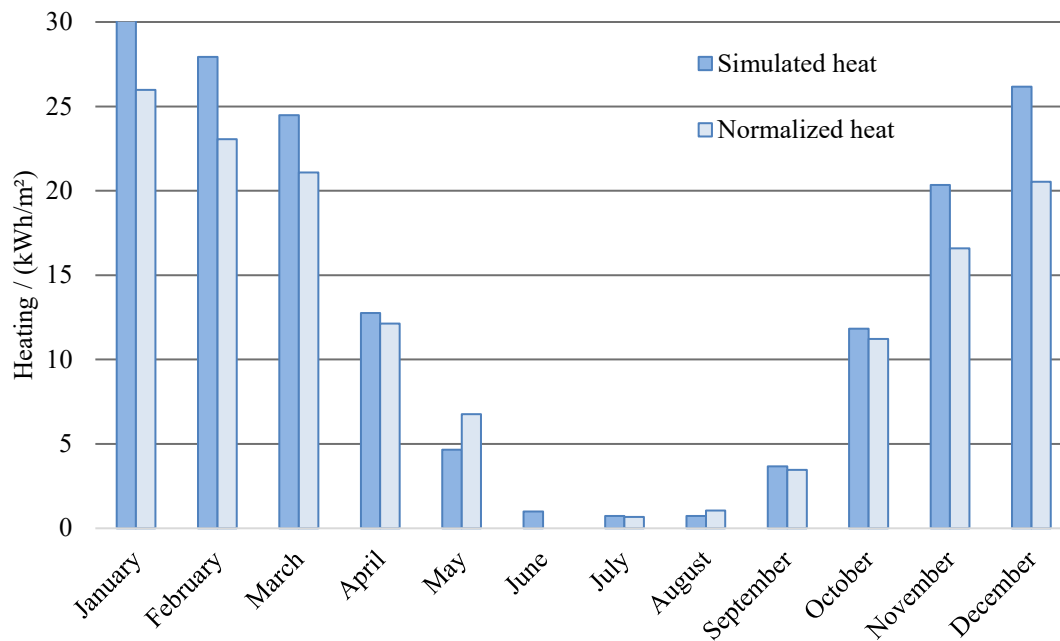


Figure 39. Monthly heating for the simulated model and the actual building B.

The breakdown of energy losses from the model of building B is illustrated in Figure 40. While the distribution resembles that of building A, the losses related to the building envelope were greater mainly due to the attic being heated with no insulation in the roof. Additionally, the window losses were also larger, because a higher proportion of building B's windows are old windows, which have not been replaced in the last 50 years.

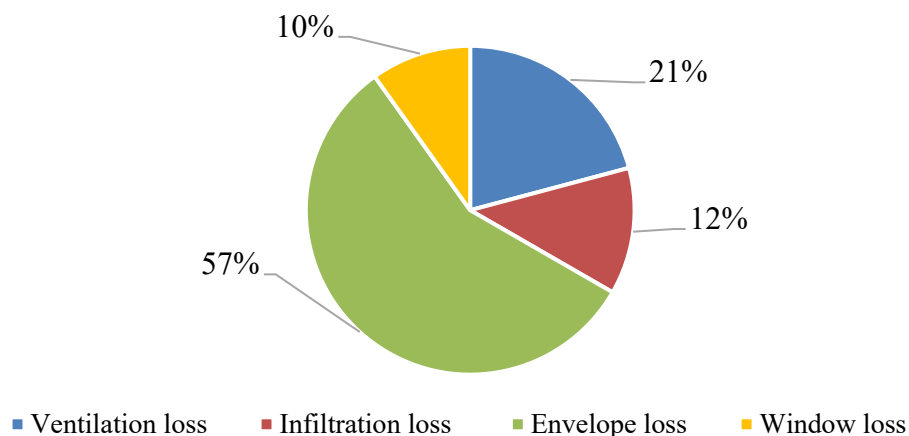


Figure 40. Distribution of heat losses from building B.

Moisture safety of current construction

The external walls of this building are also constructed with bricks, which is a material resistant to mold. The water content of the facade is illustrated in Figure 41, showing an initial increase until it reaches equilibrium after approximately four years. The increase indicates that the facade does not dry out, and in cases where the temperature in the facade drops below freezing point, there is a risk of frost damage, leading to increased costs due to potential repairs.

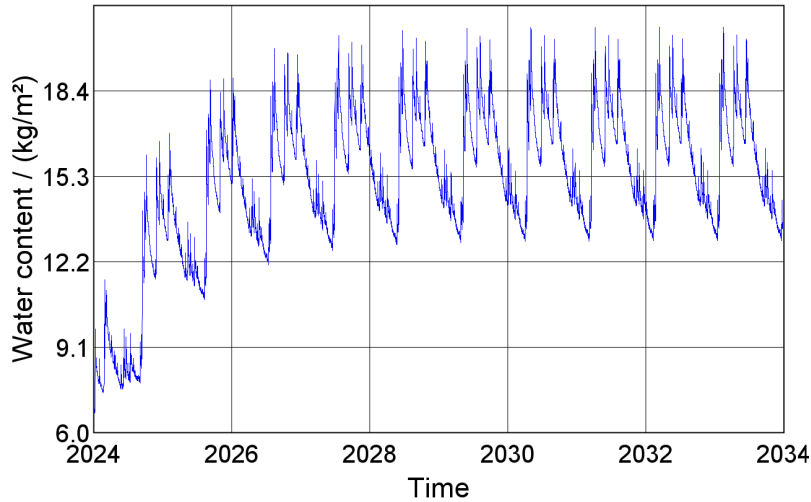


Figure 41. The water content of the base case façade construction, building B.

The roof construction consisting of wooden beams is susceptible to mold and to investigate its moisture safety a mold index analysis is done. The external part of the wooden beam layer was chosen for analysis, due to it being colder and any damage to it can lead to several problems, such as affecting its load-bearing capacity, and health risks. The mold index analysis results of that layer are illustrated in Figure 42. The result indicates that the construction is at risk of mold growth in the long-term.

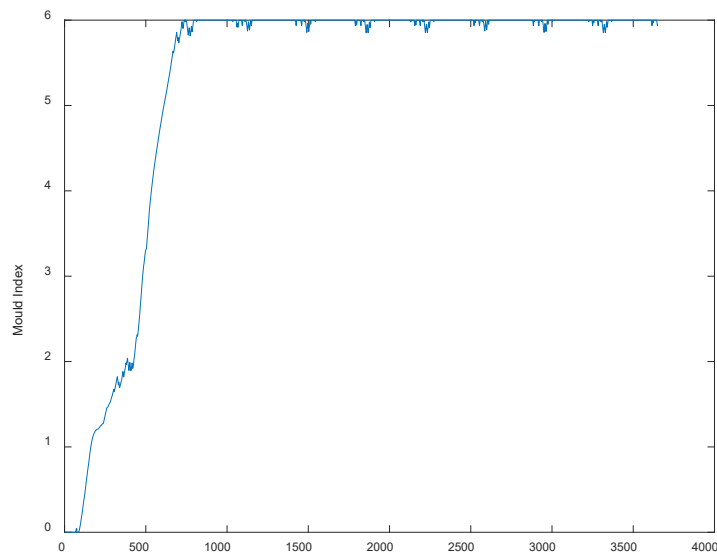


Figure 42. Mold index of the base case roof construction in building B.

5.2.2 Envelope & systems

To enhance the energy performance of the building envelope, the external walls in building B are improved using the same technique as building A. Given that buildings were located in similar climates it is reasonable to conclude that the enhanced external wall constructions are safe to use in building B as well, thus there were no analysis performed for this construction to building B. However, the roof in building B is insulated with 20 mm extra insulation, due to thicker wooden beams compared to building A. The improved roof constructions are analyzed regarding mold growth with the results presented in Figure 43. The results indicate that all the improvement options are moisture safe, as the maximum mold index observed across the options is 0.3, meaning minimal microscopic growth. Furthermore, this level of mold index is only present initially and decreases over time. Based on the results, the constructions could be described as moisture safe.

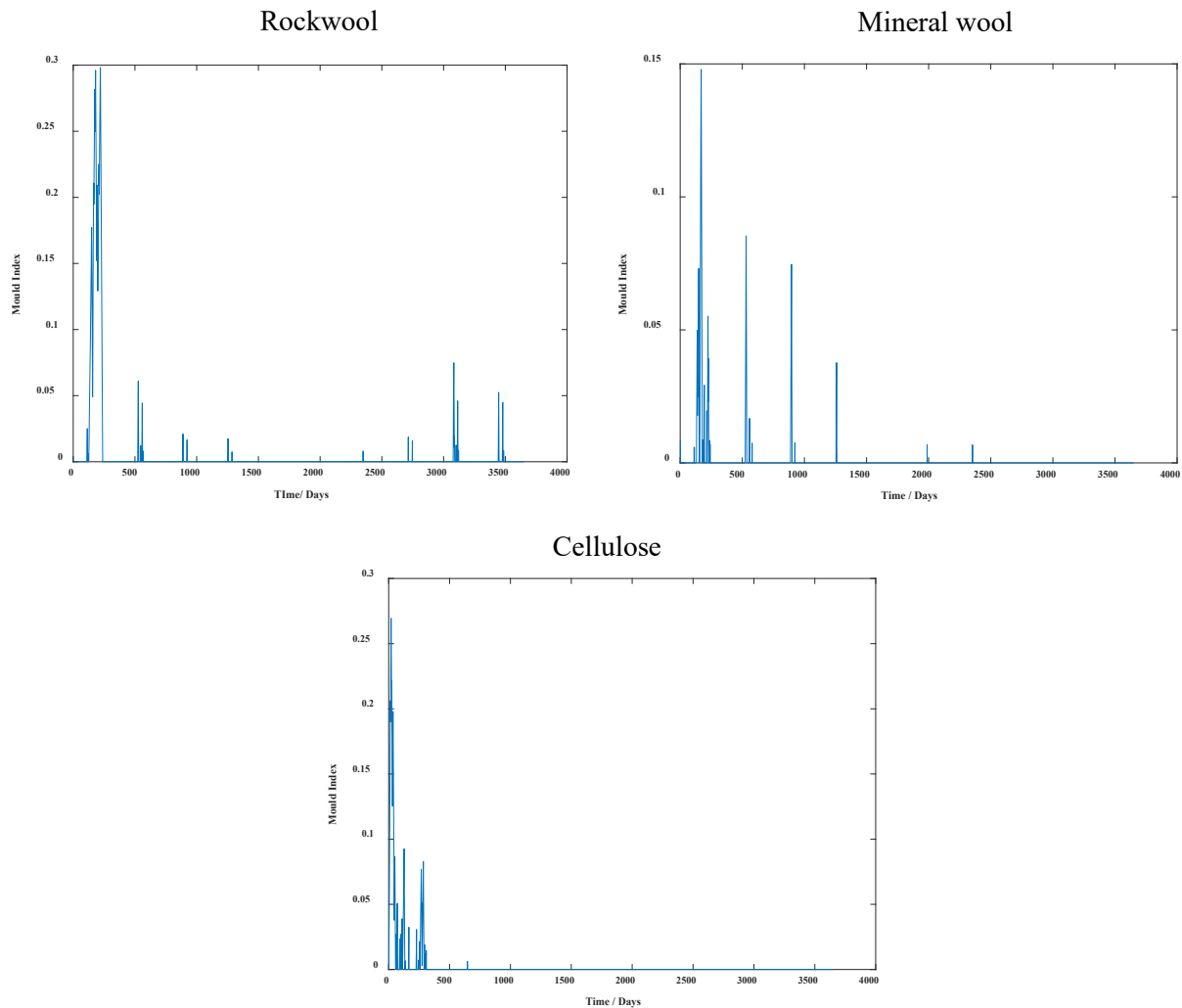


Figure 43. Mold index of the proposed roof constructions, building B.

Ventilation

The duct layout of the MVHR-system designed for building B is illustrated in Figure 44. The supply and return air ducts are represented by the colors blue and red respectively. The design of the system was done with both economic- and energy efficiency in mind. The air for building B was calculated to be 160 l/s, which equals 0.38 ($l/(s \cdot m^2)$). The supply-to-exhaust air ratio was calculated using a value of 1:1. Strategically, the AHU should have been placed at the same location as the AHU in building A, but since the attic area had been retrofitted into an apartment, the only available area left was the basement. The supply air system consists of 14 wall-mounted diffusers of the same size throughout the building, and while the exhaust air system also consists of 14 diffusers, half is wall mounted and the other half is mounted to the ceiling. Similar to the previous building the critical path for both supply and return systems is located on floor 1, highlighted in Figure 44. An overview of the supply and exhaust system sizing and balancing is provided in Appendix G.

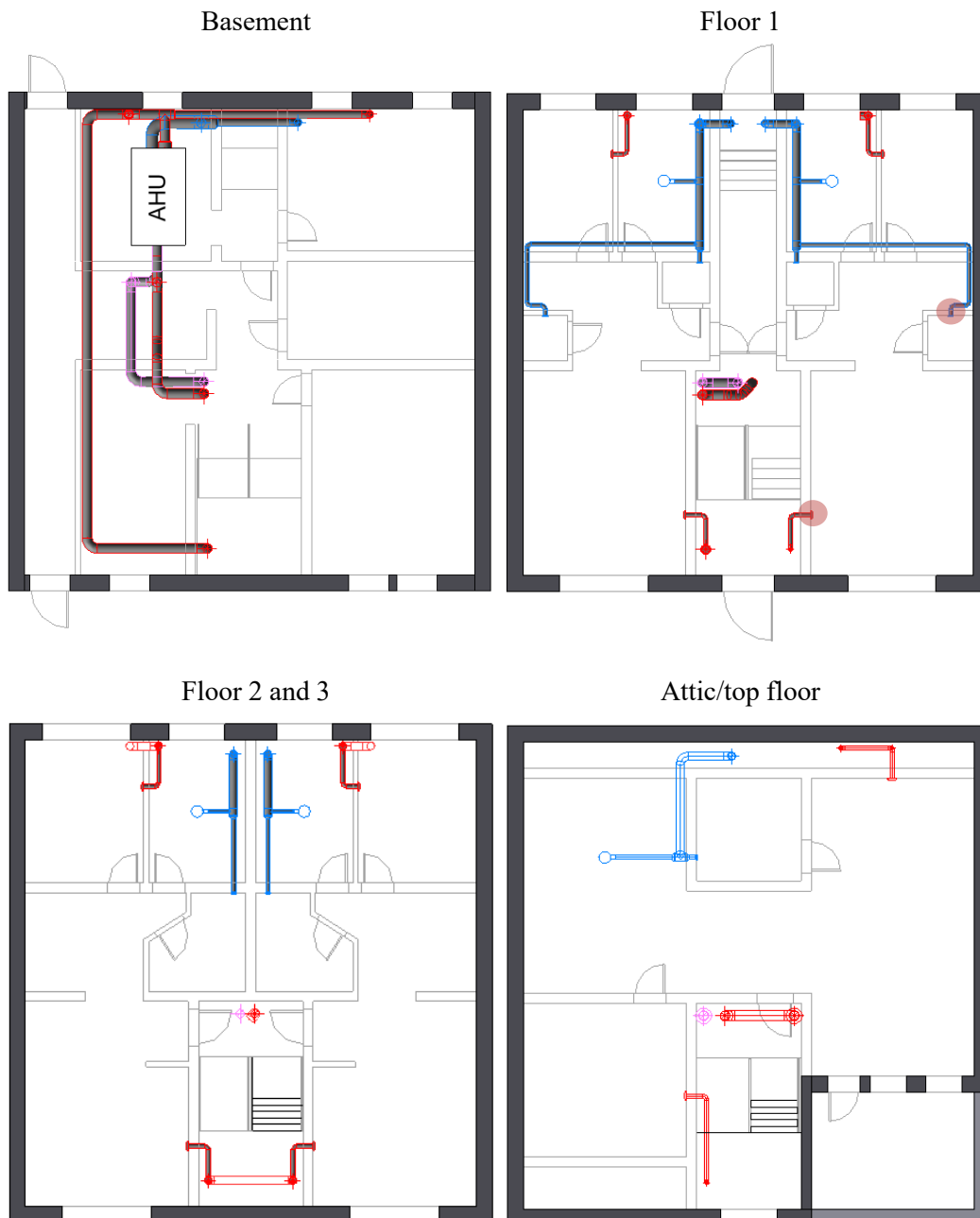


Figure 44. Plan view of the proposed ventilation system, building B.

To avoid intake of polluted exhaust air, the inlet and outlet were placed at a safe distance from each other, and the pressure drop between these two ducting systems and the AHU were calculated to 50 Pa and 62 Pa, for supply and exhaust respectively. The critical paths of the supply and extract systems were calculated to be 74 Pa and 32 Pa respectively. Using this information and the total airflow, an AHU was designed utilizing the ACON designer tool. The AHU consists of different components such as a heating coil with a power output of 3 kW, a plate heat exchanger with an 89 % counterflow heat recovery efficiency, and fans with an SFP of 0.85 kW/(m³·s). Introducing the MVHR-system leads to additional energy use due to the operation of fans and the heating coil. The annual energy use of the ventilation system amounts to 2 200 kWh, where all the energy is supplied by electricity.

Heating system

The new heating system was designed to cover 70 % of the highest peak load scenario, which is the base case, requiring a heating peak load of 21.5 kW and an additional 3.5 kW for DHW. This new system contained new radiators and pipe systems, air-to-water HPs, and circulation pumps, but not an accumulator tank. Three HPs (NIBE S2125) were selected, consisting of one with a size of 12 kW and two at 8 kW each, collectively satisfying the building's peak power demand of 25 kW. Each HP was connected to an indoor combi tank (NIBE

VVM S325) each with a volume capacity of 172 liters, sufficing the calculated peak volume of 500 liters. The critical path was calculated and together with the calculated mass flow rate was used when choosing the circulation pumps. Similar to Building A, two circulation pumps were chosen to circulate the water (Grundfos Magna3 40-120 F).

Similar to building B, the simulated cases with the proposed heating system used a COP of 3.8 for heating and DHW. The COP was based on data gathered from the manufacturer, based on the climate in which the buildings were located. The heat distribution to the rooms was done through copper pipes connected to radiators which were strategically placed under the windows in rooms requiring heating, to mitigate cold draught. The new heating system was designed to reduce energy use by effectively performing low-temperature heating with a supply water temperature of 49° C and a return mean water temperature of 43° C. The size of the radiators was selected based on the simulated heating demand of each room. The radiator and piping layout adhered to the same layout and design as the existing DH system. Detailed information regarding radiator piping and balancing can be seen in Figure 61 in Appendix H.

5.2.3 Energy

The retrofitting measures were implemented both individually and in combination with each other. Figure 45 illustrates the individual effects of each measure on purchased annual energy and peak load. An analysis of the results reveals that the most significant reduction in purchased energy is achieved by implementing an HP-system. However, this did not affect the losses or the total energy use of the building, keeping the peak load unchanged. On the contrary, installing new windows led to the smallest reduction in purchased energy, also reducing peak load marginally. The reduced peak load when installing MVHR-system was a result of reduced ventilation losses and heat recovery. The largest reduction of peak load was achieved by adding insulation on the roof, which could be explained by the combining surface area and reduced U -value.

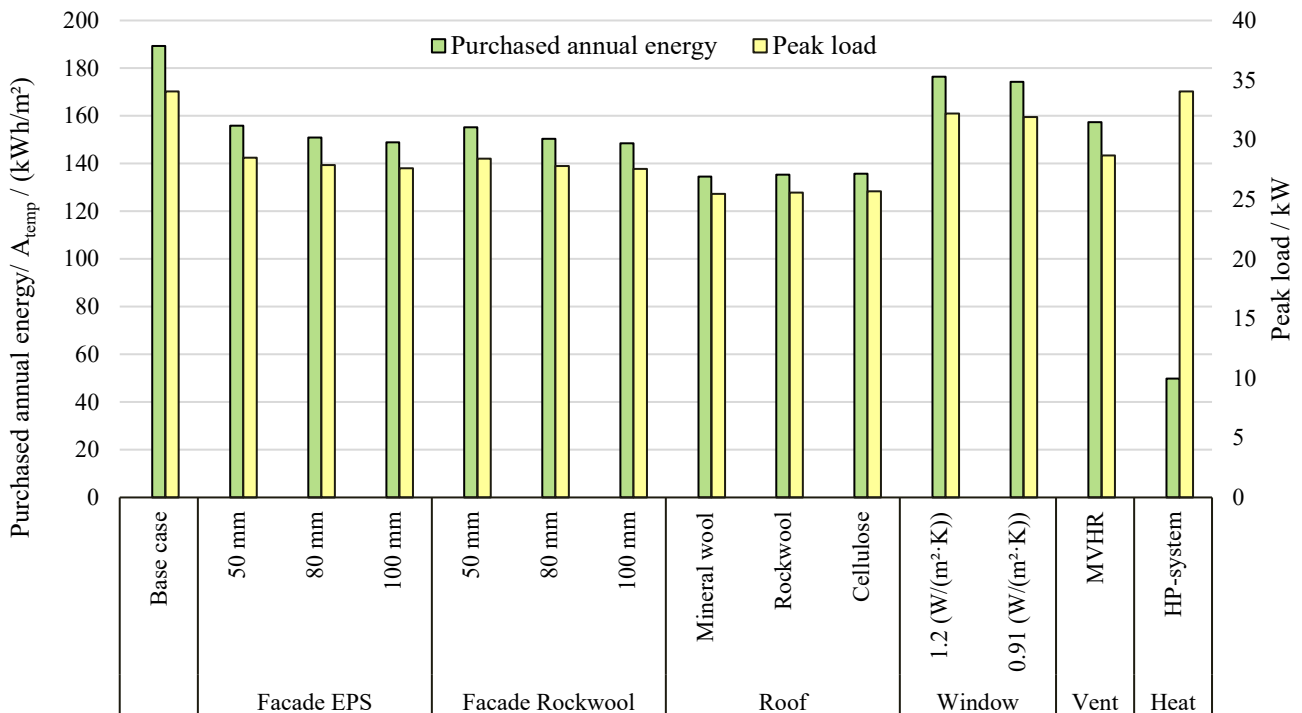


Figure 45. Purchased annual energy and peak load of each measure individually, for building B.

Figure 46 illustrates the purchased annual energy use and peak load for all 560 cases. A clear trend is visible in the results, primarily due to the type of heating system. Implementation of the HP-system decreases the purchased energy for a case, but the building's heating peak load remains unchanged. However, integrating an MVHR system decreases the heating peak load and annual energy use of the building. Similar conclusions can be drawn for other measures. Moreover, the effect of an improvement is much more visible if the DH system is in use than if the HP-system is used. Because the effects of other measures are quite low in comparison to the effect of the HP-system itself on the purchased annual energy. The three cases with the lowest annual purchased

energy are highlighted with corresponding colors in Table 18, note that the “-“ refers to no alteration being made.

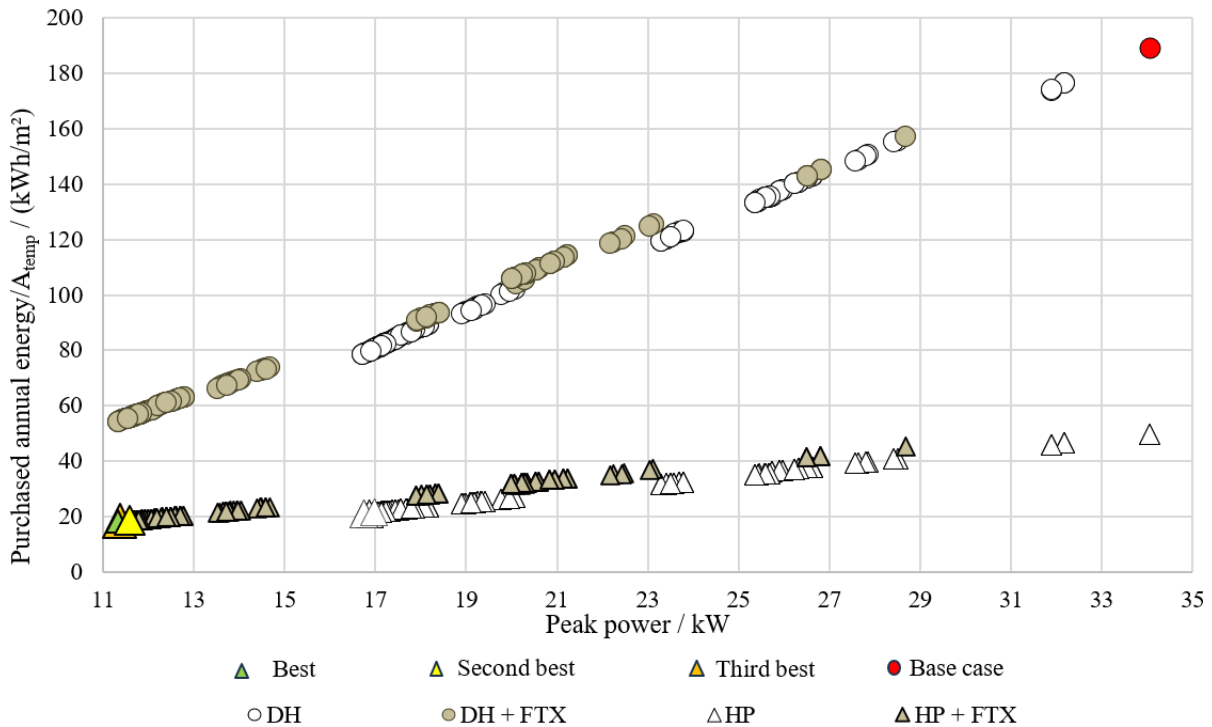


Figure 46. Purchased annual energy use and peak power for all 560 cases in building B.

Table 18. The three best combinations for building B, regarding energy use.

Rank	Façade insulation	Roof insulation	U-value window	Heating type	Ventilation type	Energy use / (kWh/(m ² A _{temp} ·y))
Best	100 mm RW	Mineral wool	0.91	HP-syst	MVHR	18.1
2 nd Best	100 mm RW	Mineral wool	0.91- Alu	HP-syst	MVHR	18.1
3 rd Best	100 mm EPS	Mineral wool	0.91	HP-syst	-	18.2
Base case	-	-	-	-	-	189

The results highlight that the most effective approach for reducing purchased energy is to implement all the measures together, forming a combination of mineral wool as roof insulation, 100 mm of different facade insulations, new windows with a U -value of 0.91 (W/(m²·K)), HP-system, and an MVHR system. The results indicate that using an HP-system together with an MVHR-system decreases both the energy use and peak load of the cases, which makes them a good choice when energy efficiency is the focus.

5.2.4 LCC

Figure 47 illustrates the initial cost of each measure in addition to the net present value of the investment, containing initial costs and maintenance-related costs. A more detailed cost breakdown, including their sources, is provided in Appendix I.

According to the results, insulating the roof had the lowest cost, while installing a new heating system with HP had the highest cost, followed by the installation of a new MVHR-system. While designing the new heating system, all system components were renewed, which is costly. Additionally, the design of the new heating system is based on a worst-case scenario, having the highest heating peak load, resulting in an oversized heating system for cases with a lower peak load.

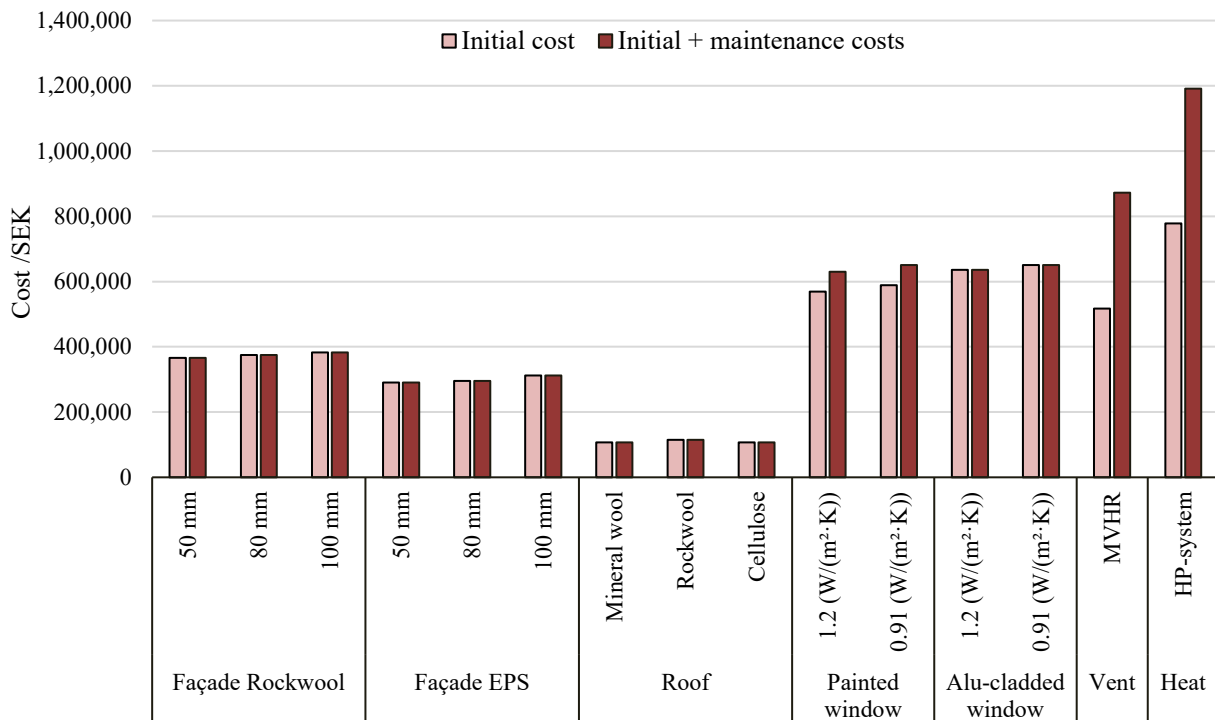


Figure 47. Cost for both initial and initial + maintenance for each measure individually.

The total NPV of all 560 combinations is presented in Figure 48 with their total investment costs. The NPV varies from -4 000 SEK/m²A_{temp} to 1 900 SEK/m²A_{temp} with most cases being negative. Interestingly, the cases that include MVHR-system or HP-system display a negative NPV, due to high investment costs in these cases, making the saving from operational energy not sufficient. The three most profitable cases are highlighted in Figure 48 and described further in Table 19.

The best performing cases from an LCC perspective have a combination of EPS façade insulation with different thicknesses, and different roof insulation, with no additional measure. The positive results in this case indicate that the saved operational costs outweigh the costs.

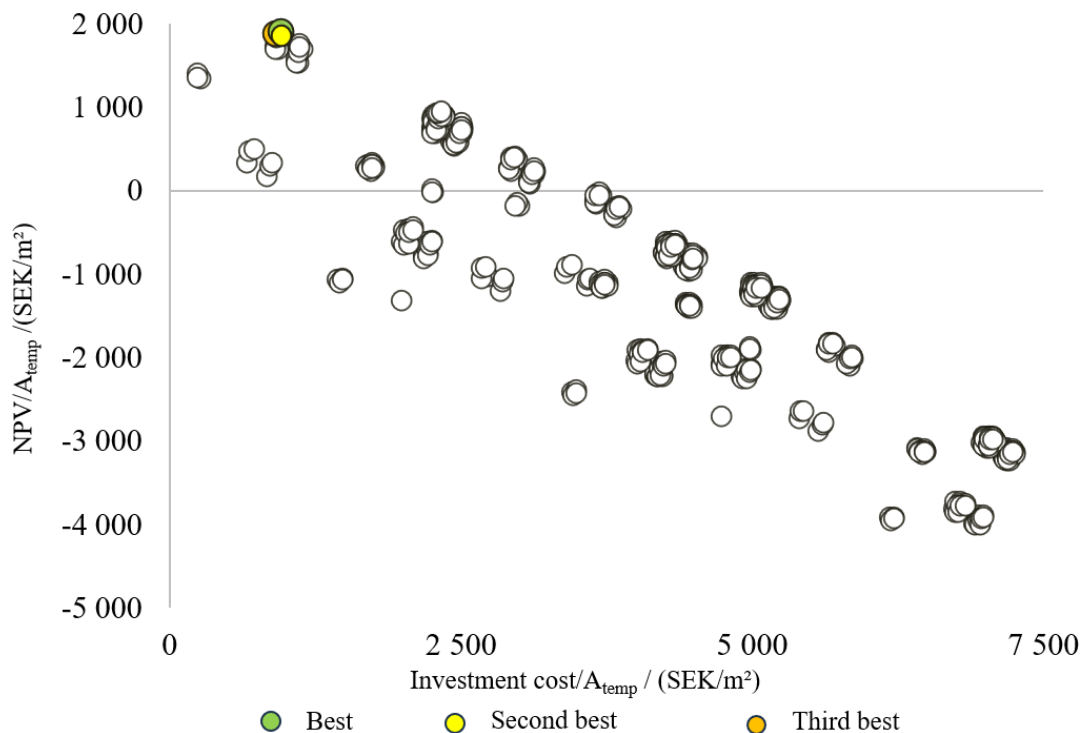


Figure 48. NPV and total investment cost for all 560 cases in building B.

Table 19. The three best combinations for building B, regarding NPV.

Rank	Façade insulation	Roof insulation	U-value window	Heating type	Ventilation type	Invest. cost /((SEK/m ² A _{temp}))	NPV /((SEK/m ² A _{temp}))
Best	100 mm EPS	Mineral wool	-	-	-	962	1 890
2 nd Best	80 mm EPS	Mineral wool	-	-	-	925	1 870
3 rd Best	100 mm EPS	Cellulose	-	-	-	961	1 860

Sensitivity analysis- Interest rates

The same scenarios used in building A were used to conduct the sensitivity analysis for the life cycle costs of retrofitting for building B. The effect of varying interest rates of 1 % and 7 % are investigated in scenarios 2 and 3 respectively, with the condition of maintaining a constant nominal price change rate of 2 % and electricity prices for the year 2022. The results of this sensitivity analysis are presented in Figure 49 and Figure 50, and the best-performing cases in these scenarios are described in Table 20.

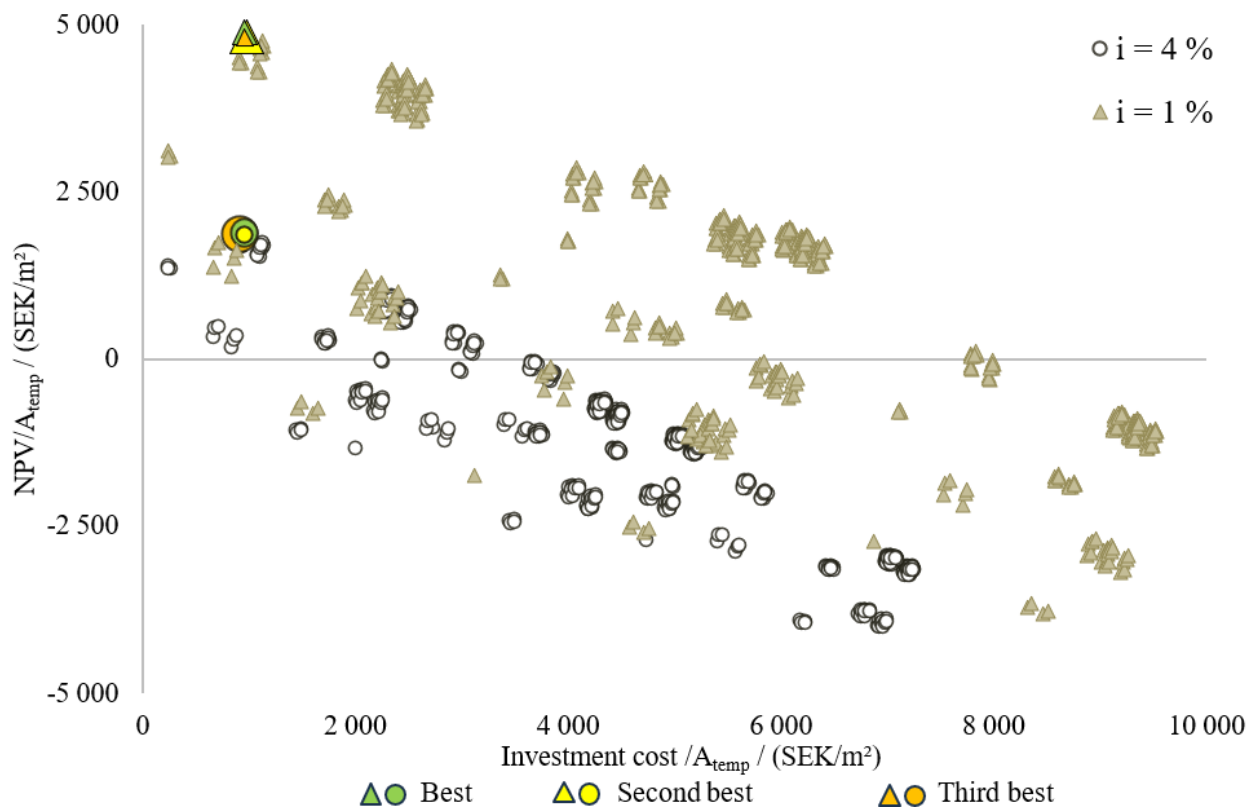


Figure 49. Scenario 2 and base scenario- Sensitivity analysis with interest rates of 1 % and 4 %.

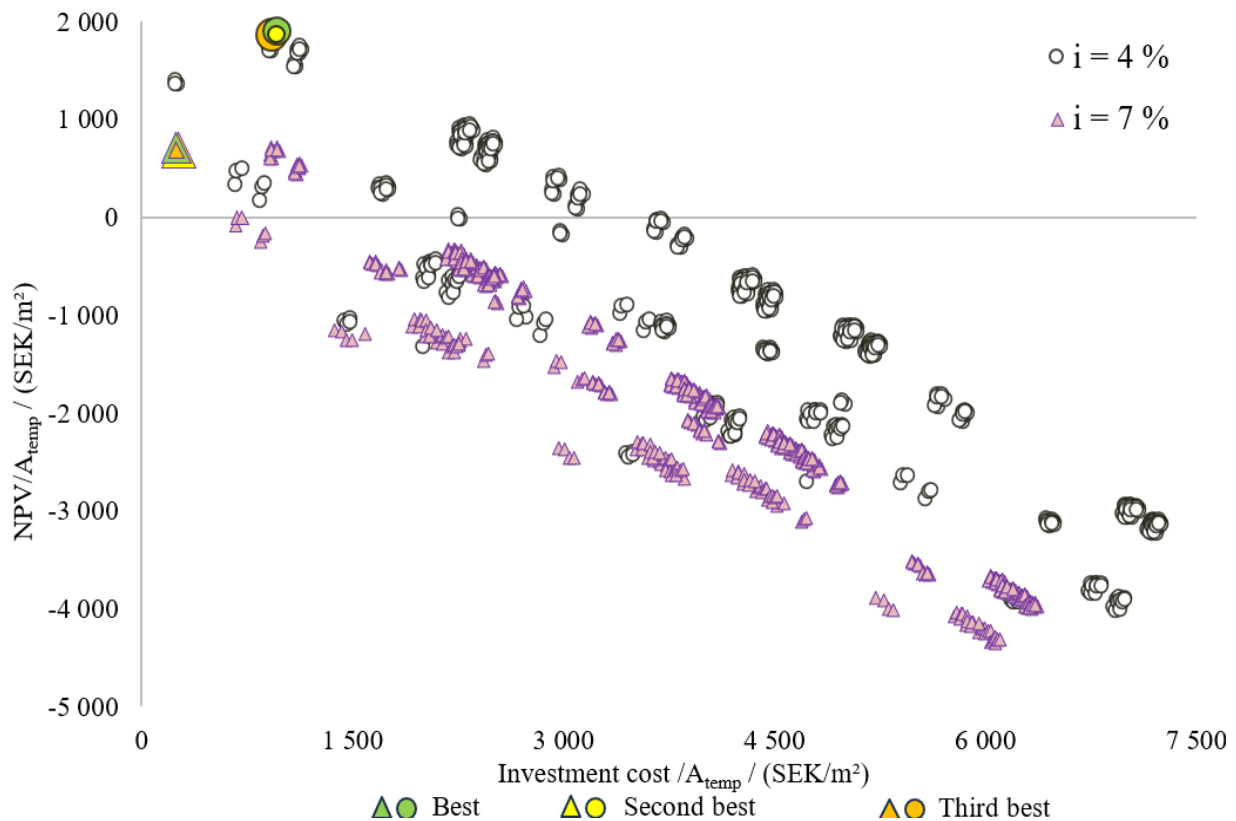


Figure 50. Scenario 3 and base scenario- Sensitivity analysis with interest rates of 1 % and 7 %.

As shown in Figure 49 and Figure 50, both the profitability and investment costs of a case increase with lower interest rates and decrease when the interest rates are increasing, meaning that when the interest rate is 1 %, the majority of cases are profitable. However, with a 7 % interest rate only a few cases are profitable.

Table 20. The three best combinations for building B of the base scenario and scenarios 2 & 3, regarding NPV.

Rank	Façade insulation	Roof insulation	U-value window	Heating type	Ventilation type	Invest. cost / (SEK/m ² A _{temp})	NPV / (SEK/m ² A _{temp})
Base scenario							
(Interest rate 4 %)							
Best	100 mm EPS	Mineral wool	-	-	-	962	1 890
2 nd Best	80 mm EPS	Mineral wool	-	-	-	925	1 870
3 rd Best	100 mm EPS	Cellulose	-	-	-	961	1 860
Scenario 2							
(Interest rate 1 %)							
Best	100 mm EPS	Mineral wool	-	-	-	962	4 890
2 nd Best	100 mm EPS	Rockwool	-	-	-	979	4 820
3 rd Best	100 mm EPS	Cellulose	-	-	-	961	4 810
Scenario 3							
(Interest rate 7 %)							
Best	-	Mineral wool	-	-	-	246	712
2 nd Best	80 mm EPS	Mineral wool	-	-	-	925	710
3 rd Best	100 mm EPS	Mineral wool	-	-	-	962	708

A common factor of the results in scenarios 2 and 3 is the combinations of façade and roof insulations. The roof insulation that is mostly used in the best cases is mineral wool, while the best insulation option for the façade is different thicknesses of EPS insulation. Moreover, the results indicate that the high investment cost of new windows, the HP-system and MVHR-system prevents them from being a viable alternative.

Sensitivity analysis - Energy prices

Scenarios 4 and 5 define the 1 120 cases formed, based on the condition of having a constant nominal price change rate of 2 % and, a nominal interest rate of 4 %, but the different price for the energy compared to the year 2022 with a 30 % decrease and increase respectively. The results of the sensitivity analysis with different energy prices are shown in Figure 51 and Figure 52, where all cases in scenarios 4 and 5 are shown in comparison to the base scenario.

In the scenarios with higher energy prices, cases with higher energy savings will be more profitable, resulting in a higher NPV, while lower energy prices lead to a lower total NPV. The three cases with the highest profitability are highlighted in Figure 51 and Figure 52 and described further in Table 21.

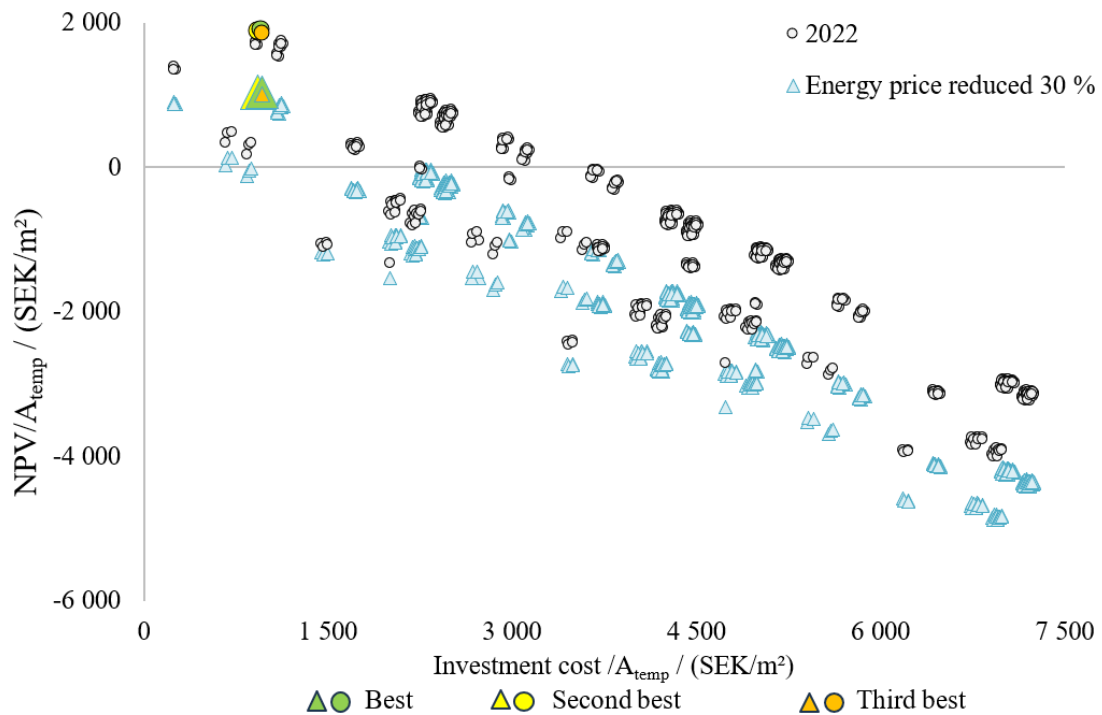


Figure 51. Scenario 4 and base scenario - Sensitivity analysis with electricity price for 2022 and 30 % reduced prices.

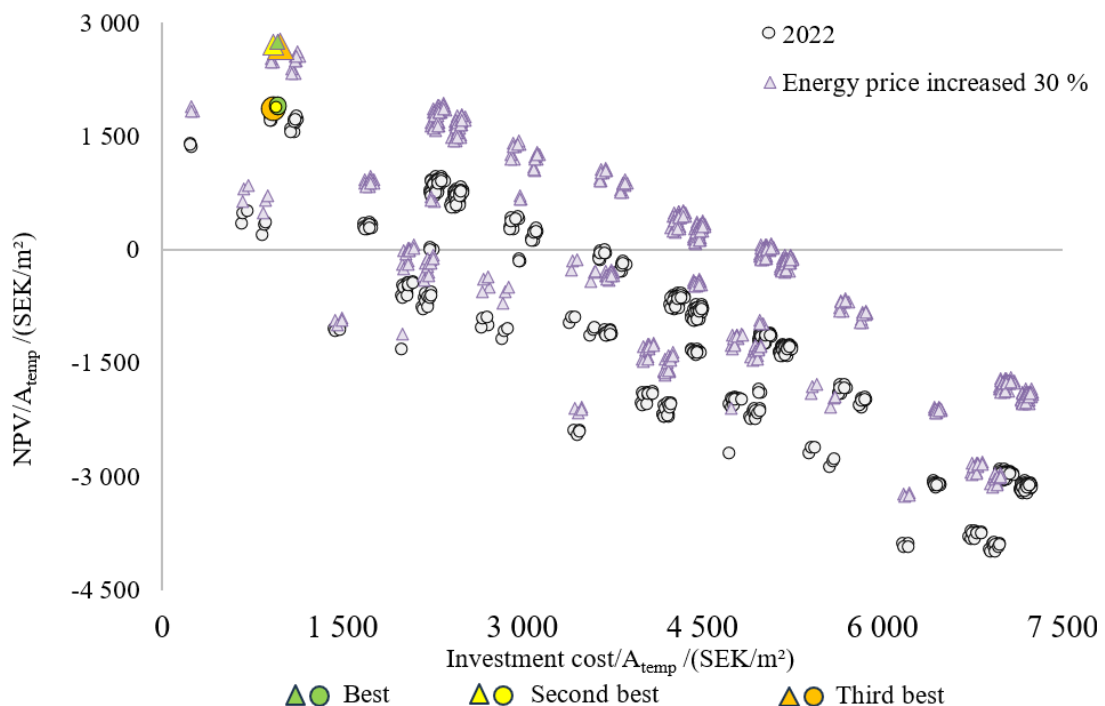


Figure 52. Scenario 5 and base scenario - Sensitivity analysis with electricity price for 2022 and 30 % increased prices.

Table 21. The three best combinations for building B of the base scenario and scenarios 4 & 5, regarding NPV.

Rank	Façade insulation	Roof insulation	U-value window	Heating type	Ventilation type	Invest. cost /((SEK/m ² A _{temp}))	NPV /((SEK/m ² A _{temp}))
Base scenario (energy price 2022)							
Best	100 mm EPS	Mineral wool	-	-	-	962	1 890
2 nd Best	80 mm EPS	Mineral wool	-	-	-	925	1 870
3 rd Best	100 mm EPS	Cellulose	-	-	-	961	1 860
Scenario 4 (30% reduced energy price)							
Best	100 mm EPS	Mineral wool	-	-	-	962	1 040
2 nd Best	80 mm EPS	Mineral wool	-	-	-	925	1 030
3 rd Best	100 mm EPS	Cellulose	-	-	-	961	1 010
Scenario 5 (30% increased energy price)							
Best	100 mm EPS	Mineral wool	-	-	-	962	2 750
2 nd Best	80 mm EPS	Mineral wool	-	-	-	925	2 710
3 rd Best	100 mm EPS	Cellulose	-	-	-	961	2 700

As illustrated in Table 21, the variations in energy prices do not affect the investment costs, therefore, the cases maintain the same investment costs across these scenarios. Notably, the best cases evaluated based on total NPV remain unchanged across scenarios 4, 5, and the base scenario. These involve combinations of different EPS insulation thicknesses for the façade paired with different roof insulation types, without incorporating other measures. This leads to the conclusion that façade insulation using EPS with thicknesses of 80 mm and 100 mm and roof insulation of mineral wool or cellulose are the most viable options across all scenarios.

5.2.5 LCA

The embodied GWP-GHG of all the investigated measures when implemented separately are presented in Figure 53. The results indicate that the HP-system demonstrates the highest individual impact, followed by the ventilation system, while adding cellulose insulation on the roof had the lowest individual impact. The reason could be that cellulose is mostly made of recycled waste materials, preventing extraction of new raw materials, and leading to less embodied impact for the measure. Among the insulation options categories, rockwool insulation registers the highest individual impact both in façade and roof construction. It is worth noting that the environmental impact of the HP-system is overestimated in most cases since the system is designed to cover the demand of the case with the highest peak load. A smaller system could have been designed for the cases with a smaller peak load, resulting in a lower embodied energy impact.

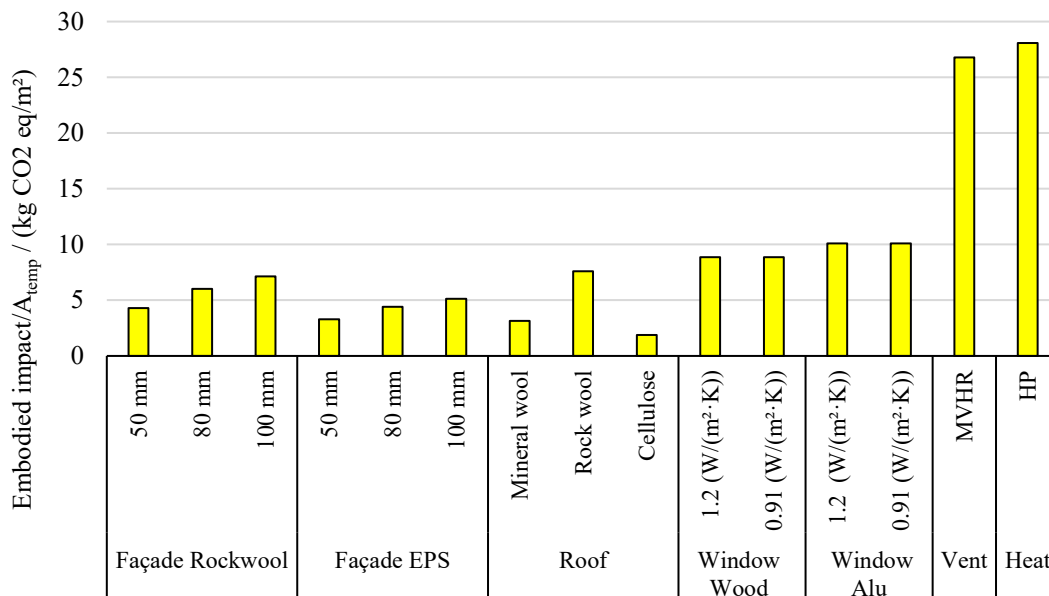


Figure 53. Embodied impact of different individual measures, building B.

Figure 54 depicts all the combinations and their environmental impact with the amount of annual purchased operational energy. The base case is presented by the case with the highest environmental impact. The total impact from the base case consists only of operational energy impacts since there are no additional materials used in the base case, thus no embodied impacts are included, meaning this is an underestimation of the impact from the base case. As shown in Figure 54, all cases lead to a reduction of environmental impacts in comparison to the base case which is due to the reduced operational energy impacts as a result of energy-reducing improvements. The three cases with the lowest environmental impact are highlighted in Figure 54, these cases are described further in Table 22.

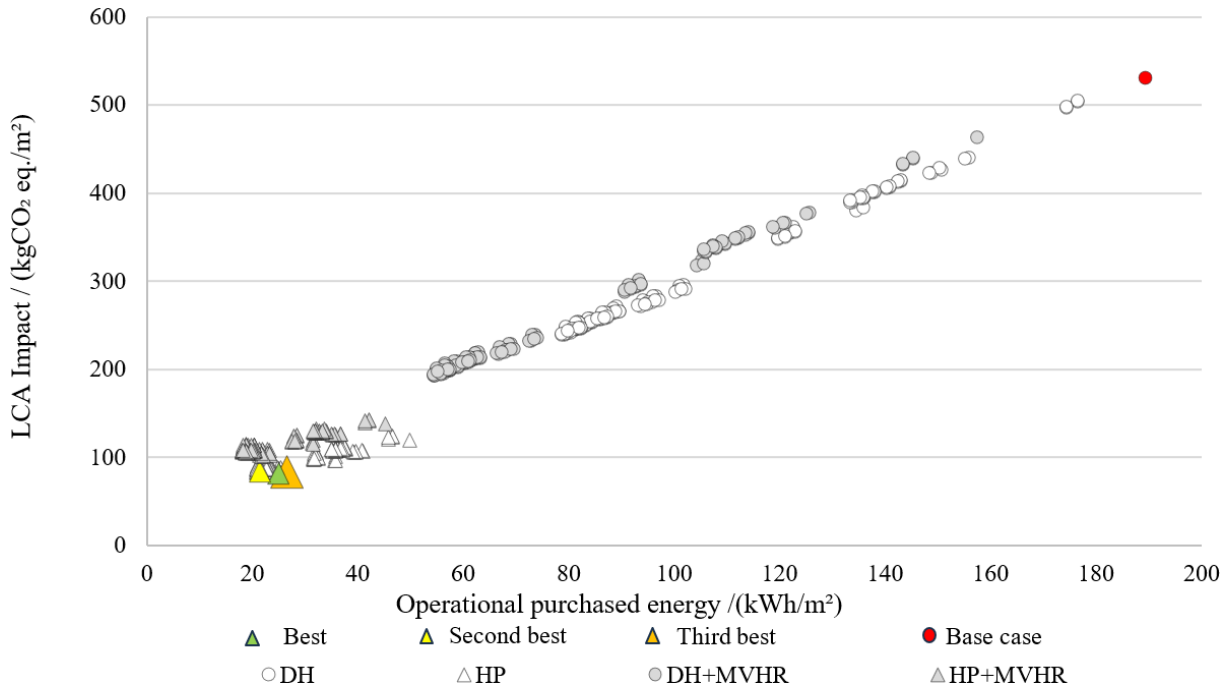


Figure 54. Total environmental impact and purchased operational energy of different cases in building B.

Table 22. The three best combinations for building B, regarding environmental impact.

Rank	Façade insulation	Roof insulation	U-value window	Heating type	Ventilation type	LCA-impact / (kg CO ₂ eq. /m ² A _{temp})
Best	100 mm EPS	Cellulose	-	HP-system	-	81.4
2 nd Best	80 mm EPS	Cellulose	-	HP-system	-	81.6
3 rd Best	100 mm EPS	Mineral wool	-	HP-system	-	82.0
Base case	-	-	-	-	-	530

Analyzing the results, a pattern emerges indicating that cases involving roof insulation, especially the cellulose insulation and EPS insulation on the façade with HPs as a heat source, have a lower environmental impact than other cases. These cases consist of combinations where the reduction in the operational energy impact surpasses the embodied energy impact. Likewise, similar to the results for building A, the cases in building B also exhibit a generally higher environmental impact when a mechanical ventilation system is used in combination with HPs, primarily due to the high embodied impact associated with the MVHR system, which is less than the impact reductions from the saved energy. Consequently, installing a mechanical ventilation system is a less desirable measure from an environmental standpoint.

5.2.6 Thermal comfort

Unlike the thermal comfort of building A, this building illustrates a base case above the overheating threshold of 10 %, which is illustrated as a red line in Figure 55. A vast difference between the analyzed zone in this building and the zone in Building A is the locations relative to the floors. While this zone is located on the top floor with exterior air surrounding it, the zone in Building A had a cold attic above it. Similar to the results in Building A, the MVHR-system illustrated the most significant decrease in overheating, likely due to its increased airflow rate, whilst insulating the façade illustrated the worst performance regarding overheating.

Comparing rockwool and EPS, the latter had the largest effect, possibly due to its smaller thermal conductivity. The HP-system had no impact on this metric, as it only affects the purchased energy, not the energy usage. Additionally, the effect from windows illustrated a small increase in overheating, like the façade insulation this measure also reduces the transmission losses. Similar to the roof insulation in Building A, this building also experiences a reduction of overheating when implementing roof insulation, which could be explained by the prevention of heat transfer into the building.

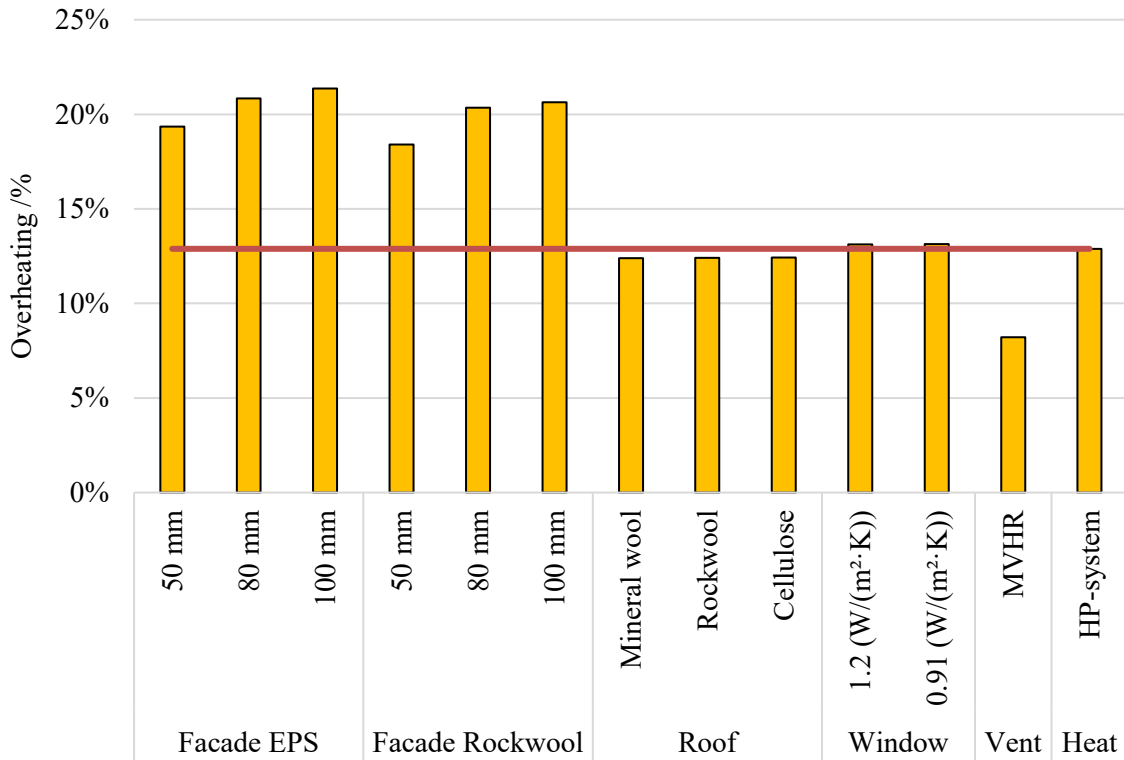


Figure 55. Overheating percentage of cases when a measure is applied individually compared to the base case.

In Figure 56 the base case is illustrated as a line of reference regarding overheating, and each measure both individually and in combination is illustrated regarding its impact on thermal comfort for each of the 560 cases. As illustrated, none of the cases is below the threshold of 10 % overheating. A total of 23 cases are performing better compared to the base case, all of which consist of MVHR. Some cases also consist of new windows and/or added roof insulation. Additionally, the results illustrate the possibility of decreasing heat loss in the building while still improving thermal comfort simultaneously. The three cases with the lowest overheating are highlighted in Figure 56, these cases are described further in Table 23.

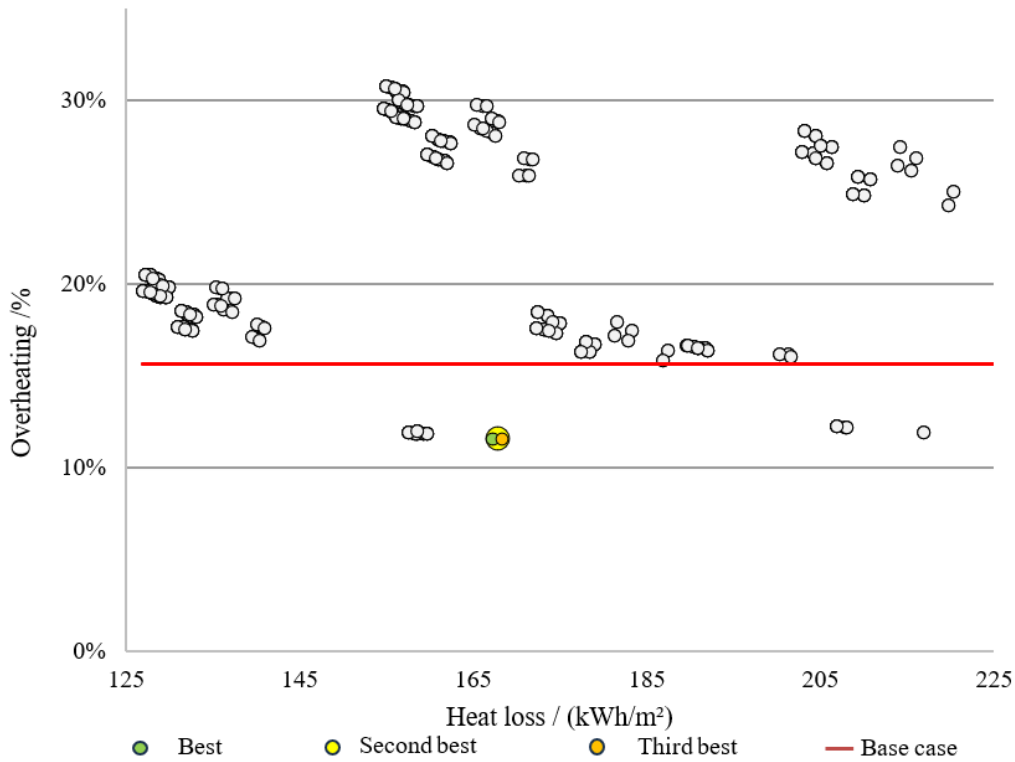


Figure 56. The overheating percentages of all cases, building B.

Table 23. The three best combinations for building B, regarding thermal comfort.

Rank	Façade insulation	Roof insulation	U-value window	Heating type	Ventilation type	Heat loss / (kWh/m ²)	Overheating /%
Best	-	Mineral wool	-	-	MVHR	167	11.54
2 nd Best	-	Rockwool	-	-	MVHR	168	11.57
3 rd Best	-	Cellulose	-	-	MVHR	169	11.57

5.2.7 Summary

The best-performing cases across all analyzed categories are presented in Table 24 to be further analyzed. Similar to Building A, the best cases in building B are different across the categories, dependent on different factors being analyzed. While analyzing operational energy and LCA, the optimal cases consisted of combinations that significantly reduced the operational energy, leading to a reduction in operational energy impacts as well. The roof insulation proved to be very effective in all analysis categories since the best-performing cases in all categories have some type of roof insulation. Another measure proving to be effective in many categories is façade insulation, where EPS is the preferred insulation type due to its low environmental impact and initial cost. However, insulating the façade is not the best measure if the main focus is thermal comfort.

In contrast to building A, none of the measures in this building have an overheating below 10% and the best-performing cases in other analysis categories have an overheating of 19 % to 30 %, which could be explained by the cold attic above the analyzed zone in building A, while the analyzed zone in building B had outdoor air above it, which means it got more solar gains during the summer. Moreover, the MVHR-system and roof insulation are a very good retrofitting option regarding thermal comfort. With mineral wool insulation on the roof and an MVHR system, a positive NPV can also be achieved, however, the environmental impact of these measures is quite high, making them less desirable from an environmental perspective. The measure of installing a new HP-system is effective for reducing the purchased energy and environmental impact, however, it is not part of the best cases if economic efficiency is considered.

Table 24. Results summary for building B.

Rank	Façade insulation	Roof insulation	U-value window	Heat. type	Vent. type	Energy /(kWh/m^2)	NPV /(SEK/m^2)	LCA /($\text{kgCO}_2\text{eq.}/\text{m}^2$)	Overheating /%
Annual purchased energy									
Best	100 mm RW	Mineral wool	0.91-Alu	HP-syst	MVHR	18.1	- 3 120	109	19.6
2 nd Best	100 mm RW	Mineral wool	0.91	HP-syst	MVHR	18.1	- 3 100	108	19.6
3 rd Best	100 mm EPS	Mineral wool	0.91	HP-syst	MVHR	18.2	- 2 940	106	20.5
LCC									
Best	100 mm EPS	Mineral wool	-	-	-	94	1 890	271	29.8
2 nd Best	80 mm EPS	Mineral wool	-	-	-	96	1 870	276	29
3 rd Best	100 mm EPS	Cellulose	-	-	-	95	1 860	273	29.6
LCA									
Best	100 mm EPS	Cellulose	-	HP-syst	-	25.0	-52	81.6	29.6
2 nd Best	80 mm EPS	Cellulose	-	HP-syst	-	25.6	-56	81.6	28.8
3 rd Best	100 mm EPS	Mineral wool	-	HP-syst	-	24.7	-28	82.0	29.8
Overheating									
Best	-	Mineral wool	-	-	MVHR	104	12	116	11.54
2 nd Best	-	Rockwool	-	-	MVHR	105	- 29	121	11.56
3 rd Best	-	Cellulose	-	-	MVHR	106	- 23	115	11.57

6 Conclusions

Given the need for retrofitting a portion of the building stock, it is important to analyze the retrofitting options carefully concerning costs, environmental implications, energy efficiency, and thermal comfort. After an analysis of the database, two similar buildings of the most common building type were chosen for further analysis. Following the aim of the study, parametric analysis was used to produce comprehensive results, which were utilized for comparison of the retrofitting options in the analyzed categories. This facilitates a comprehensive assessment that considers multiple factors at an early stage, to help with the identification of effective retrofitting early in the process and ensure the alignment of proposed retrofitting with regulations set by relevant agencies.

To achieve the aim of this study, the objectives were to find the best-performing measures within the categories of energy use, profitability, environmental impact, and thermal comfort, illustrating several measures that can be applied to similar multifamily residential buildings.

The first objective was achieved by comparing the operational energy use between all cases. The three best-performing combinations consist of thick wall insulation, mineral wool roof insulation, new windows (U -value of $0.91 \text{ W}/(\text{m}^2 \cdot \text{K})$), an air-to-water heat pump, and a mechanical ventilation system with heat recovery. These three cases each reduced the purchased energy to approximately $26 \text{ kWh}/\text{m}^2$ (80 % reduction) and $18 \text{ kWh}/\text{m}^2$ (88 % reduction) for buildings A and B respectively. However, the resulting life cycle costs are very high due to investment costs, and it is worth mentioning that the heat pump system includes the installation of new radiators, piping, thermostats, and circulation pumps for both buildings and was designed for the highest peak load, which is the base case. The system is oversized due to reduced transmission, leakage, and ventilation losses, leading to overestimated costs and environmental impact. Matching the system with the specific case would yield better results. Furthermore, the roof insulation proves to be more impactful in building B compared to building A because the attic in building B is heated, which increases the energy savings when insulating. Installing new windows is however not effective in either building, even though the window area was three times larger (54 m^2) in building B compared to building A (18 m^2). This ineffectiveness is due to the large heat loss from the façade, which shows a greater reduction when insulated compared to installing new windows. The environmental impact of the three cases, approximately $83 \text{ kg CO}_2 \text{ eq.}/\text{m}^2$ and $110 \text{ kg CO}_2 \text{ eq.}/\text{m}^2$ for building A and building B respectively, was close to the best-performing cases in the analyzed environmental impact category, which had an impact of $81 \text{ kg CO}_2 \text{ eq.}/\text{m}^2$ and $82 \text{ kg CO}_2 \text{ eq.}/\text{m}^2$. Furthermore, the overheating of these cases increased in both buildings, with building A below the limit of 10 % overheating and building B above. The overheating difference in both buildings is explained by the analyzed zone in building A being located below the cold attic, while the zone in building B is located in the attic. In summary, aiming for the lowest energy reduction can achieve a low environmental impact but results in higher overheating and low profitability.

Through a detailed life cycle cost analysis, the second objective was achieved. The three best combinations consisted of EPS façade insulation, and mineral wool or cellulose roof insulation. These retrofitting options display a profitability of approximately $500 \text{ SEK}/\text{m}^2$ and $1\,900 \text{ SEK}/\text{m}^2$ for building A and building B respectively. The profitability is mainly due to high energy cost savings combined with a low investment cost. The sensitivity analysis illustrated an increased profitability for all cases, and in the number of cases, when the interest rate decreases and the electricity price increases. The energy use of the best-performing cases was reduced by approximately 24 % for both buildings to a level of $102 \text{ kWh}/\text{m}^2$ and $95 \text{ kWh}/\text{m}^2$ for buildings A and B respectively. While overheating reached a level below 10 % for building A, and above for building B. Additionally, the environmental impact reached the highest level for all best cases in the analyzed category of life cycle costs. To conclude, aiming for the most profitable investment one could expect a decrease in operational energy, an increase in overheating, and a high environmental impact.

The third objective was achieved by performing a life cycle assessment. The three best combinations consist of EPS wall insulation, cellulose or mineral wool roof insulation, and integration of a heating system consisting of heat pumps, radiators, piping, thermostats, and circulation pumps. The installation of mechanical ventilation systems and renewal of windows were not preferred measures from an environmental standpoint, since their embodied impact was higher than their saved operational impact. The result showed an impact of $81 \text{ kg CO}_2 \text{ eq.}/\text{m}^2$ to $82 \text{ kg CO}_2 \text{ eq.}/\text{m}^2$ for both buildings, which is a significant reduction compared to the environmental impact of base cases, which is $440 \text{ kg CO}_2 \text{ eq.}/\text{m}^2$ and $530 \text{ kg CO}_2 \text{ eq.}/\text{m}^2$ for building A and building B

respectively. The main reason for the low LCA impact is the reduced purchased energy of 79 % and 82 % for buildings A and B respectively. The profitability was however negative in both buildings, and to a larger extent in building A mainly due to a larger investment cost and a difference in reduced purchased energy of 3 %. Since façade insulation is applied and mechanical ventilation is not present, the overheating increased in both buildings. Building A was below the limit of 10 % while building B was above. In summary, aiming for the lowest environmental impact will yield significantly less energy use, but a negative profitability and an increase in overheating.

The fourth objective was achieved by analyzing the thermal comfort from April to September. The results indicate that mechanical ventilation is the most favorable option for both buildings, in combination with new windows for building A, and roof insulation for building B. The reduction in overheating is mainly due to the capability of the ventilation system to cool the indoor air through increased constant airflow. Even though it utilizes heat recovery it comes with significant costs and environmental impact. Even with the implementation of mechanical ventilation in building B, overheating remains above satisfactory levels, reaching a minimum of 11 %, and falling short of the desired threshold of 10 %. The roof insulation was also an appropriate choice of measure for building B to reduce the overheating percentage since it will reduce the heat transfer from outside into the attic, which is the assessed zone. Overall, there was no profitability using these measures for either building. However, if the interest rate decreased or the electricity price increased, the profitability would increase to a level that would make the best cases profitable for building B. In summary, these measures do not only yield the least overheating degree, reduced energy use, and environmental impact but also a chance of profitability.

A common conclusion from the analysis is that the most effective combinations of measures vary across categories depending on the analyzed factor and that there are not many measures that perform well in all categories. However, roof insulation can reduce heat transfer to and from the building to a certain extent. Its profitability depends on the low investment cost and relatively high amount of reduced energy, which additionally is favorable in terms of environmental impact. Thus, indicating that roof insulation is a prudent choice. In general, the results indicate that most retrofit measures decrease the environmental impact by reducing greenhouse gas emissions. However, absorption and emission of biogenic emissions are not included according to Boverket's guidelines and were therefore excluded. The base case did not include any renovations to keep the building in its current state. The inclusion of biogenic emissions and renovation of the base cases could have altered the outcome of the results and rendered the comparison more comprehensive.

Furthermore, refurbishing an attic into an apartment can yield unsatisfactory temperatures, and the implementation of interior blinds, natural ventilation, and mechanical ventilation will not provide enough thermal comfort within the limits set by FEBY18. Notably, all the measures were analyzed in different categories to identify the best-performing measures. However, these categories are not fully independent, since a choice of measure can affect all the categories, which is evident from our results.

6.1 Further studies

A Grasshopper template could be developed to perform faster simulations while still including as many relevant factors as possible. The template could include a manual to standardize the simulation process for all buildings of interest, thus, ensuring a common methodology for the users and making it more user-friendly. Additionally, A weighting system could be developed to assess the importance and effects of various measures on all the analyzed aspects, helping to identify the most appropriate measure when considering all analysis criteria.

There are several factors used as metrics in certifications, thus, a script could be developed and integrated with the Grasshopper environment to be used to automatically collect the necessary data required to determine if a building reaches a certain degree in a certification system. With the potential of increasing productivity and generating results faster compared with manual labour.

References

- Abdul Hamid, A., Farsäter, K., Wahlström, Å., & Wallentén, P. (2018). Literature review on renovation of multifamily buildings in temperate climate conditions. *Energy and Buildings*, 172, 414–431. <https://doi.org/10.1016/J.ENBUILD.2018.04.032>
- Arfvidsson, J., Harderup, L.-E., & Samuelson, I. (2017). *Fukthandboken - Praktik och teori* (Fourth edition). AB Svensk Byggtjänst.
- ASHRAE. (2021). *ASHRAE 90.1 Section 11 and Appendix G Submittal Review Manual*.
- Avelin, A., Dahlquist, E., & Wallin, F. (2017). Effect of different renovation actions, their investment cost and future potential. *Energy Procedia*, 143, 73–79. <https://doi.org/10.1016/J.EGYPRO.2017.12.650>
- Awbi, H. (2003). *Ventilation of buildings* (Second). Routledge.
- Bahramian, M., & Yetilmmezsoy, K. (2020). Life cycle assessment of the building industry: An overview of two decades of research (1995–2018). *Energy and Buildings*, 219. <https://doi.org/10.1016/j.enbuild.2020.109917>
- Ban, A., & Bungâu, C. (2022). *LIFE CYCLE COST ANALYSIS FOR SYSTEMS EQUIPPED WITH A HEAT PUMP.*: *Lund University Libraries*. 21(3), 268–276. <https://eds-p-ebshost-com.ludwig.lub.lu.se/eds/pdfviewer/pdfviewer?vid=5&sid=ffabfc15-11d9-4f6d-92f4-2a7e29615119%40redis>
- Bastian, Z., Schnieders, J., Conner, W., Kaufmann, B., Lepp, L., Norwood, Z., Simmonds, A., & Theoboldt, I. (2022). Retrofit with Passive House components. *Energy Efficiency*, 15(1). <https://doi.org/10.1007/S12053-021-10008-7>
- Baumann, H., & Tillman, A. M. (2004). The hitch hiker's guide to LCA : an orientation in life cycle assessment. *Lund, Sweden: Studentlitteratur AB*, 11(2), 543. <https://www.studentlitteratur.se/kurslitteratur/naturvetenskap-och-miljo/miljo/the-hitch-hikers-guide-to-lca/>
- BjäreKraft. (2022). *1 september höjer vi ersättningen för nätnytta och avgiften för elöverföring | Bjäre Kraft*. <https://www.bjarekraft.se/privat/om-oss/nyheter/1-september-hojer-vi-ersattningen-for-natnytta-och-avgiften-for-eloverforing>
- Björk, C., Kallstenius, P., & Reppen, L. (2021). *Så byggdes husen 1880 - 2020 - Arkitektur, konstruktion och material i våra flerbostadshus under 140 år* (8th ed.).
- Björklund, J., & Ohlsson, P. (2018). *Systemkunskap* (4th ed., Vol. 1). Liber AB.
- Bolliger, R., Ott, W., & Von Grünigen, S. (2015). Finding the balance between energy efficiency measures and renewable energy measures in building renovation: An assessment based on generic calculations in 8 European countries. *Energy Procedia*, 78, 2372–2377. <https://doi.org/10.1016/J.EGYPRO.2015.11.191>
- Bournas, I., Abugabbara, M., Balcerzak, A., Dubois, M. C., & Javed, S. (2016). Energy renovation of an office building using a holistic design approach. *Journal of Building Engineering*, 7, 194–206. <https://doi.org/10.1016/J.JOBE.2016.06.010>
- Boverket. (2016). *Handbok för energihushållning enligt Boverkets byggregler - utgåva två*.
- Boverket. (2017). *BFS 2017:6 - BEN 2*.
- Boverket. (2021a). *Boverkets byggregler (2011:6) - föreskrifter och allmänna råd, BBR*. <https://www.boverket.se/sv/lag--ratt/forfattningssamling/gallande/bbr---bfs-20116/>
- Boverket. (2021b). *Klimatdeklaration av byggnader*. <https://www.boverket.se/sv/byggande/hallbart-byggande-och-forvaltning/klimatdeklaration/>
- Boverket. (2024). *Boverkets klimatdatabas*.
- Circular Ecology. (2024). *Environmental Impacts - Circular Ecology*. <https://circularecology.com/environmental-impacts.html>
- ClimateOneBuilding. (2024). *climate.onebuilding.org*. 2024. <https://climate.onebuilding.org/>
- Decorte, Y., Van Den Bossche, N., & Steeman, M. (2024). Importance of technical installations in whole-building LCA: Single-family case study in Flanders. *Building and Environment*, 250, 111209. <https://doi.org/10.1016/J.BUILDENV.2024.111209>
- Dubois, M.-C., Gentile, N., Laike, T., Bournas, I., & Alenius, M. (2019). *Daylighting and lighting - Under a nordic sky* (1st ed., Vol. 1). Studentlitteratur AB.
- ECB. (2024). *Vad är räntor och vad är skillnaden mellan nominell ränta och realränta?*
- Ekström, T., & Blomsterberg, Å. (2016). Renovation of Swedish Single-family Houses to Passive House Standard – Analyses of Energy Savings Potential. *Energy Procedia*, 96, 134–145. <https://doi.org/10.1016/J.EGYPRO.2016.09.115>

- EnergiFöretagen. (2023). *Fjärrvärmepreiser - Energiföretagen Sverige*.
<https://www.energiforetagen.se/statistik/fjarrvarmestatistik/fjarrvarmepreiser/>
- Energimarknadsbyrån. (2023). *Fjärrvärme - pris och kostnad | Energimarknadsbyrån*.
<https://www.energimarknadsbyran.se/fjarrvarme/fjarrvarmeavtal-och-kostnader/fjarrvarme-pris-och-kostnad/>
- European Commission. (2020). *In focus: Energy efficiency in buildings*.
https://commission.europa.eu/news/focus-energy-efficiency-buildings-2020-02-17_en
- European Commission. (2021). *Level(s) common framework*.
- European Commission. (2024). *Nytt utsläppsmål för 2040 ska se till att EU är klimatneutralt vid 2050 - Europeiska kommissionen*. https://commission.europa.eu/news/recommendation-2040-target-reach-climate-neutrality-2050-2024-02-06_sv
- Farinha, C., Brito, J. de, & Veiga, M. Do. (2021). Life cycle assessment. *Eco-Efficient Rendering Mortars*, 205–234. <https://doi.org/10.1016/B978-0-12-818494-3.00008-8>
- FEBY18. (2024). *Kravspecifikation för energieffektiva byggnader*. www.feby.se
- Flodin, J., Landeman, M., Julstad, B., Larsson, J., Sörbom, P., Lindgren, E., Kalbro, T., Haapaniemi, M., Berghöök, J., Grauer Henning, P., Gustafsson, C., Persson, E., Lind, H., Lundgren, B., Nordlund, B., Råckle, G., Hermansson, C., Nyström, J., Palm, P., ... Högberg, L. (2021). *Fastighetsnomenklatur - Fastighetsekonomi och fastighetsrätt* (14th ed.). Studentlitteratur AB.
- Grynning, S., Gustavsen, A., Time, B., & Jelle, B. P. (2013). Windows in the buildings of tomorrow: Energy losers or energy gainers? *Energy and Buildings*, 61, 185–192. <https://doi.org/10.1016/J.ENBUILD.2013.02.029>
- Gustafsson, M., Gustafsson, M. S., Myhren, J. A., Bales, C., & Holmberg, S. (2016). Techno-economic analysis of energy renovation measures for a district heated multi-family house. *Applied Energy*, 177, 108–116. <https://doi.org/10.1016/J.APENERGY.2016.05.104>
- Hagentoft, C.-E., & Sandin, K. (2017). *Byggnadsfysik - Så fungerar hus* (1:1). Studentlitteratur AB.
- Heide, V., Thingbø, H. S., Lien, A. G., & Georges, L. (2022). Economic and Energy Performance of Heating and Ventilation Systems in Deep Retrofitted Norwegian Detached Houses †. *Energies*, 15(19). <https://doi.org/10.3390/EN15197060>
- Hukka, A., & Viitanen, H. A. (1999). A mathematical model of mold growth on wooden material. *Wood Science and Technology*, 33(6), 475–485. <https://doi.org/10.1007/S002260050131>
- International Energy Agency, I. (2023). *World Energy Outlook 2023*. www.iea.org/terms
- IPCC. (2007). *2.10.2 Direct Global Warming Potentials - AR4 WGI Chapter 2: Changes in Atmospheric Constituents and in Radiative Forcing*. https://archive.ipcc.ch/publications_and_data/ar4/wg1/en/ch2s2-10-2.html
- Jaemoon, K., Duhwan, L., & Seunghoon, N. (2023). Potential for environmental impact reduction through building LCA(Life Cycle Assessment) of school facilities in material production stage. *Building and Environment*, 238, 110329. <https://doi.org/https://doi.org/10.1016/j.buildenv.2023.110329>
- Janson, U. (2008). *Passive houses in Sweden Experiences from design and construction phase*. Lunds Tekniska Högskola.
- Jelle, B. P., Hynd, A., Gustavsen, A., Arasteh, D., Goudey, H., & Hart, R. (2012). Fenestration of today and tomorrow: A state-of-the-art review and future research opportunities. *Solar Energy Materials and Solar Cells*, 96(1), 1–28. <https://doi.org/10.1016/J.SOLMAT.2011.08.010>
- Jradi, M., Veje, C., & Jørgensen, B. N. (2017). Deep energy renovation of the Mærsk office building in Denmark using a holistic design approach. *Energy and Buildings*, 151, 306–319. <https://doi.org/10.1016/J.ENBUILD.2017.06.047>
- Kansal, R., & Kadambari, G. (2010). Green Buildings: An Assessment of Life Cycle Cost. *IUP Journal of Infrastructure*, 8(4), 50–57.
- Konsumenternas Energimarknadsbyrå. (2024). *Energiskatt - skattesatser och kostnader*. <https://www.energimarknadsbyran.se/el/dina-avtal-och-kostnader/elrakningen/energiskatt-skattesatser-och-kostnader>
- La Fleur, L., Rohdin, P., & Moshfegh, B. (2019). Investigating cost-optimal energy renovation of a multifamily building in Sweden. *Energy and Buildings*, 203, 109438. <https://doi.org/10.1016/J.ENBUILD.2019.109438>
- Lavy, S., & Shohet, I. M. (2007). On the effect of service life conditions on the maintenance costs of healthcare facilities. *Construction Management and Economics*, 25(10), 1087–1098. <https://doi.org/10.1080/01446190701393034>

- Li, Y., Tao, X., Zhang, Y., & Li, W. (2024). Combining use of natural ventilation, external shading, cool roof and thermal mass to improve indoor thermal environment: Field measurements and simulation study. *Journal of Building Engineering*, *86*, 108904. <https://doi.org/10.1016/j.job.2024.108904>
- Liu, L., Rohdin, P., & Moshfegh, B. (2015). Evaluating indoor environment of a retrofitted multi-family building with improved energy performance in Sweden. *Energy and Buildings*, *102*, 32–44. <https://doi.org/10.1016/j.enbuild.2015.05.021>
- Menassa, C. C. (2011). Evaluating sustainable retrofits in existing buildings under uncertainty. *Energy and Buildings*, *43*(12), 3576–3583. <https://doi.org/10.1016/J.ENBUILD.2011.09.030>
- Milić, V., Ekelöw, K., Andersson, M., & Moshfegh, B. (2019). Evaluation of energy renovation strategies for 12 historic building types using LCC optimization. *Energy and Buildings*, *197*, 156–170. <https://doi.org/10.1016/J.ENBUILD.2019.05.017>
- Naturvårdsverket. (2023). *Sveriges miljömål*. <https://www.naturvardsverket.se/om-miljoarbetet/sveriges-miljomal/>
- Niemelä, T., Kosonen, R., & Jokisalo, J. (2017). Cost-effectiveness of energy performance renovation measures in Finnish brick apartment buildings. *Energy and Buildings*, *137*, 60–75. <https://doi.org/10.1016/j.enbuild.2016.12.031>
- Park, C. (2018). *Fundamentals of Engineering Economics* (4th ed., Vol. 1). Pearson.
- Poirazis, H., Blomsterberg, Å., & Wall, M. (2008). Energy simulations for glazed office buildings in Sweden. *Energy and Buildings*, *40*(7), 1161–1170. <https://doi.org/10.1016/J.ENBUILD.2007.10.011>
- Ramírez-Villegas, R., Eriksson, O., & Olofsson, T. (2019). Life cycle assessment of building renovation measures—trade-off between building materials and energy. *Energies*, *12*(3). <https://doi.org/10.3390/EN12030344>
- Rønneseth, Ø., Sandberg, N. H., & Sartori, I. (2019). Is It Possible to Supply Norwegian Apartment Blocks with 4th Generation District Heating? *Energies 2019, Vol. 12, Page 941*, *12*(5), 941. <https://doi.org/10.3390/EN12050941>
- Santamouris, M., Tsangrassoulis, A., & Klitsikas, N. (2000). *World Renewable Energy Congress VI (WREC2000)*.
- SGBC. (2022). *Miljöbyggnad 4.0*. www.sgbc.se
- Siegenthaler, J. (2023). *Modern hydronic heating & cooling - For residential and light commercial buildings*. (4th ed., Vol. 1). Cengage.
- Skatteverket. (2029). *Typkoder för fastighetstaxering | Skatteverket*. <https://www.skatteverket.se/privat/fastigheterochbostad/fastighetstaxering/typkoder.4.2b543913a42158acf800022661.html>
- Sveby. (2012). *Brucarindata bostäder*.
- Sveby. (2022). *Uppdaterade DVUT-värden för nya normalperioden | Sveby*. <https://www.sveby.org/okategoriserad/uppdaterade-dvut-varden-for-nya-normalperioden/>
- Svensk Ventilation. (2024, January). *Värmeväxlare - Svensk Ventilation*. 2024. <https://www.svenskventilation.se/ventilation/varmevaxlare/>
- Swedish Institute for Standards. (2021). *Svensk Standard SS-EN 15804:2012 +A2:2019/AC:2021 Hållbarhet hos byggnadsverk-Miljödeklarationer-Produktspecifika regler*. www.sis.se
- Swedish Standard Institute. (2006). *Miljöledning - Livscykelanalys - Krav och vägledning (ISO 14044:2006)*.
- Swedish Standard Institute. (2020). *Hållbarhet hos byggnadsverk – Regler för miljödeklarationer för byggprodukter och byggtjänster (ISO 21930:2017, IDT)*.
- Terés-Zubiaga, J., Campos-Celador, A., González-Pino, I., & Escudero-Revilla, C. (2015). Energy and economic assessment of the envelope retrofitting in residential buildings in Northern Spain. *Energy and Buildings*, *86*, 194–202. <https://doi.org/10.1016/J.ENBUILD.2014.10.018>
- Vattenfall. (2024). *Timpris för dig som kan styra elanvändning - Vattenfall*. <https://www.vattenfall.se/elavtal/elpriser/timpris/>
- Wang, N., Chang, Y. C., & El-Sheikh, A. A. (2012). Monte Carlo simulation approach to life cycle cost management. *Structure and Infrastructure Engineering*, *8*(8), 739–746. <https://doi.org/10.1080/15732479.2010.481304>
- Wang, Q., Ploskić, A., Song, X., & Holmberg, S. (2016). Ventilation heat recovery jointed low-temperature heating in retrofitting - An investigation of energy conservation, environmental impacts and indoor air quality in Swedish multifamily houses. *Energy and Buildings*, *121*, 250–264. <https://doi.org/10.1016/J.ENBUILD.2016.02.050>
- Warfvinge, C., & Dahlblom, M. (2010). *Projektering av VVS-installationer* (1:14). Studentlitteratur AB.

Zou, Y., Guo, J., Xia, D., Lou, S., Huang, Y., Yang, X., & Zhong, Z. (2023). Quantitative analysis and enhancement on passive survivability of vernacular houses in the hot and humid region of China. *Journal of Building Engineering*, 71, 106431. <https://doi.org/10.1016/J.JOBE.2023.106431>

Appendix

Appendix A

Table 25. Input data for WUFI, building A.

Name	Facade	Roof
Weather file	Malmö	Malmö
Simulation duration /Years	10	10
Inclination /°	-	29 and 36.5
Adhering rain fraction /(-)	0.7	0
Indoor climate	EN 13788	EN 13788
Humidity class	2	2
Indoor temperature /°C	21	21
Orientation (critical)	Southwest	North
Long wave radiation emissivity	0.9	0.9
Initial water content /%	80	80

Table 26. Input data for WUFI, building B.

Name	Facade	Roof
Weather file	Helsingborg	Helsingborg
Simulation duration /Years	10	10
Inclination /°	-	30
Adhering rain fraction /(-)	0.7	0
Indoor climate	EN 13788	EN 13788
Humidity class	2	2
Indoor temperature /°C	21	21
Orientation (critical)	Southwest	North
Long wave radiation	0.9	0.9
Initial water content /%	80	80

Appendix B

Table 27. Product data used in the LCA calculation.

Type	Product & declared unit	EPD	Lifespan /years	Life cycle stages	EPD Impact /stages	Source
MVHR-system	Ductwork kg CO ₂ eq./m ²		50+	A1-A5	2.79	Lindab circular duct EPD
	Diffusers kg CO ₂ eq./kg		50+	A1-A5	3.58	Galvanized steel Boverket CDB
	Fittings kg CO ₂ eq./kg		50+	A1-A5	3.69	Lindab Fittings EPD
	AHU kg CO ₂ eq./kg		20	A1-A5	2 470	Swegon AHU EPD
	AHU-replacement kg CO ₂ eq./kg		-	B4	4 950	Swegon AHU EPD A1-A5
	Filter kg CO ₂ eq./ filterbag		1	B2	6.85	Filter EPD
Heating	Accumulator tank kg CO ₂ eq./kg		25	A1-A5	3.67	Steel and Polyisocyanurate insulation, Boverket CDB
	Accumulator tank- replacement kg CO ₂ eq./kg		-	B4	3.67	Steel and Polyisocyanurate insulation, Boverket CDB A1-A5
	HP Outdoor part kg CO ₂ eq./kg		25	A1-A5	4.85	Steel, Aluminum, Copper, Polyisocyanurate insulation, Boverket CDB
	HP Outdoor part- replacement kg CO ₂ eq./kg		-	B4	4.85	Steel, Aluminum, Copper, Polyisocyanurate insulation, Boverket CDB A1-A5
	HP indoor part kg CO ₂ eq./kg		25	A1-A5	2.69	Steel, Aluminum, Copper, Polyisocyanurate insulation, Boverket CDB
	HP indoor part - replacement kg CO ₂ eq./kg		-	B4	2.69	Steel, Aluminum, Copper, Polyisocyanurate insulation, Boverket CDB A1-A5
	Radiators kg CO ₂ eq./kW		50	A1-A5	70.1	Purmo radiators EPD
	Thermostats kg CO ₂ eq./piece		10	A1-A5	0.676	Danfoss Thermostat EPD
	Thermostats- replacement kg CO ₂ eq./piece		-	B4	2.71	Danfoss Thermostat EPD A1-A5
	Circulator pumps kg CO ₂ eq./piece		10	A1-A5	53.6	Grundfos pump EPD
	Circulator pumps- replacement kg CO ₂ eq./piece		-	B4	214	Grundfos pump EPD A1-A5
	Copper pipes kg CO ₂ eq./kg		50	A1-A5	3.20	Copper pipe, Boverket CDB
	Fitting kg CO ₂ eq./kg		50	A1-A5	3.20	Copper pipe, Boverket CDB
Roof	Gypsum Board kg CO ₂ eq./kg		50+	A1-A5	0.344	gypsum board, Boverket CDB
	Mineral wool kg CO ₂ eq./m ²		50+	A1-A5	3.99	Knauf Insulation- Glass wool EPD
	Rock wool kg CO ₂ eq./m ²		50+	A1-A5	4.81	Rockwool EPD
	Cellulose kg CO ₂ eq./kg		50+	A1-A5	0.175	Cellulose- Boverket CDB
	Vapour Barrier		50	A1-A5	3.08	Vapour Barrier – Boverket CDB

	kg CO ₂ eq./kg				
Facade	Plaster kg CO ₂ eq./kg	50+	A1-A5	0.256	Plaster, Boverket CDB
	Rockwool kg CO ₂ eq./m ²	50+	A1-A5	4.81	Rockwool EPD
	EPS kg CO ₂ eq./kg	50+	A1-A5	4.32	EPS insulation, Boverket CDB
Window	Paint kg CO ₂ eq./kg	30	B2	3.29	Outdoor paint - Boverket CDB
	Window Openable kg CO ₂ eq./m ²	50	A1-A5	71.9	Svenska Fönster, openable window EPD
	Window not openable kg CO ₂ eq./m ²	50	A1-A5	55.8	Svenska Fönster, not openable Window EPD

Appendix C

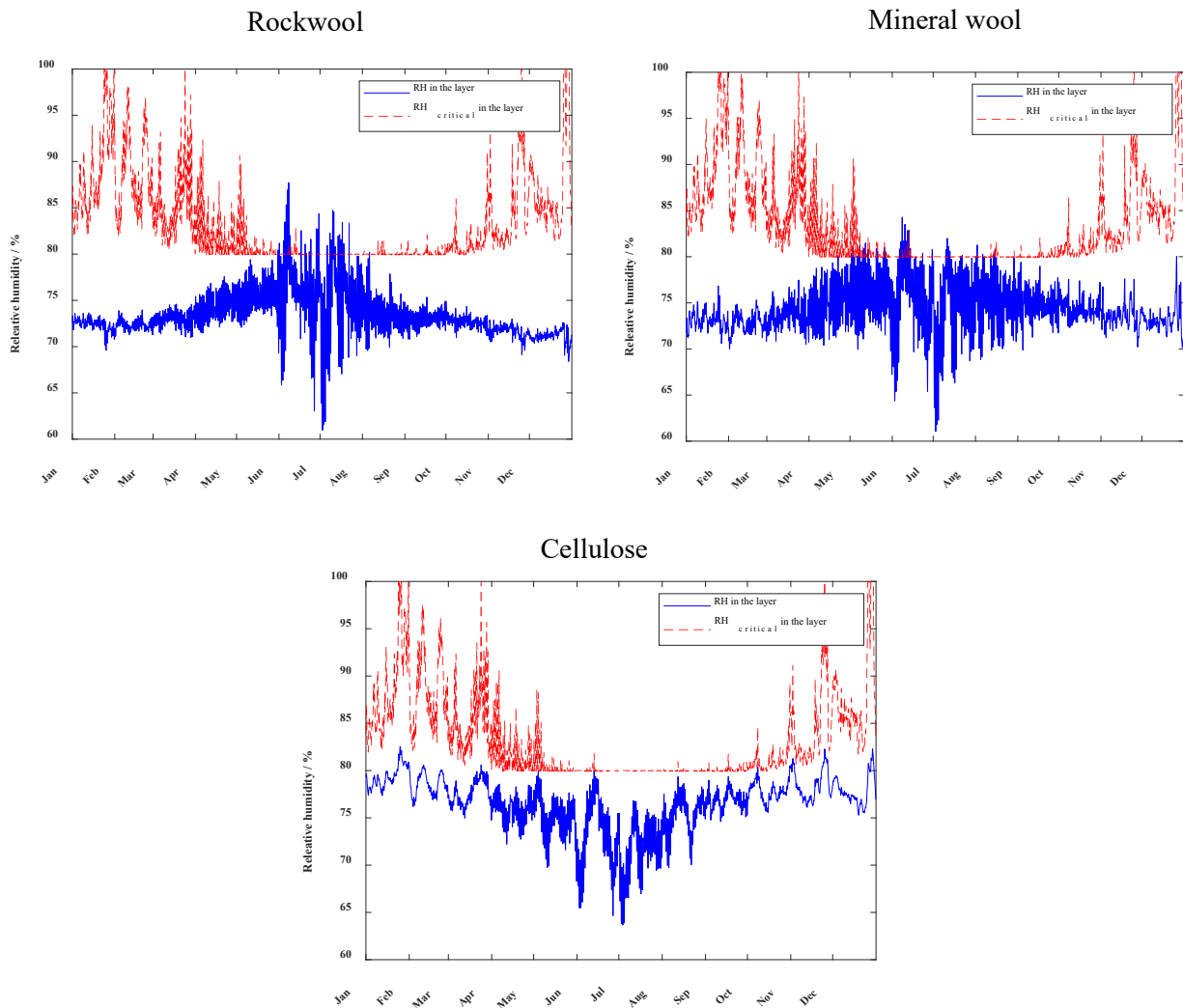


Figure 57. Relative humidity of the roof constructions in building A, relative to the critical level.

Appendix D



Ductwork Balancing Report

Project Information			
Software version:	MagiCAD for Revit 2023 UR-2	Calculation date:	2024-02-28 23:58
Project name:	Project Name	Project number:	0001
Project address:	Enter address here	Client name:	Owner
Project issue date:	Issue Date	Organization name:	
Organization description:		Author:	

Project Calculation Data			
Systems:	-	Total pressure:	72.7 Pa
Total flow:	260.0 l/s		

Calculation Input Values			
Air Density:	1.20 kg/m3	Air Dynamic Viscosity:	0.00001813 Pa*s
Min. dp air devices:	20.0 Pa	Balancing target pressure:	By air handling equipment
Out of dp-range warning tolerance:	0 %		

Calculation Results / Supply

Location	Level	Node	Type	Series	Product	Size	L [m]	Insulation	qv set [l/s]	qv [l/s]	v [m/s]	dpt [Pa]	K factor	dp/L [Pa/m]	pt [Pa]	pst [Pa]	adj.	qv [%]	Warnings
			DUCT	44	INSR-250	250 (L)	1,2		260,0	260,0	5,3	2,3		2,00	72,7	55,9			
		40	T-BRANCH	44	INTCU-250-2	250/250			260,0	260,0	5,3	19,0	1,126			70,4			
			DUCT	44	INSR-250	250	1,2		120,0	120,0	2,4	0,5		0,44	51,5	47,9			
		41	T-BRANCH	44	INTCU-250-2	250/200			120,0	120,0	2,4	4,1	1,157			50,9			
			DUCT	44	INSR-200	200	2,0		68,0	68,0	2,2	1,0		0,47	46,6	44,0			
			BEND-90	44	INBU-200-90	200			68,0	68,0	2,2	1,2	0,418			45,8			
			DUCT	44	INSR-200	200	1,3		68,0	68,0	2,2	0,6		0,47	44,7	41,8			
			BEND-90	44	INBU-200-90	200			68,0	68,0	2,2	1,2	0,418			44,1			
			DUCT	44	INSR-200	200	1,9		68,0	68,0	2,2	0,9		0,47	42,9	40,1			
		21	X-BRANCH	44	BDEX-1	FAB 200/100/100			68,0	68,0	2,2	3,1	1,100			42,0			
			DUCT	44	INSR-100	100	0,9		12,0	12,0	1,5	0,5		0,60	38,9	37,5			
			BEND-90	44	INBU-100-90	100			12,0	12,0	1,5	0,8	0,563			38,4			
			DUCT	44	INSR-100	100	0,3		12,0	12,0	1,5	0,2		0,60	37,6	36,2			
		22	SUPPLY		SHH-100	100			12,0	12,0	1,5	37,4			37,4		6,9	100	
			DUCT	44	INSR-100	100	0,4		12,0	12,0	1,5	0,3		0,60	38,9	37,5			
			BEND-90	44	INBU-100-90	100			12,0	12,0	1,5	0,8	0,563			38,6			
			DUCT	44	INSR-100	100	0,3		12,0	12,0	1,5	0,2		0,60	37,8	36,4			
		23	SUPPLY		SHH-100	100			12,0	12,0	1,5	37,6			37,6		6,9	100	
			DUCT	44	INSR-200	200 (L)	2,8		44,0	44,0	1,4	0,6		0,20	41,8	40,6			
		24	X-BRANCH	44	BDEX-1	FAB 200/100/100			44,0	44,0	1,4	1,5	1,238			41,2			
			DUCT	44	INSR-100	100	0,9		12,0	12,0	1,5	0,5		0,60	39,7	38,3			
			BEND-90	44	INBU-100-90	100			12,0	12,0	1,5	0,8	0,563			39,2			
			DUCT	44	INSR-100	100	0,3		12,0	12,0	1,5	0,2		0,60	38,4	37,0			
		25	SUPPLY		SHH-100	100			12,0	12,0	1,5	38,2			38,2		6,9	100	
			DUCT	44	INSR-100	100	0,4		12,0	12,0	1,5	0,3		0,60	39,7	38,3			
			BEND-90	44	INBU-100-90	100			12,0	12,0	1,5	0,8	0,563			39,5			
			DUCT	44	INSR-100	100	0,3		12,0	12,0	1,5	0,2		0,60	38,7	37,3			
		26	SUPPLY		SHH-100	100			12,0	12,0	1,5	38,5			38,5		6,8	100	
			REDUCER	44	INRCFU-200-200/100				20,0	20,0	0,6				40,8				
			DUCT	44	INSR-100	100	2,8		20,0	20,0	2,5	4,4		1,60	40,8	36,9			
			BEND-90	44	INBU-100-90	100			20,0	20,0	2,5	1,9	0,488			36,3			
			DUCT	44	INSR-100	100	0,5		20,0	20,0	2,5	0,9		1,60	34,4	30,5			
			BEND-90	44	INBU-100-90	100			20,0	20,0	2,5	1,9	0,488			33,8			
			DUCT	44	INSR-100	100	0,3		20,0	20,0	2,5	0,5		1,60	31,7	27,8			
		27	SUPPLY		SHH-100	100			20,0	20,0	2,5	31,2			31,2		13	100	
			REDUCER	44	INRCFU-250-250/200				52,0	52,0	1,1				50,7				
			DUCT	44	INSR-200	200	2,5		52,0	52,0	1,7	0,7		0,28	50,7	49,0			
			BEND-90	44	INBU-200-90	200			52,0	52,0	1,7	0,7	0,451			50,0			
			DUCT	44	INSR-200	200	2,8		52,0	52,0	1,7	0,8		0,28	49,3	47,6			
			BEND-30	44	INBU-200-30	200			52,0	52,0	1,7	0,2	0,142			48,5			
			DUCT	44	INSR-200	200	1,8		52,0	52,0	1,7	0,5		0,28	48,2	46,6			
			BEND-90	44	MAGIB-C4-6	200			52,0	52,0	1,7	0,5	0,324			47,7			
			DUCT	44	INSR-200	200	0,2		52,0	52,0	1,7	0,0		0,28	47,2	45,5			
		2	T-BRANCH	44	INTCU-200-1	200/100			52,0	52,0	1,7	1,8	1,076			47,1			
			DUCT	44	INSR-100	100	2,0		8,0	8,0	1,0	0,5		0,28	45,4	44,7			
			BEND-90	44	INBU-100-90	100			8,0	8,0	1,0	0,4	0,631			44,8			
			DUCT	44	INSR-100	100	0,4		8,0	8,0	1,0	0,1		0,28	44,4	43,8			
			BEND-90	44	INBU-100-90	100			8,0	8,0	1,0	0,4	0,631			44,3			
			DUCT	44	INSR-100	100	0,4		8,0	8,0	1,0	0,1		0,28	43,9	43,3			
		3	SUPPLY		SHH-100	100			8,0	8,0	1,0	43,8			43,8		4,0	100	
			DUCT	44	INSR-200	200	0,3		44,0	44,0	1,4	0,1		0,20	47,1	45,9			
		4	T-BRANCH	44	INTCU-200-1	200/100			44,0	44,0	1,4	1,3	1,106			47,0			
			DUCT	44	INSR-100	100	0,4		8,0	8,0	1,0	0,1		0,28	45,7	45,1			
		5	SUPPLY		SHH-100	100			8,0	8,0	1,0	45,6			45,6		3,9	100	
			DUCT	44	INSR-200	200	1,8		36,0	36,0	1,1	0,3		0,14	46,9	46,1			
		6	T-BRANCH	44	INTCU-200-1	200/100			36,0	36,0	1,1	0,9	1,158			46,7			
			DUCT	44	INSR-100	100	2,0		8,0	8,0	1,0	0,6		0,28	45,8	45,1			
			BEND-90	44	INBU-100-90	100			8,0	8,0	1,0	0,4	0,631			45,2			
			DUCT	44	INSR-100	100	0,9		8,0	8,0	1,0	0,2		0,28	44,8	44,2			
			BEND-90	44	INBU-100-90	100			8,0	8,0	1,0	0,4	0,631			44,6			

Location	Level	Node	Type	Series	Product	Size	L [m]	Insulation	qv set [l/s]	qv [l/s]	v [m/s]	dpt [Pa]	K factor	dp/L [Pa/m]	pt [Pa]	pst [Pa]	adj.	qv [%]	Warnings
	Level 2		DUCT	44	INSR-100	100	0,3		8,0	8,0	1,0	0,1		0,28	44,2	43,6			
	Level 2	7	SUPPLY		SHH-100	100			8,0	8,0	1,0	44,1			44,1		4,0	100	
	Level 2		DUCT	44	INSR-200	200	0,9		28,0	28,0	0,9	0,1		0,09	46,6	46,2			
	Level 2	8	T-BRANCH	44	INTCU-200-1	200/100			28,0	28,0	0,9	0,6	1,261		46,6				
	Level 2		DUCT	44	INSR-100	100	0,4		8,0	8,0	1,0	0,1		0,28	46,0	45,3			
	Level 2	9	SUPPLY		SHH-100	100			8,0	8,0	1,0	45,8			45,8		3,9	100	
	Level 2		REDUCER	44	INRCFU-200	200/100			20,0	20,0	0,8				45,8				
	Level 1		DUCT	44	INSR-100	100	2,8		20,0	20,0	2,5	4,5		1,80	45,8	41,9			
	Level 1		BEND-90	44	INBU-100-90	100			20,0	20,0	2,5	1,9	0,488		41,3				
	Level 1		DUCT	44	INSR-100	100	0,4		20,0	20,0	2,5	0,7		1,80	39,4	35,5			
	Level 1	10	SUPPLY		SHH-100	100			20,0	20,0	2,5	38,8			38,8		12	100	
	Level 3		DUCT	44	INSR-250	250	1,2		140,0	140,0	2,9	0,7		0,80	51,2	46,3			
	Golv/Vinden	42	T-BRANCH	44	INTCU-250-2	250/200			140,0	140,0	2,9	5,7	1,159		50,5				
	Golv/Vinden		DUCT	44	INSR-200	200	2,0		80,0	80,0	2,5	1,3		0,64	44,8	41,0			
	Level 3		BEND-90	44	INBU-200-90	200			80,0	80,0	2,5	1,8	0,400		43,5				
	Level 3		DUCT	44	INSR-200	200	2,8		80,0	80,0	2,5	1,8		0,64	42,0	38,1			
	Level 3		BEND-90	44	INBU-200-90	200			80,0	80,0	2,5	1,6	0,400		40,2				
	Level 3		DUCT	44	INSR-200	200	1,9		80,0	80,0	2,5	1,2		0,64	38,6	34,7			
	Level 3	28	X-BRANCH	44	BDEX-1 FAB	200/100/100			80,0	80,0	2,5	4,2	1,072		37,4				
	Level 3		DUCT	44	INSR-100	100	0,6		12,0	12,0	1,5	0,3		0,80	32,4	31,8			
	Level 3		BEND-90	44	INBU-100-90	100			12,0	12,0	1,5	0,8	0,563		32,9				
	Level 3		DUCT	44	INSR-100	100	0,3		12,0	12,0	1,5	0,2		0,80	32,1	30,7			
	Level 3	29	SUPPLY		SHH-100	100			12,0	12,0	1,5	31,9			31,9		7,5	100	
	Level 3		DUCT	44	INSR-100	100	0,7		12,0	12,0	1,5	0,4		0,80	33,2	31,8			
	Level 3		BEND-90	44	INBU-100-90	100			12,0	12,0	1,5	0,8	0,563		32,8				
	Level 3		DUCT	44	INSR-100	100	0,3		12,0	12,0	1,5	0,2		0,80	32,0	30,6			
	Level 3	30	SUPPLY		SHH-100	100			12,0	12,0	1,5	31,8			31,8		7,5	100	
	Level 3		REDUCER	44	INRCFU-200	200/160			56,0	56,0	1,8				37,2				
	Level 2		DUCT	44	INSR-160	160 (L)	2,7		56,0	56,0	2,8	2,7		1,02	37,2	32,6			
	Level 2		REDUCER	44	INRCFU-200	200/160			56,0	56,0	2,8	0,9	0,187		34,5				
	Level 2	31	X-BRANCH	44	BDEX-1 FAB	200/100/100			56,0	56,0	1,8	2,2	1,147		33,6				
	Level 2		DUCT	44	INSR-100	100	0,5		12,0	12,0	1,5	0,3		0,80	31,4	30,0			
	Level 2		BEND-90	44	INBU-100-90	100			12,0	12,0	1,5	0,8	0,563		31,1				
	Level 2		DUCT	44	INSR-100	100	0,3		12,0	12,0	1,5	0,2		0,80	30,3	28,9			
	Level 2	32	SUPPLY		SHH-100	100			12,0	12,0	1,5	30,1			30,1		7,7	100	
	Level 2		DUCT	44	INSR-100	100	0,8		12,0	12,0	1,5	0,5		0,80	31,4	30,0			
	Level 2		BEND-90	44	INBU-100-90	100			12,0	12,0	1,5	0,8	0,563		31,0				
	Level 2		DUCT	44	INSR-100	100	0,3		12,0	12,0	1,5	0,2		0,80	30,2	28,8			
	Level 2	33	SUPPLY		SHH-100	100			12,0	12,0	1,5	30,0			30,0		7,7	100	
	Level 1		DUCT	44	INSR-200	200	2,8		32,0	32,0	1,0	0,3		0,11	33,4	32,8			
	Level 1	34	T-BRANCH	44	INTCU-200-2	200/200			32,0	32,0	1,0	1,5	2,333		33,1				
	Level 1		REDUCER	44	INRCFU-200	200/100			20,0	20,0	0,8				31,7				
	Level 1		DUCT	44	INSR-100	100	0,5		20,0	20,0	2,5	0,8		1,80	31,7	27,8			
	Level 1		BEND-90	44	INBU-100-90	100			20,0	20,0	2,5	1,9	0,488		30,8				
	Level 1		DUCT	44	INSR-100	100	0,3		20,0	20,0	2,5	0,5		1,80	28,9	25,0			
	Level 1	35	SUPPLY		SHH-100	100			20,0	20,0	2,5	28,4			28,4		14	100	
	Level 1		REDUCER	44	INRCFU-200	200/100			12,0	12,0	0,4				32,2				
	Level 1		DUCT	44	INSR-100	100	0,7		12,0	12,0	1,5	0,4		0,80	32,2	30,8			
	Level 1		BEND-90	44	INBU-100-90	100			12,0	12,0	1,5	0,8	0,563		31,7				
	Level 1		DUCT	44	INSR-100	100	0,3		12,0	12,0	1,5	0,2		0,80	30,9	29,5			
	Level 1	36	SUPPLY		SHH-100	100			12,0	12,0	1,5	30,7			30,7		7,6	100	
	Golv/Vinden		REDUCER	44	INRCFU-250	250/200			60,0	60,0	1,2				50,1				
	Level 3		DUCT	44	INSR-200	200	1,8		60,0	60,0	1,9	0,6		0,37	50,1	48,0			
	Level 3		BEND-90	44	INBU-200-90	200			60,0	60,0	1,9	0,9	0,433		49,5				
	Level 3		DUCT	44	INSR-200	200	2,8		60,0	60,0	1,9	1,0		0,37	48,5	46,4			
	Level 3		BEND-30	44	INBU-200-30	200			60,0	60,0	1,9	0,3	0,136		47,5				
	Level 3		DUCT	44	INSR-200	200	1,8		60,0	60,0	1,9	0,7		0,37	47,2	45,0			
	Level 3		BEND-60	44	MAGIB-C4-6	200			60,0	60,0	1,9	0,7	0,311		46,5				
	Level 3		DUCT	44	INSR-200	200	0,2		60,0	60,0	1,9	0,1		0,37	45,9	43,7			
	Level 3	11	T-BRANCH	44	INTCU-200-1	200/100			60,0	60,0	1,9	2,3	1,057		45,8				
	Level 3		DUCT	44	INSR-100	100	2,0		8,0	8,0	1,0	0,6		0,28	43,5	42,9			
	Level 3		BEND-90	44	INBU-100-90	100			8,0	8,0	1,0	0,4	0,631		42,9				
	Level 3		DUCT	44	INSR-100	100	0,4		8,0	8,0	1,0	0,1		0,28	42,5	41,9			
	Level 3		BEND-90	44	INBU-100-90	100			8,0	8,0	1,0	0,4	0,631		42,4				
	Level 3		DUCT	44	INSR-100	100	0,4		8,0	8,0	1,0	0,1		0,28	42,0	41,4			
	Level 3	12	SUPPLY		SHH-100	100			8,0	8,0	1,0	41,9			41,9		4,1	100	
	Level 3		DUCT	44	INSR-200	200	0,3		52,0	52,0	1,7	0,1		0,28	45,7	44,1			
	Level 3	13	T-BRANCH	44	INTCU-200-1	200/100			52,0	52,0	1,7	1,8	1,076		45,6				
	Level 3		DUCT	44	INSR-100	100	0,3		8,0	8,0	1,0	0,1		0,28	43,8	43,2			
	Level 3	14	SUPPLY		SHH-100	100			8,0	8,0	1,0	43,8			43,8		4,0	100	
	Level 2		DUCT	44	INSR-200	200	1,8		44,0	44,0	1,4	0,4		0,20	45,5	44,4			
	Level 2	15	T-BRANCH	44	INTCU-200-1	200/100			44,0	44,0	1,4	1,3	1,106		45,2				
	Level 2		DUCT	44	INSR-100	100	2,0		8,0	8,0	1,0	0,6		0,28	43,9	43,2			
	Level 2		BEND-90	44	INBU-100-90	100			8,0	8,0	1,0	0,4	0,631		43,3				
	Level 2		DUCT	44	INSR-100	100	0,9		8,0	8,0	1,0	0,2		0,28	42,9	42,3			
	Level 2		BEND-90	44	INBU-100-90	100			8,0	8,0	1,0	0,4	0,631		42,7				
	Level 2		DUCT	44	INSR-100	100	0,4		8,0	8,0	1,0	0,1		0,28	42,3	41,7			
	Level 2	16	SUPPLY		SHH-100	100			8,0	8,0	1,0	42,2			42,2		4,1	100	
	Level 2		DUCT	44	INSR-200	200	0,9		36,0	36,0	1,1	0,1		0,14	45,1	44,3			
	Level 2		T-BRANCH	44	INTCU-200-1	200/100			36,0	36,0	1,1	0,9	1,158		45,0				
	Level 2		DUCT	44	INSR-100	100	0,3		8,0	8,0	1,0	0,1		0,28	44,1	43,4			
	Level 2	18	SUPPLY		SHH-100	100			8,0	8,0	1,0	44,0			44,0		4,0	100	
	Level 1		DUCT	44	INSR-200	200	1,8		28,0	28,0	0,9	0,2		0,09	44,9	44,5			
	Level 1.1	39	T-BRANCH	44	INTCU-200-1	200/100			28,0	28,0	0,9	0,6	1,261		44,8				
	Level 1.1		DUCT	44	INSR-100	100	2,0		8,0	8,0	1,0	0,6		0,28	44,2	43,6			
	Level 1.1		BEND-90	44	INBU-100-90	100			8,0	8,0	1,0	0,4	0,631		43,6				
	Level 1.1		DUCT	44	INSR-100	100	0,9		8,0	8,0	1,0	0,2		0,28	43				

Appendix E



Hydronic Network Balancing Report

Project Information			
Software version:	MagiCAD for Revit 2023 UR-2	Calculation date:	2024-04-09 14:22
Project name:	Project Name	Project number:	0001
Project address:	Enter address here	Client name:	Owner
Project issue date:	Issue Date	Organization name:	
Organization description:		Author:	

Project Calculation Data			
Total pressure:	37015.9 Pa	Systems:	Hydronic Supply / Hydronic Return
Fluid type:	Water	Total flow:	1.2 l/s
Fluid density:	988 / 990.9 kg/m3	Fluid temperature:	49 / 43 °C
Fluid spec. heat capacity:	4180 / 4179 J/kg*K	Fluid dyn. viscosity:	0.00055723 / 0.00061428 Pa*s
		Volume of the system:	360.0 l
Pipe series:	Standard / Material	Thermal conductivity:	
Copper and copper alloys - Seaml	Default / Metal		20.00000 W/m*K

Calculation Input Values			
Pressure drop standard(s):	Default	Ambient air temperature(s):	21.0°C
Min. dp radiator valves:	3.0 Pa	Balancing target pressure:	Minimum

Calculation Results / Supply

Location	Level	Node	Type	Series	Product	Size	L [m]	Insulation	P [W]	qv [l/s]	v [m/s]	T [°C]	Q [W]	dp/L [Pa/m]	dpt [Pa]	K factor	pt [Pa]	adj.	Warnings
	Level 0		PIPE	17	EN 1057 - R250		1.3		28510	1.2	0.69	48.9	58.2	98.4	130.8		37015.9		
	Level 0	76	BRANCH	17	Tee Soldered50/50				28510	1.2	0.69				232.3	1.000	36885.1		
	Level 0		REDUCER	17	Reducer Stra 50/32				9990	0.4	0.23				44.1	0.256	36652.8		
	Level 0		PIPE	17	EN 1057 - R232		1.0		9990	0.4	0.59	48.9	26.8	134.0	128.3		36608.7		
	Level 0	77	BRANCH	17	Tee Soldered32/32				9990	0.4	0.59				172.2	1.000	36480.4		
	Level 0		PIPE	17	EN 1057 - R232		3.3		6990	0.3	0.43	48.9	91.3	76.6	250.0		36308.2		
	Level 0	2	BRANCH	17	Tee Soldered32/32				6990	0.3	0.43				91.5	1.000	36058.2		
	Level 0		REDUCER	17	Reducer Stra 32/20				3010	0.1	0.19				35.2	0.269	35966.7		
	Level 0		PIPE	17	EN 1057 - R220		3.0		3010	0.1	0.51	48.8	52.7	198.3	599.0		35931.5		
	Level 0	78	BRANCH	17	Tee Soldered20/20				3010	0.1	0.51				130.9	1.000	35332.5		
	Level 0		PIPE	17	EN 1057 - R220		0.5		1300	0.1	0.22	48.7	9.5	46.2	25.1		35201.5		
	Level 0		BEND-90	17	Elbow Solder 20				1300	0.1	0.22				10.1	0.414	35176.4		
	Level 0		PIPE	17	EN 1057 - R220		2.1		1300	0.1	0.22	48.7	37.0	46.2	25.1		35166.3		
	Level 0		REDUCER	17	Reducer Stra 20/10				1300	0.1	0.22				211.0	0.337	35067.8		
	Level 1	79	RADIATOR V17		RA-N_Straig 10 (L)				1300	0.1					33070.9		34856.8	7.0	
	Level 0	80	HEATING: R		TPV4 22-914 20				1300	0.1		48.5					1785.9		
	Level 0		PIPE	17	EN 1057 - R220		1.6		1710	0.1	0.29	48.7	27.9	74.2	118.9		35332.5		
	Level 0		BEND-90	17	Elbow Solder 20				1710	0.1	0.29				17.5	0.414	35213.6		
	Level 0		PIPE	17	EN 1057 - R220		3.5		1710	0.1	0.29	48.6	61.3	74.2	262.5		35196.0		
	Level 0		BEND-90	17	Elbow Solder 20				1710	0.1	0.29				17.5	0.414	34933.5		
	Level 0		PIPE	17	EN 1057 - R220		1.3		1710	0.1	0.29	48.4	22.6	74.2	97.4		34916.0		
	Level 3		BEND-90	17	Elbow Solder 20				1710	0.1	0.29				17.5	0.414	34818.6		
	Level 3		PIPE	17	EN 1057 - R220		0.6		1710	0.1	0.29	48.3	9.8	74.2	42.2		34801.1		
	Level 1	27	BRANCH	17	Tee Soldered20/20 (L)				1710	0.1	0.29				42.3	1.000	34758.9		
	Level 1		PIPE	17	EN 1057 - R220		0.1		750	0.0	0.13	48.3	1.9	18.0	2.0		34716.6		
	Level 1	28	RADIATOR V17		RA-N_Straig 10 (L)				750	0.0					32504.6		34714.6	4.9	
	Level 1	29	HEATING: R		TPV4 22-612 20				750	0.0		48.3					2210.1		
	Level 1		REDUCER	17	Reducer Stra 20/16				960	0.0	0.16				6.0	0.166	34758.9		
	Level 3		PIPE	17	EN 1057 - R216		3.0		960	0.0	0.27	48.3	41.3	89.8	270.2		34752.9		
	Level 2	7	BRANCH	17	Tee Soldered16/16				960	0.0	0.27				36.4	1.000	34482.6		
	Level 2		PIPE	17	EN 1057 - R216		0.2		480	0.0	0.14	48.1	2.2	27.4	4.5		34446.2		
	Level 2	8	RADIATOR V17		RA-N_Straig 10 (L)				480	0.0					31943.0		34441.7	3.3	
	Level 2	9	HEATING: R		TPV4 22-410 15				480	0.0		48.0					2498.7		
	Level 3		PIPE	17	EN 1057 - R216		3.0		480	0.0	0.14	48.1	41.1	27.4	83.0		34482.6		
	Level 3		BEND-90	17	Elbow Solder 16				480	0.0	0.14				3.6	0.396	34399.7		
	Level 3		PIPE	17	EN 1057 - R216		0.2		480	0.0	0.14	47.6	2.2	27.4	4.4		34396.1		
	Level 3	10	RADIATOR V17		RA-N_Straig 10 (L)				480	0.0					31614.2		34391.6	3.3	
	Level 3	11	HEATING: R		TPV4 22-410 15				480	0.0		47.6					2577.4		
	Level 0		REDUCER	17	Reducer Stra 32/25				3980	0.2	0.25				14.9	0.173	36058.2		
	Level 0		PIPE	17	EN 1057 - R225		2.0		3980	0.2	0.42	48.8	43.7	100.8	202.1		36043.3		
	Level 0	81	BRANCH	17	Tee Soldered25/25				3980	0.2	0.42				85.9	1.000	35841.2		
	Level 0		REDUCER	17	Reducer Stra 25/20				1300	0.1	0.14				4.0	0.163	35755.3		
	Level 0		PIPE	17	EN 1057 - R220		0.5		1300	0.1	0.22	48.7	9.1	46.2	24.0		35751.4		
	Level 0		BEND-90	17	Elbow Solder 20				1300	0.1	0.22				10.1	0.414	35727.3		
	Level 0		PIPE	17	EN 1057 - R220		1.3		1300	0.1	0.22	48.7	22.4	46.2	59.5		35717.2		
	Level 1		BEND-90	17	Elbow Solder 20				1300	0.1	0.22				10.1	0.414	35657.7		
	Level 1		PIPE	17	EN 1057 - R220		0.0		1300	0.1	0.22	48.6	0.5	46.2	1.4		35647.6		
	Level 1		REDUCER	17	Reducer Stra 20/10				1300	0.1	0.22				211.0	0.337	35646.2		
	Level 1	82	RADIATOR V17		RA-N_Straig 10 (L)				1300	0.1					34149.1		35435.2	7.0	
	Level 0	83	HEATING: R		TPV4 22-914 20				1300	0.1		48.6					1286.1		
	Level 0		REDUCER	17	Reducer Stra 25/20				2680	0.1	0.28				16.9	0.163	35841.2		
	Level 0		PIPE	17	EN 1057 - R220		1.4		2680	0.1	0.46	48.7	24.6	161.8	228.8		35824.3		
	Level 2		BEND-90	17	Elbow Solder 20				2680	0.1	0.46				43.0	0.414	35595.5		
	Level 2		PIPE	17	EN 1057 - R220		0.6		2680	0.1	0.46	48.7	9.9	161.8	92.1		35552.5		

Location	Level	Node	Type	Series	Product	Size	L [m]	Insulation	P [W]	qv [l/s]	v [m/s]	T [°C]	Q [W]	dpL [Pa/m]	dpt [Pa]	K factor	pt [Pa]	adj.	Warnings
	Level 2	14	BRANCH	17	Tee Soldered	20/20			2680	0,1	0,46				103,8	1,000	35460,5		
	Level 2		REDUCER	17	Reducer Stra	20/16			760	0,0	0,13				3,8	0,166	35356,7		
	Level 2		PIPE	17	EN 1057 - R216		0,6		760	0,0	0,21	48,7	8,3	60,1	35,9		35352,9		
	Level 1	15	RADIATOR V17		RA-N_Straig	10 (L)			760	0,0					33739,5		35317,0	4,8	
	Level 1	16	HEATING: R		TPv4 22-611	15			760	0,0		48,6					1577,5		
	Level 2		PIPE	17	EN 1057 - R220		3,0		1920	0,1	0,33	48,7	52,4	90,7	274,0		35460,5		
	Level 2	17	BRANCH	17	Cross Solder	20/20/20			1920	0,1	0,33				53,3	1,000	35186,4		
	Level 2		REDUCER	17	Reducer Stra	20/16			480	0,0	0,08				1,5	0,166	35133,2		
	Level 2		PIPE	17	EN 1057 - R216		1,1		480	0,0	0,14	48,5	15,4	27,4	30,5		35131,7		
	Level 2	18	RADIATOR V17		RA-N_Straig	10 (L)			480	0,0					33252,5		35101,1	3,3	
	Level 2	19	HEATING: R		TPv4 22-410	15			480	0,0		48,3					1848,6		
	Level 2		REDUCER	17	Reducer Stra	20/16			480	0,0	0,08				1,5	0,166	35133,2		
	Level 2		PIPE	17	EN 1057 - R216		0,6		480	0,0	0,14	48,5	8,9	27,4	17,7		35131,7		
	Level 2	20	RADIATOR V17		RA-N_Straig	10 (L)			480	0,0					33275,7		35113,9	3,3	
	Level 2	21	HEATING: R		TPv4 22-410	15			480	0,0		48,4					1838,3		
	Level 2		REDUCER	17	Reducer Stra	20/16			960	0,0	0,16				6,0	0,166	35186,4		
	Level 3		PIPE	17	EN 1057 - R216		3,0		960	0,0	0,27	48,5	41,6	89,8	270,3		35180,4		
	Level 3	22	BRANCH	17	Tee Soldered	16/16			960	0,0	0,27				36,4	1,000	34910,2		
	Level 3		PIPE	17	EN 1057 - R216		1,1		480	0,0	0,14	48,3	15,5	27,4	31,1		34873,8		
	Level 3	23	RADIATOR V17		RA-N_Straig	10 (L)			480	0,0					32674,6		34842,7	3,3	
	Level 3	24	HEATING: R		TPv4 22-410	15			480	0,0		48,1					2168,1		
	Level 3		PIPE	17	EN 1057 - R216		0,7		480	0,0	0,14	48,3	9,1	27,4	18,3		34873,8		
	Level 3	25	RADIATOR V17		RA-N_Straig	10 (L)			480	0,0					32697,9		34855,5	3,3	
	Level 3	26	HEATING: R		TPv4 22-410	15			480	0,0		48,2					2157,6		
	Level 0		REDUCER	17	Reducer Stra	32/20			2600	0,1	0,16				26,3	0,269	36480,4		
	Level 0		PIPE	17	EN 1057 - R220		1,1		2600	0,1	0,44	48,9	18,7	153,4	164,1		36454,2		
	Level 0	84	BRANCH	17	Tee Soldered	20/20			2600	0,1	0,44				97,7	1,000	36290,1		
	Level 0		PIPE	17	EN 1057 - R220		0,7		1300	0,1	0,22	48,8	12,3	46,2	32,5		36192,4		
	Level 1		BEND-90	17	Elbow Solder	20			1300	0,1	0,22				10,1	0,414	36160,0		
	Level 1		PIPE	17	EN 1057 - R220		0,6		1300	0,1	0,22	48,8	9,9	46,2	26,3		36149,8		
	Level 1		BEND-90	17	Elbow Solder	20			1300	0,1	0,22				10,1	0,414	36123,6		
	Level 1		PIPE	17	EN 1057 - R220		0,1		1300	0,1	0,22	48,7	0,9	46,2	2,5		36113,5		
	Level 1		REDUCER	17	Reducer Stra	20/10			1300	0,1	0,22				211,0	0,337	36111,0		
	Level 1	85	RADIATOR V17		RA-N_Straig	10 (L)			1300	0,1					35023,1		35900,0	7,0	
	Level 1	86	HEATING: R		TPv4 22-914	20			1300	0,1		48,7					876,9		
	Level 0		PIPE	17	EN 1057 - R220		1,5		1300	0,1	0,22	48,8	25,5	46,2	67,5		36290,1		
	Level 0		BEND-90	17	Elbow Solder	20			1300	0,1	0,22				10,1	0,414	36222,6		
	Level 0		PIPE	17	EN 1057 - R220		0,7		1300	0,1	0,22	48,7	12,2	46,2	32,3		36212,5		
	Level 1		BEND-90	17	Elbow Solder	20			1300	0,1	0,22				10,1	0,414	36180,2		
	Level 1		PIPE	17	EN 1057 - R220		0,6		1300	0,1	0,22	48,7	9,9	46,2	26,2		36170,1		
	Level 1		BEND-90	17	Elbow Solder	20			1300	0,1	0,22				10,1	0,414	36143,8		
	Level 1		PIPE	17	EN 1057 - R220		0,1		1300	0,1	0,22	48,6	0,9	46,2	2,5		36133,7		
	Level 1		REDUCER	17	Reducer Stra	20/10			1300	0,1	0,22				211,0	0,337	36131,2		
	Level 1	87	RADIATOR V17		RA-N_Straig	10 (L)			1300	0,1					34987,9		35920,3	7,0	
	Level 1	88	HEATING: R		TPv4 22-914	20			1300	0,1		48,6					932,4		
	Level 0		REDUCER	17	Reducer Stra	50/40			18920	0,8	0,45				40,8	0,157	36652,8		
	Level 0		PIPE	17	EN 1057 - R240		0,9		18920	0,8	0,73	48,9	33,0	145,3	137,0		36612,0		
	Level 0	27	BRANCH	17	Tee Soldered	40/40			18920	0,8	0,73				260,4	1,000	36475,0		
	Level 0		REDUCER	17	Reducer Stra	40/20			2860	0,1	0,11				38,5	0,326	36214,5		
	Level 1		PIPE	17	EN 1057 - R220		0,7		2860	0,1	0,49	48,9	11,7	181,3	121,4		36176,0		
	Level 0	28	BRANCH	17	Tee Soldered	20/20			2860	0,1	0,49				118,2	1,000	36054,7		
	Level 0		REDUCER	17	Reducer Stra	20/16			1560	0,1	0,27				15,9	0,166	35936,5		
	Level 0		PIPE	17	EN 1057 - R216		3,2		1560	0,1	0,44	48,8	44,6	208,3	664,7		35920,5		
	Level 0		BEND-90	17	Elbow Solder	16			1560	0,1	0,44				38,1	0,396	35255,8		
	Level 0		PIPE	17	EN 1057 - R216		6,1		1560	0,1	0,44	48,7	85,4	208,3	1279,5		35217,7		
	Level 1		BEND-90	17	Elbow Solder	16			1560	0,1	0,44				38,1	0,396	33938,2		
	Level 1		PIPE	17	EN 1057 - R216		0,2		1560	0,1	0,44	48,4	3,3	208,3	50,6		33900,2		
	Level 1		BEND-90	17	Elbow Solder	16			1560	0,1	0,44				38,1	0,396	33849,6		
	Level 1		PIPE	17	EN 1057 - R216		0,6		1560	0,1	0,44	48,4	8,0	208,3	121,1		33811,5		
	Level 1	29	BRANCH	17	Tee Soldered	16/16			1560	0,1	0,44				96,1	1,000	33690,4		
	Level 1		PIPE	17	EN 1057 - R216		0,1		600	0,0	0,17	48,3	1,7	40,1	5,1		33594,3		
	Level 1	74	RADIATOR V17		RA-N_Straig	10 (L)			600	0,0					30241,5		33589,3	3,9	
	Level 1	75	HEATING: R		TPv4 21-611	15			600	0,0		48,3					3347,7		
	Level 1		PIPE	17	EN 1057 - R216		3,0		960	0,0	0,27	48,3	41,6	89,8	272,0		33690,4		
	Level 2	32	BRANCH	17	Tee Soldered	16/16 (L)			960	0,0	0,27				36,4	1,000	33418,4		
	Level 2		PIPE	17	EN 1057 - R216		0,1		480	0,0	0,14	48,1	1,7	27,4	3,4		33382,0		
	Level 2	33	RADIATOR V17		RA-N_Straig	10 (L)			480	0,0					29753,9		33378,6	3,4	
	Level 2	34	HEATING: R		TPv4 22-410	15			480	0,0		48,1					3624,7		
	Level 1		PIPE	17	EN 1057 - R216		3,0		480	0,0	0,14	48,1	41,2	27,4	83,0		33418,4		
	Level 1		BEND-90	17	Elbow Solder	16 (L)			480	0,0	0,14				3,6	0,396	33335,4		
	Level 3		PIPE	17	EN 1057 - R216		0,1		480	0,0	0,14	47,6	1,6	27,4	3,3		33331,8		
	Level 3	35	RADIATOR V17		RA-N_Straig	10 (L)			480	0,0					29625,2		33328,5	3,4	
	Level 3	36	HEATING: R		TPv4 22-410	15			480	0,0		47,6					3703,4		
	Level 1		PIPE	17	EN 1057 - R220 (L)		1,2		1300	0,1	0,22	48,8	20,4	46,2	53,9		36054,7		
	Level 1		BEND-90	17	Elbow Solder	20			1300	0,1	0,22				10,1	0,414	36000,8		
	Level 1		PIPE	17	EN 1057 - R220 (L)		0,6		1300	0,1	0,22	48,8	9,9	46,2	26,2		35990,7		
	Level 1		BEND-90	17	Elbow Solder	20			1300	0,1	0,22				10,1	0,414	35964,4		
	Level 1		PIPE	17	EN 1057 - R220		0,1		1300	0,1	0,22	48,7	1,5	46,2	3,9		35954,3		
	Level 1		REDUCER	17	Reducer Stra	20/10			1300	0,1	0,22				211,0	0,337	35950,4		
	Level 1	89	RADIATOR V17		RA-N_Straig	10 (L)			1300	0,1					34610,8		35739,5	7,0	

Location	Level	Node	Type	Series	Product	Size	L [m]	Insulation	P [W]	qv [l/s]	v [m/s]	T [°C]	Q [W]	dpl [Pa/m]	dpt [Pa]	K factor	pt [Pa]	adj.	Warnings
	Level 1	90	HEATING: R		TPv4 22-914 20				1300	0,1		48,7					1128,6		
	Level 1		PIPE	17	EN 1057 - R240		0,8		16060	0,7	0,62	48,9	28,2	108,1	87,3		36214,5		
	Level 0	39	BRANCH	17	Tee Soldered40/40				16060	0,7	0,62					187,7	1,000	36127,3	
	Level 0		REDUCER	17	Reducer Stra 40/32				8620	0,4	0,33					22,0	0,158	35939,6	
	Level 0		PIPE	17	EN 1057 - R232		1,5		8620	0,4	0,53	48,9	40,6	111,0	161,1		35917,6		
	Level 1		BEND-90	17	Elbow Solder 32				8620	0,4	0,53					61,3	0,440	35756,5	
	Level 1		PIPE	17	EN 1057 - R232		4,5		8620	0,4	0,53	48,8	125,9	111,0	499,8		35695,3		
	Level 1		BEND-90	17	Elbow Solder 32				8620	0,4	0,53					61,3	0,440	35195,5	
	Level 1		PIPE	17	EN 1057 - R232		0,5		8620	0,4	0,53	48,8	15,2	111,0	60,4		35134,2		
	Level 1	40	BRANCH	17	Cross Solder 32/32/32				8620	0,4	0,53					139,2	1,000	35073,8	
	Level 1		REDUCER	17	Reducer Stra 32/16				1510	0,1	0,09					29,6	0,329	34934,7	
	Level 1		PIPE	17	EN 1057 - R216		0,9		1510	0,1	0,43	48,7	11,9	196,8	168,6		34905,1		
	Level 1	41	RADIATOR V17		RA-N_Straig 10 (L)				1510	0,1						32695,4		34736,5	7,1
	Level 1	42	HEATING: R		TPv4 22-623 15				1510	0,1		48,7						2041,1	
	Level 1		REDUCER	17	Reducer Stra 32/16				1510	0,1	0,09					29,6	0,329	34934,7	
	Level 1		PIPE	17	EN 1057 - R216		0,8		1510	0,1	0,43	48,7	11,2	196,8	158,2		34905,1		
	Level 1	43	RADIATOR V17		RA-N_Straig 10 (L)				1510	0,1						32693,1		34746,8	7,1
	Level 1	44	HEATING: R		TPv4 22-623 15				1510	0,1		48,7						2053,7	
	Level 1		REDUCER	17	Reducer Stra 32/25				5600	0,2	0,34					29,4	0,173	35073,8	
	Level 1		PIPE	17	EN 1057 - R225		3,0		5600	0,2	0,59	48,7	64,9	184,0	548,3		35044,4		
	Level 2	45	BRANCH	17	Cross Solder 25/25/25				5600	0,2	0,59					170,0	1,000	34496,1	
	Level 2		REDUCER	17	Reducer Stra 25/16				1300	0,1	0,14					17,6	0,264	34326,1	
	Level 2		PIPE	17	EN 1057 - R216		0,9		1300	0,1	0,37	48,7	12,2	151,7	133,3		34308,4		
	Level 2	46	RADIATOR V17		RA-N_Straig 10 (L)				1300	0,1						31603,2		34175,1	7,0
	Level 2	47	HEATING: R		TPv4 22-523 15				1300	0,1		48,6						2572,0	
	Level 2		REDUCER	17	Reducer Stra 25/16				1300	0,1	0,14					17,6	0,264	34326,1	
	Level 2		PIPE	17	EN 1057 - R216		0,8		1300	0,1	0,37	48,7	11,3	151,7	123,4		34308,4		
	Level 2	48	RADIATOR V17		RA-N_Straig 10 (L)				1300	0,1						31605,4		34185,0	7,0
	Level 2	49	HEATING: R		TPv4 22-523 15				1300	0,1		48,6						2579,6	
	Level 2		REDUCER	17	Reducer Stra 25/20				3000	0,1	0,31					21,2	0,163	34496,1	
	Level 1		PIPE	17	EN 1057 - R220		3,0		3000	0,1	0,51	48,7	52,1	197,2	591,0		34474,9		
	Level 1	50	BRANCH	17	Tee Soldered20/20				3000	0,1	0,51					130,1	1,000	33883,9	
	Level 1		REDUCER	17	Reducer Stra 20/16				1500	0,1	0,26					14,7	0,166	33753,9	
	Level 1		PIPE	17	EN 1057 - R216		1,2		1500	0,1	0,42	48,6	17,1	194,5	240,3		33739,1		
	Level 3	51	RADIATOR V17		RA-N_Straig 10 (L)				1500	0,1						30077,8		33498,8	7,1
	Level 3	52	HEATING: R		TPv4 22-916 15				1500	0,1		48,5						3421,0	
	Level 1		REDUCER	17	Reducer Stra 20/16				1500	0,1	0,26					14,7	0,166	33753,9	
	Level 1		PIPE	17	EN 1057 - R216		1,2		1500	0,1	0,42	48,6	16,2	194,5	227,6		33739,1		
	Level 3	53	RADIATOR V17		RA-N_Straig 10 (L)				1500	0,1						30081,2		33511,5	7,1
	Level 3	54	HEATING: R		TPv4 22-916 15				1500	0,1		48,5						3430,3	
	Level 0		REDUCER	17	Reducer Stra 40/32				7440	0,3	0,29					16,4	0,158	36127,3	
	Level 0		PIPE	17	EN 1057 - R232		4,5		7440	0,3	0,46	48,9	125,2	85,5	382,7		36110,9		
	Level 1		BEND-90	17	Elbow Solder 32				7440	0,3	0,46					45,6	0,440	35728,2	
	Level 1		PIPE	17	EN 1057 - R232		6,3		7440	0,3	0,46	48,8	174,8	85,5	536,1		35682,6		
	Level 2		BEND-90	17	Elbow Solder 32				7440	0,3	0,46					45,6	0,440	35146,4	
	Level 2		PIPE	17	EN 1057 - R232		0,5		7440	0,3	0,46	48,6	15,1	85,5	46,5		35100,8		
	Level 1	55	BRANCH	17	Cross Solder 32/32/32				7440	0,3	0,46					103,7	1,000	35054,2	
	Level 1		REDUCER	17	Reducer Stra 32/16				1000	0,0	0,06					13,0	0,329	34950,6	
	Level 1		PIPE	17	EN 1057 - R216		0,8		1000	0,0	0,28	48,6	10,9	96,3	75,4		34937,6		
	Level 1	56	RADIATOR V17		RA-N_Straig 10 (L)				1000	0,0						32761,6		34862,2	5,9
	Level 1	57	HEATING: R		TPv4 22-614 15				1000	0,0		48,6						2100,6	
	Level 1		REDUCER	17	Reducer Stra 32/16				840	0,0	0,05					9,2	0,329	34950,6	
	Level 1		PIPE	17	EN 1057 - R216		1,0		840	0,0	0,24	48,6	13,6	71,3	69,9		34941,4		
	Level 1		BEND-90	17	Elbow Solder 16				840	0,0	0,24					11,0	0,396	34871,5	
	Level 1		PIPE	17	EN 1057 - R216		3,1		840	0,0	0,24	48,5	43,4	71,3	224,2		34860,5		
	Level 1	61	RADIATOR V17		RA-N_Straig 10 (L)				840	0,0						32279,4		34636,3	5,3
	Level 1	62	HEATING: R		TPv4 22-613 15				840	0,0		48,2						2357,0	
	Level 1		REDUCER	17	Reducer Stra 32/25				5600	0,2	0,34					29,4	0,173	35054,2	
	Level 2		PIPE	17	EN 1057 - R225		3,0		5600	0,2	0,59	48,6	64,6	184,0	548,3		35024,8		
	Level 2	63	BRANCH	17	Cross Solder 25/25/25				5600	0,2	0,59					170,0	1,000	34476,5	
	Level 2		REDUCER	17	Reducer Stra 25/16				1300	0,1	0,14					17,6	0,264	34306,5	
	Level 2		PIPE	17	EN 1057 - R216		0,8		1300	0,1	0,37	48,6	11,5	151,7	126,3		34288,8		
	Level 2	64	RADIATOR V17		RA-N_Straig 10 (L)				1300	0,1						31424,6		34162,6	7,0
	Level 2	65	HEATING: R		TPv4 22-523 15				1300	0,1		48,5						2737,9	
	Level 2		REDUCER	17	Reducer Stra 25/16				1300	0,1	0,14					17,6	0,264	34306,5	
	Level 2		PIPE	17	EN 1057 - R216		0,9		1300	0,1	0,37	48,6	11,9	151,7	130,5		34288,8		
	Level 2	66	RADIATOR V17		RA-N_Straig 10 (L)				1300	0,1						31389,7		34158,4	7,0
	Level 2	67	HEATING: R		TPv4 22-523 15				1300	0,1		48,5						2768,7	
	Level 2		REDUCER	17	Reducer Stra 25/20				3000	0,1	0,31					21,2	0,163	34476,5	
	Level 3		PIPE	17	EN 1057 - R220		3,0		3000	0,1	0,51	48,6	51,8	197,2	591,0		34455,3		
	Level 3	68	BRANCH	17	Tee Soldered20/20				3000	0,1	0,51					130,1	1,000	33864,3	
	Level 3		REDUCER	17	Reducer Stra 20/16				1500	0,1	0,26					14,7	0,166	33734,3	
	Level 3		PIPE	17	EN 1057 - R216		1,2		1500	0,1	0,42	48,5	16,4	194,5	231,3		33719,5		
	Level 3	69	RADIATOR V17		RA-N_Straig 10 (L)				1500	0,1						29904,8		33488,3	7,1
	Level 3	70	HEATING: R		TPv4 22-916 15				1500	0,1		48,4						3583,4	
	Level 3		REDUCER	17	Reducer Stra 20/16				1500	0,1	0,26					14,7	0,166	33734,3	
	Level 3		PIPE	17	EN 1057 - R216		1,2		1500	0,1	0,42	48,5	16,8	194,5	236,7		33719,5		
	Level 3	71	RADIATOR V17		RA-N_Straig 10 (L)				1500	0,1						29859,7		33482,9	7,1
	Level 3	72	HEATING: R		TPv4 22-916 15				1500	0,1		48,4						3623,1	

Figure 59. Balancing and sizes of the supply piping, with an illustration of the critical path in building A.

Appendix F

Table 28. Detailed description of the retrofitting costs related to building A.

Type	Specification	Price /SEK	Note	Source
Ventilation	AHU	140 000	Replaced every 20 years.	Wikells
	Ducts and bends	96 000	(-)	Lindab webshop
	Diffusers	25 000	(-)	Lindab webshop
	Inlet & outlet	7 000	(-)	Lindab webshop
	Filter	1 500	Replaced every year.	Luftbutikens webshop
	Core drilling	165 000	Includes labor.	GK
	Fire sealant	7 000	Includes labor.	Wikells
	Adjustment of system	16 000	Performed every 20 years.	GK
	Labor	100 000	All except core drilling, adjustment, and fire sealant.	Wikells
Heating	HP & tank	390 000	Replaced once during the calculation period.	Wikells, Velltra, VVSButiken
	Radiators	115 000	(-)	Bygghemma
	Pipes & bends	25 000	(-)	Bauhaus, Golvvarmebutiken
	Thermostats	7 000	Replaced every 10 years.	Amazon
	Circulation pumps	35 000	Replaced every 10 years.	Bygghemma
	Core drilling	26 000	Includes labor.	GK
	Fire sealant	4 000	Includes labor.	Wikells
	Labor	180 000	All except core drilling, and fire sealant.	Wikells
Facade	Scaffolding	75 000	Included in each façade retrofitting.	Wikells
	Rockwool 50 /mm	428 000	Serporoc system	Wikells
	Rockwool 80 /mm	440 000	Serporoc system	Wikells
	Rockwool 100 /mm	450 000	Serporoc system	Wikells
	EPS 50 /mm	326 000	StoTherm Vario	Wikells
	EPS 80 /mm	333 000	StoTherm Vario	Wikells
	EPS 100 /mm	355 000	StoTherm Vario	Wikells
	Labor	(-)	Is included in each set.	
Roof	Scaffolding	(-)	The work was performed from the interior.	Wikells
	Mineral wool	63 000	(-)	Wikells/Bygghemma
	Rockwool	74 000	(-)	Wikells/Bygghemma
	Cellulose	63 000	(-)	Wikells/Bygghemma
	PE-membrane, duct-tape	59 000	Included in each roof retrofitting.	Wikells
	Gypsum board	63 000	Included in each roof retrofitting.	Wikells
	Labor	(-)	Included in each set.	
Window	Scaffolding	18 000	The windows are only being replaced on one façade.	Wikells
	Demolition of existing windows	7 000	Included in each retrofitting.	Wikells
	Painted <i>U-value</i> : 1.2	136 000	Painted once during the calculation period.	Beijerbygg
	Painted <i>U-value</i> : 0.9	143 000	Painted once during the calculation period.	Beijerbygg
	Alu <i>U-value</i> : 1.2	158 000	No maintenance.	Beijerbygg
	Alu <i>U-value</i> : 0.9	166 000	No maintenance.	Beijerbygg
	Labor	56 000	A complete package for finishing the window installation. Included in each window retrofitting.	Wikells

Appendix G



Ductwork Balancing Report

Project Information			
Software version:	MagiCAD for Revit 2023 UR-2	Calculation date:	2024-05-10 16:25
Project name:	Project Name	Project number:	Project Number
Project address:	Enter address here	Client name:	Owner
Project issue date:	Issue Date	Organization name:	
Organization description:		Author:	

Project Calculation Data			
Systems:	- / - / - / -	Total pressure:	74.4 Pa
Total flow:	160.0 l/s		

Calculation Input Values			
Air Density:	1.20 kg/m ³	Air Dynamic Viscosity:	0.00001813 Pa*s
Min. dp air devices:	20.0 Pa	Balancing target pressure:	Minimum
Out of dp-range warning tolerance:	0 %		

Calculation Results / Supply																			
Location	Level	Node	Type	Series	Product	Size	L [m]	Insulation	qv set [l/s]	qv [l/s]	v [m/s]	dpt [Pa]	K factor	dp/L [Pa/m]	pt [Pa]	pst [Pa]	adj.	qv [%]	Warnings
	Basement	28	AHE/AHU		Acon_05113_				160.0	160.0		+50.0			26.3				Inufficient dp
	Basement		REDUCER	44	INRCFU-315-315/250				160.0	160.0	2.1	0.2	0.033		74.4				
	Basement		DUCT	44	INSR-250 (250 (L))		0.3		160.0	160.0	3.3	0.3		0.77	74.2	67.9			
	Basement	29	T-BRANCH	44	INTCU-250-2 250/250				160.0	160.0	3.3	7.1	1.108		74.0				
	Basement		REDUCER	44	INRCFU-250-250/200				36.0	36.0	0.7				66.9				
	Basement		DUCT	44	INSR-200 (200)		4.6		36.0	36.0	1.1	0.6		0.14	66.9	66.1			
	Tak		BEND-90	44	INBU-200-90 200				36.0	36.0	1.1	0.4	0.500		66.3				
	Tak		DUCT	44	INSR-200 (200)		4.0		36.0	36.0	1.1	0.6		0.14	65.9	65.1			
	Level 1		T-BRANCH	44	INTCU-200-1 200/100				36.0	36.0	1.1	0.9	1.158		65.3				
	Level 1		DUCT	44	INSR-100 (100)		0.7		8.0	8.0	1.0	0.2		0.28	64.4	63.8			
	Level 1		BEND-90	44	INBU-100-90 100				8.0	8.0	1.0	0.4	0.631		64.2				
	Level 1		DUCT	44	INSR-100 (100)		0.2		8.0	8.0	1.0	0.1		0.28	63.8	63.2			
	Level 1	9	SUPPLY		SHH-100 (100)				8.0	8.0	1.0	63.7			63.7		3.3	100	
	Level 1		DUCT	44	INSR-200 (200)		0.6		28.0	28.0	0.9	0.1		0.09	65.3	64.6			
	Level 1		BEND-90	44	INBU-200-90 200				28.0	28.0	0.9	0.3	0.536		65.2				
	Level 1		DUCT	44	INSR-200 (200 (L))		0.3		28.0	28.0	0.9	0.0		0.09	65.0	64.5			
	Level 1		BEND-90	44	INBU-200-90 200				28.0	28.0	0.9	0.3	0.536		64.9				
	Level 1		DUCT	44	INSR-200 (200)		1.9		28.0	28.0	0.9	0.2		0.09	64.7	64.2			
	Level 2	10	T-BRANCH	44	INTCU-200-1 200/100				28.0	28.0	0.9	0.6	1.261		64.5				
	Level 2		DUCT	44	INSR-100 (100)		0.8		8.0	8.0	1.0	0.2		0.28	63.9	63.3			
	Level 2		BEND-90	44	INBU-100-90 100				8.0	8.0	1.0	0.4	0.631		63.7				
	Level 2		DUCT	44	INSR-100 (100)		0.3		8.0	8.0	1.0	0.1		0.28	63.3	62.7			
	Level 2	11	SUPPLY		SHH-100 (100)				8.0	8.0	1.0	63.2			63.2		3.3	100	
	Level 1		DUCT	44	INSR-200 (200)		2.9		20.0	20.0	0.6	0.1		0.05	64.5	64.2			
	Level 3	12	T-BRANCH	44	INTCU-200-1 200/100				20.0	20.0	0.6	0.4	1.512		64.3				
	Level 3		DUCT	44	INSR-100 (100)		0.8		8.0	8.0	1.0	0.2		0.28	64.0	63.4			
	Level 3		BEND-90	44	INBU-100-90 100				8.0	8.0	1.0	0.4	0.631		63.8				
	Level 3		DUCT	44	INSR-100 (100)		0.3		8.0	8.0	1.0	0.1		0.28	63.4	62.7			
	Level 3	13	SUPPLY		SHH-100 (100)				8.0	8.0	1.0	63.3			63.3		3.3	100	
	Level 3		REDUCER	44	INRCFU-200-200/100				12.0	12.0	0.4				64.1				
	Level 3		DUCT	44	INSR-100 (100)		0.6		12.0	12.0	1.5	0.4		0.60	64.1	62.7			
	Level 3		BEND-90	44	INBU-100-90 100				12.0	12.0	1.5	0.8	0.593		63.8				
	Level 3		DUCT	44	INSR-100 (100)		1.1		12.0	12.0	1.5	0.8		0.60	63.0	61.6			
	Level 3		BEND-90	44	INBU-100-90 100				12.0	12.0	1.5	0.8	0.593		62.3				
	Level 3		DUCT	44	INSR-100 (100)		0.6		12.0	12.0	1.5	0.4		0.60	61.5	60.1			
	Level 3		BEND-90	44	INBU-100-90 100				12.0	12.0	1.5	0.8	0.593		61.2				
	Tak		DUCT	44	INSR-100 (100)		0.7		12.0	12.0	1.5	0.4		0.60	60.4	59.0			
	Tak	14	SUPPLY		SHH-100 (100)				12.0	12.0	1.5	60.0			60.0		5.4	100	
	Basement		DUCT	44	INSR-250 (250)		0.5		124.0	124.0	2.5	0.2		0.47	66.3	62.5			
	Basement		BEND-90	44	INBU-250-90 250				124.0	124.0	2.5	1.7	0.439		66.1				
	Tak		DUCT	44	INSR-250 (250)		1.0		124.0	124.0	2.5	0.5		0.47	64.4	60.6			
	Basement	2	T-BRANCH	44	INTCU-250-2 250/250				124.0	124.0	2.5	4.3	1.130		63.9				
	Basement		DUCT	44	INSR-250 (250)		0.6		100.0	100.0	2.0	0.2		0.31	59.6	57.1			
	Basement		BEND-90	44	INBU-250-90 250				100.0	100.0	2.0	1.1	0.459		59.4				
	Basement		DUCT	44	INSR-250 (250)		10.3		100.0	100.0	2.0	3.2		0.31	58.3	55.8			
	Basement		BEND-90	44	INBU-250-90 250				100.0	100.0	2.0	1.1	0.459		55.1				
	Basement		DUCT	44	INSR-250 (250)		2.5		100.0	100.0	2.0	0.8		0.31	53.9	51.4			
	Tak		BEND-90	44	INBU-250-90 250				100.0	100.0	2.0	1.1	0.459		53.1				
	Tak		DUCT	44	INSR-250 (250)		2.6		100.0	100.0	2.0	0.8		0.31	52.0	49.5			
	Level 1	15	T-BRANCH	44	INTCU-250-1 250/100				100.0	100.0	2.0	3.4	1.378		51.2				
	Level 1		DUCT	44	INSR-100 (100)		0.6		22.0	22.0	2.8	1.2		1.92	47.7	43.0			
	Level 1		BEND-90	44	INBU-100-90 100				22.0	22.0	2.8	2.2	0.475		46.6				
	Level 1		DUCT	44	INSR-100 (100)		0.4		22.0	22.0	2.8	0.8		1.92	44.3	39.6			
	Level 1	16	SUPPLY		SHH-100 (100)				22.0	22.0	2.8	43.5			43.5		13	100	
	Level 1		REDUCER	44	INRCFU-250-250/200				78.0	78.0	1.8				51.0				
	Tak		DUCT	44	INSR-200 (200)		1.4		78.0	78.0	2.5	0.8		0.61	51.0	47.3			
	Tak	17	T-BRANCH	44	INTCU-200-2 200/200				78.0	78.0	2.5	4.0	1.070		50.2				
	Tak		DUCT	44	INSR-200 (200)		1.9		46.0	46.0	1.5	0.4		0.22	46.2	44.9			
	Tak	18	T-BRANCH	44	INTCU-200-2 200/200				46.0	46.0	1.5	1.5	1.138		45.8				
	Tak		DUCT	44	INSR-200 (200)		1.2		24.0	24.0	0.8	0.1		0.07	44.3	44.0			

Level 2	19 T-BRANCH	44	INTCU-200-1 200/100		24.0	24.0	0.8	0.6	1.800		44.3		
Level 2	DUCT	44	INSR-100 100	0.6	12.0	12.0	1.5	0.4		0.60	43.6	42.2	
Level 2	BEND-90	44	INBU-100-90 100		12.0	12.0	1.5	0.8	0.563		43.2		
Level 2	DUCT	44	INSR-100 100	0.4	12.0	12.0	1.5	0.2		0.60	42.5	41.1	
Level 2	20 SUPPLY		SHH-100 100		12.0	12.0	1.5	42.2			42.2	8.5	100
Level 2	REDUCER	44	INRCFU-200-200/100		12.0	12.0	0.4				44.1		
Tak	DUCT	44	INSR-100 100	2.8	12.0	12.0	1.5	1.7		0.60	44.1	42.7	
Tak	BEND-90	44	INBU-100-90 100		12.0	12.0	1.5	0.8	0.563		42.4		
Level 3	DUCT	44	INSR-100 100	0.7	12.0	12.0	1.5	0.4		0.60	41.6	40.2	
Level 3	BEND-90	44	INBU-100-90 100		12.0	12.0	1.5	0.8	0.563		41.2		
Level 3	DUCT	44	INSR-100 100	0.4	12.0	12.0	1.5	0.2		0.60	40.4	39.0	
Level 3	21 SUPPLY		SHH-100 100		12.0	12.0	1.5	40.2			40.2	6.7	100
Tak	REDUCER	44	INRCFU-200-200/100		22.0	22.0	0.7				43.5		
Tak	DUCT	44	INSR-100 100	1.3	22.0	22.0	2.8	2.6		1.92	43.5	38.8	
Tak	BEND-90	44	INBU-100-90 100		22.0	22.0	2.8	2.2	0.475		40.9		
Level 1	DUCT	44	INSR-100 100	0.7	22.0	22.0	2.8	1.3		1.92	38.6	33.9	
Level 1	BEND-90	44	INBU-100-90 100		22.0	22.0	2.8	2.2	0.475		37.4		
Level 1	DUCT	44	INSR-100 100	0.4	22.0	22.0	2.8	0.8		1.92	35.1	30.4	
Level 1	22 SUPPLY		SHH-100 100		22.0	22.0	2.8	34.4			34.4	14	100
Tak	DUCT	44	INSR-200 200	1.2	32.0	32.0	1.0	0.1		0.11	49.6	48.9	
Level 2	23 T-BRANCH	44	INTCU-200-1 200/100		32.0	32.0	1.0	0.9	1.450		49.4		
Level 2	DUCT	44	INSR-100 100	0.6	12.0	12.0	1.5	0.4		0.60	48.5	47.1	
Level 2	BEND-90	44	INBU-100-90 100		12.0	12.0	1.5	0.8	0.563		48.1		
Level 2	DUCT	44	INSR-100 100	0.4	12.0	12.0	1.5	0.2		0.60	47.4	46.0	
Level 2	24 SUPPLY		SHH-100 100		12.0	12.0	1.5	47.1			47.1	6.2	100
Tak	DUCT	44	INSR-200 200	2.9	20.0	20.0	0.6	0.1		0.05	49.4	49.1	
Level 3	25 T-BRANCH	44	INTCU-200-1 200/100		20.0	20.0	0.6	0.5	2.152		49.2		
Level 3	DUCT	44	INSR-100 100	0.6	12.0	12.0	1.5	0.4		0.60	48.7	47.3	
Level 3	BEND-90	44	INBU-100-90 100		12.0	12.0	1.5	0.8	0.563		48.3		
Level 3	DUCT	44	INSR-100 100	0.4	12.0	12.0	1.5	0.2		0.60	47.5	46.1	
Level 3	26 SUPPLY		SHH-100 100		12.0	12.0	1.5	47.3			47.3	6.2	100
Level 3	REDUCER	44	INRCFU-200-200/100		8.0	8.0	0.3				49.2		
Tak	DUCT	44	INSR-100 100	1.2	8.0	8.0	1.0	0.3		0.28	49.2	48.6	
Tak	BEND-90	44	MAGIB-C4-6 100		8.0	8.0	1.0	0.3	0.441		48.9		
Tak	DUCT	44	INSR-100 100	2.3	8.0	8.0	1.0	0.6		0.28	48.6	48.0	
Tak	BEND-90	44	INBU-100-90 100		8.0	8.0	1.0	0.4	0.631		47.9		
Tak	DUCT	44	INSR-100 100	0.4	8.0	8.0	1.0	0.1		0.28	47.6	46.9	
Tak	27 SUPPLY		SHH-100 100		8.0	8.0	1.0	47.4			47.4	3.8	100
Basement	REDUCER	44	INRCFU-250-250/200		24.0	24.0	0.5				63.1		
Tak	DUCT	44	INSR-200 200	2.6	24.0	24.0	0.8	0.2		0.07	63.1	62.8	
Level 1	3 T-BRANCH	44	INTCU-200-1 200/100		24.0	24.0	0.8	0.5	1.356		62.9		
Level 1	DUCT	44	INSR-100 100	0.7	8.0	8.0	1.0	0.2		0.28	62.5	61.8	
Level 1	BEND-90	44	INBU-100-90 100		8.0	8.0	1.0	0.4	0.631		62.3		
Level 1	DUCT	44	INSR-100 100	0.2	8.0	8.0	1.0	0.1		0.28	61.9	61.2	
Level 1	4 SUPPLY		SHH-100 100		8.0	8.0	1.0	61.8			61.8	3.4	100
Level 1	DUCT	44	INSR-200 200	0.7	16.0	16.0	0.5	0.0		0.03	62.9	62.6	
Level 1	BEND-90	44	INBU-200-90 200		16.0	16.0	0.5	0.1	0.627		62.9		
Level 1	DUCT	44	INSR-200 200	0.3	16.0	16.0	0.5	0.0		0.03	62.8	62.6	
Tak	BEND-90	44	INBU-200-90 200		16.0	16.0	0.5	0.1	0.627		62.8		
Tak	DUCT	44	INSR-200 200	1.8	16.0	16.0	0.5	0.1		0.03	62.7	62.5	
Level 2	5 T-BRANCH	44	INTCU-200-1 200/100		16.0	16.0	0.5	0.3	1.800		62.6		
Level 2	DUCT	44	INSR-100 100	0.8	8.0	8.0	1.0	0.2		0.28	62.3	61.7	
Level 2	BEND-90	44	INBU-100-90 100		8.0	8.0	1.0	0.4	0.631		62.1		
Level 2	DUCT	44	INSR-100 100	0.3	8.0	8.0	1.0	0.1		0.28	61.7	61.1	
Level 2	6 SUPPLY		SHH-100 100		8.0	8.0	1.0	61.7			61.7	3.4	100
Level 2	REDUCER	44	INRCFU-200-200/100		8.0	8.0	0.3				62.6		
Tak	DUCT	44	INSR-100 100	2.8	8.0	8.0	1.0	0.8		0.28	62.6	61.9	
Tak	BEND-90	44	INBU-100-90 100		8.0	8.0	1.0	0.4	0.631		61.8		
Level 3	DUCT	44	INSR-100 100	0.8	8.0	8.0	1.0	0.2		0.28	61.4	60.7	
Level 3	BEND-90	44	INBU-100-90 100		8.0	8.0	1.0	0.4	0.631		61.1		
Level 3	DUCT	44	INSR-100 100	0.3	8.0	8.0	1.0	0.1		0.28	60.7	60.1	
Level 3	7 SUPPLY		SHH-100 100		8.0	8.0	1.0	60.7			60.7	3.4	100

Figure 60. Balancing and sizes of the supply ducting, with an illustration of the critical path in building B.

Appendix H



Hydronic Network Balancing Report

Project Information

Software version:	MagiCAD for Revit 2023 UR-2	Calculation date:	2024-04-05 11:18
Project name:	Project Name	Project number:	Project Number
Project address:	Enter address here	Client name:	Owner
Project issue date:	Issue Date	Organization name:	
Organization description:		Author:	

Project Calculation Data

Total pressure:	67923.8 Pa	Systems:	Hydronic_Supply / Hydronic_Return
Fluid type:	Water	Total flow:	1.3 l/s
Fluid density:	988 / 990.9 kg/m ³	Fluid temperature:	49 / 43 °C
Fluid spec. heat capacity:	4180 / 4179 J/kg*K	Fluid dyn. viscosity:	0.00055723 / 0.00061428 Pa*s
		Volume of the system:	385.5 l
Pipe series:	Standard / Material	Thermal conductivity:	
Copper and copper alloys - Seaml	Default / Metal	20.00000 W/m*K:	

Calculation Input Values

Pressure drop standard(s):	Default	Ambient air temperature(s):	21.0°C
Min. dp radiator valves:	3.0 Pa	Balancing target pressure:	Minimum

Calculation Results / Supply

Location	Level	Node	Type	Series	Product	Size	L [m]	Insulation	P [W]	qv [l/s]	v [m/s]	T [°C]	Q [W]	dp/L [Pa/m]	dpt [Pa]	K factor	pt [Pa]	adj.	Warnings
Basement			PIPE	17	EN 1057 - R250		0.6		30150	1.3	0.72	48,9	27,6	108,5	68,4		67923,8		
Basement			BEND-90	17	Elbow Solder 50				30150	1,3	0,72				118,1	0,455	67855,4		
Basement			PIPE	17	EN 1057 - R250		2,7		30150	1,3	0,72	48,9	116,8	108,5	289,5		67737,3		
Basement			BEND-90	17	Elbow Solder 50				30150	1,3	0,72				118,1	0,455	67447,8		
Basement			PIPE	17	EN 1057 - R250		0,7		30150	1,3	0,72	48,9	29,3	108,5	72,7		67329,7		
Basement			BEND-90	17	Elbow Solder 50				30150	1,3	0,72				118,1	0,455	67257,0		
Basement			PIPE	17	EN 1057 - R250		0,3		30150	1,3	0,72	48,9	13,2	108,5	32,8		67138,8		
Basement	12	BRANCH	17		Tee Soldered 50/50				30150	1,3	0,72				259,8	1,000	67106,0		
Basement			REDUCER	17	Reducer Stra 50/40				14590	0,6	0,35				24,3	0,157	66846,2		
Basement			PIPE	17	EN 1057 - R240		0,2		14590	0,6	0,56	48,9	7,6	91,2	19,9		66822,0		
Level 0	13	BRANCH	17		Tee Soldered 40/40				14590	0,6	0,56				154,9	1,000	66802,1		
Level 0			REDUCER	17	Reducer Stra 40/16				1200	0,1	0,05				20,6	0,363	66647,2		
Level 0			PIPE	17	EN 1057 - R216 (L)		0,1		1200	0,1	0,34	48,9	1,0	132,0	9,7		66626,6		
Level 0			BEND-90	17	Elbow Solder 16				1200	0,1	0,34				22,5	0,396	66616,8		
Level 0			PIPE	17	EN 1057 - R216 (L)		0,4		1200	0,1	0,34	48,8	5,2	132,0	49,2		66594,3		
Level 0			BEND-90	17	Elbow Solder 16				1200	0,1	0,34				22,5	0,396	66545,1		
Level 0			PIPE	17	EN 1057 - R216 (L)		0,6		1200	0,1	0,34	48,8	8,1	132,0	77,0		66522,6		
Level 0			BEND-25	17	Elbow Solder 16				1200	0,1	0,34						66445,6		
Level 0			PIPE	17	EN 1057 - R216 (L)		0,1		1200	0,1	0,34	48,8	0,7	132,0	6,8		66445,6		
Level 0	14	RADIATOR V17			RA-N_Axial_10 (L)				1200	0,1					65059,7		66438,9	5,3	
Level 0	15	HEATING: R			TPV4 22-913 10				1200	0,1		48,8					1379,2		
Basement			PIPE	17	EN 1057 - R240		2,8		13390	0,6	0,51	48,9	98,1	78,3	219,7		66802,1		
Basement			BEND-90	17	Elbow Solder 40				13390	0,6	0,51				58,5	0,448	66582,4		
Basement			PIPE	17	EN 1057 - R240		0,7		13390	0,6	0,51	48,8	22,9	78,3	51,3		66523,9		
Basement			BEND-90	17	Elbow Solder 40				13390	0,6	0,51				58,5	0,448	66472,6		
Basement			PIPE	17	EN 1057 - R240		0,6		13390	0,6	0,51	48,8	22,4	78,3	50,2		66414,1		
Level 1	16	BRANCH	17		Tee Soldered 40/40				13390	0,6	0,51				130,4	1,000	66363,9		
Level 1			REDUCER	17	Reducer Stra 40/25				5100	0,2	0,20				37,5	0,266	66233,5		
Level 1			PIPE	17	EN 1057 - R225		0,7		5100	0,2	0,53	48,8	14,3	156,0	102,2		66195,9		
Level 1			BEND-90	17	Elbow Solder 25				5100	0,2	0,53				60,4	0,428	66093,7		
Level 1			PIPE	17	EN 1057 - R225		0,5		5100	0,2	0,53	48,8	11,1	156,0	79,1		66033,3		
Level 1	1	BRANCH	17		Tee Soldered 25/25				5100	0,2	0,53				141,0	1,000	65954,2		
Level 1			REDUCER	17	Reducer Stra 25/16				1000	0,0	0,10				10,4	0,264	65813,1		
Level 1			PIPE	17	EN 1057 - R216 (L)		0,0		1000	0,0	0,28	48,8	0,7	96,3	4,6		65802,7		
Level 1	2	RADIATOR V17			RA-N_Straig_10 (L)				1000	0,0					64090,1		65798,1	4,5	
Level 1	3	HEATING: R			TPV4 22-420 10				1000	0,0		48,8					1708,0		
Level 1			PIPE	17	EN 1057 - R225		3,0		4100	0,2	0,43	48,8	66,0	106,2	321,8		65954,2		
Level 2	4	BRANCH	17		Tee Soldered 25/25				4100	0,2	0,43				91,1	1,000	65632,4		
Level 2			REDUCER	17	Reducer Stra 25/16				1000	0,0	0,10				10,4	0,264	65541,2		
Level 2			PIPE	17	EN 1057 - R216 (L)		0,1		1000	0,0	0,28	48,7	0,9	96,3	6,5		65530,8		
Level 2	5	RADIATOR V17			RA-N_Straig_10 (L)				1000	0,0					63485,5		65524,3	4,6	
Level 2	6	HEATING: R			TPV4 22-420 10				1000	0,0		48,7					2038,8		
Level 2			REDUCER	17	Reducer Stra 25/20				3100	0,1	0,32				22,6	0,163	65632,4		
Level 1			PIPE	17	EN 1057 - R220		3,0		3100	0,1	0,53	48,7	52,4	208,9	630,1		65609,8		
Level 3	7	BRANCH	17		Tee Soldered 20/20				3100	0,1	0,53				138,9	1,000	64979,6		
Level 3			REDUCER	17	Reducer Stra 20/16				1000	0,0	0,17				6,6	0,166	64840,8		
Level 3			PIPE	17	EN 1057 - R216 (L)		0,1		1000	0,0	0,28	48,6	1,0	96,3	7,2		64834,2		
Level 3	8	RADIATOR V17			RA-N_Straig_10 (L)				1000	0,0					62125,2		64827,0	4,6	
Level 3	9	HEATING: R			TPV4 22-420 10				1000	0,0		48,6					2701,8		
Level 3			REDUCER	17	Reducer Stra 20/16 (L)				2100	0,1	0,36				28,9	0,166	64979,6		
Level 1			PIPE	17	EN 1057 - R216 (L)		2,9		2100	0,1	0,59	48,6	39,8	348,9	1002,4		64950,7		
Level 1			BEND-90	17	Elbow Solder 16				2100	0,1	0,59				69,0	0,396	63948,3		
Level 1			PIPE	17	EN 1057 - R216 (L)		0,4		2100	0,1	0,59	48,5	5,2	348,9	130,9		63879,4		
Level 1			BEND-90	17	Elbow Solder 16				2100	0,1	0,59				69,0	0,396	63748,4		

Vind	PIPE	17	EN 1057 - R216 (L)	0,1	2100	0,1	0,59	48,5	1,3	348,9	33,4	63679,5	
Vind	BEND-90	17	Elbow Solder 16		2100	0,1	0,59				69,0	0,396	63646,0
Vind	PIPE	17	EN 1057 - R216 (L)	1,2	2100	0,1	0,59	48,5	17,2	348,9	434,6		63577,1
Vind	10 RADIATOR V17		RA-N_Axial_10 (L)		2100	0,1					58525,1		63142,5 7,1
Vind	11 HEATING: R		TPv4 22-630 10		2100	0,1		48,4					4617,4
Level 1	REDUCER	17	Reducer Stra 40/32		8290	0,4	0,32				20,4	0,158	66363,9
Basement	PIPE	17	EN 1057 - R232	1,4	8290	0,4	0,51	48,8	39,2	103,6	145,6		66343,5
Basement	BEND-90	17	Elbow Solder 32		8290	0,4	0,51				56,7	0,440	66198,0
Basement	PIPE	17	EN 1057 - R232	4,5	8290	0,4	0,51	48,8	124,8	103,6	463,6		66141,3
Basement	BEND-90	17	Elbow Solder 32		8290	0,4	0,51				56,7	0,440	65677,7
Basement	PIPE	17	EN 1057 - R232	0,8	8290	0,4	0,51	48,7	21,3	103,6	79,3		65621,0
Level 1	17 BRANCH	17	TEE Soldered 32/32		8290	0,4	0,51				128,7	1,000	65541,7
Level 1	REDUCER	17	Reducer Stra 32/25		3670	0,2	0,23				12,6	0,173	65413,0
Level 1	PIPE	17	EN 1057 - R225	5,8	3670	0,2	0,38	48,7	128,1	87,4	507,9		65400,4
Level 1	BEND-90	17	Elbow Solder 25		3670	0,2	0,38				31,3	0,428	64892,5
Level 1	PIPE	17	EN 1057 - R225	0,5	3670	0,2	0,38	48,5	10,9	87,4	44,4		64861,2
Level 1	18 BRANCH	17	Cross Solder 25/25/25		3670	0,2	0,38				73,0	1,000	64816,9
Level 1	REDUCER	17	Reducer Stra 25/12		580	0,0	0,06				17,4	0,341	64743,9
Level 1	PIPE	17	EN 1057 - R212 (L)	0,1	580	0,0	0,32	48,5	1,4	184,9	25,2		64726,5
Level 1	BEND-90	17	Elbow Solder 12		580	0,0	0,32				18,5	0,363	64701,3
Level 1	PIPE	17	EN 1057 - R212 (L)	0,2	580	0,0	0,32	48,4	1,7	184,9	29,7		64682,7
Level 1	BEND-90	17	Elbow Solder 12		580	0,0	0,32				18,5	0,363	64653,0
Level 1	PIPE	17	EN 1057 - R212 (L)	0,2	580	0,0	0,32	48,4	1,9	184,9	34,0		64634,5
Level 1	19 RADIATOR V17		RA-N_Straig 10 (L)		580	0,0					61547,1		64600,5 3,1
Level 1	20 HEATING: R		TPv4 22-412 10		580	0,0		48,4					3053,4
Level 1	REDUCER	17	Reducer Stra 25/12		580	0,0	0,06				17,4	0,341	64743,9
Level 1	PIPE	17	EN 1057 - R212 (L)	0,1	580	0,0	0,32	48,5	0,7	184,9	11,9		64726,5
Level 1	BEND-90	17	Elbow Solder 12		580	0,0	0,32				18,5	0,363	64714,6
Level 1	PIPE	17	EN 1057 - R212 (L)	0,2	580	0,0	0,32	48,5	1,7	184,9	29,7		64696,1
Level 1	BEND-90	17	Elbow Solder 12		580	0,0	0,32				18,5	0,363	64666,4
Level 1	PIPE	17	EN 1057 - R212 (L)	0,6	580	0,0	0,32	48,4	6,0	184,9	107,7		64647,9
Level 1	21 RADIATOR V17		RA-N_Straig 10 (L)		580	0,0					61412,8		64540,1 3,1
Level 1	22 HEATING: R		TPv4 22-412 10		580	0,0		48,4					3127,3
Level 1	REDUCER	17	Reducer Stra 25/20		2510	0,1	0,26				14,8	0,163	64816,9
Level 2	PIPE	17	EN 1057 - R220	2,9	2510	0,1	0,43	48,5	49,5	144,2	414,3		64802,0
Level 2	BEND-90	17	Elbow Solder 20		2510	0,1	0,43				37,7	0,414	64387,7
Level 2	PIPE	17	EN 1057 - R220	0,3	2510	0,1	0,43	48,4	5,3	144,2	44,4		64350,0
Level 2	BEND-90	17	Elbow Solder 20		2510	0,1	0,43				37,7	0,414	64305,6
Level 2	PIPE	17	EN 1057 - R220	0,1	2510	0,1	0,43	48,3	1,3	144,2	11,1		64267,9
Level 2	23 BRANCH	17	Cross Solder 20/20/20		2510	0,1	0,43				91,0	1,000	64256,8
Level 2	REDUCER	17	Reducer Stra 20/12		590	0,0	0,10				15,3	0,290	64165,7
Level 2	PIPE	17	EN 1057 - R212 (L)	0,5	590	0,0	0,33	48,3	4,9	190,5	90,2		64150,4
Level 2	BEND-90	17	Elbow Solder 12		590	0,0	0,33				19,2	0,363	64060,2
Level 2	PIPE	17	EN 1057 - R212 (L)	0,2	590	0,0	0,33	48,3	1,7	190,5	30,6		64041,1
Level 2	BEND-90	17	Elbow Solder 12		590	0,0	0,33				19,2	0,363	64010,5
Level 2	PIPE	17	EN 1057 - R212 (L)	0,1	590	0,0	0,33	48,3	1,3	190,5	24,6		63991,3
Level 2	24 RADIATOR V17		RA-N_Straig 10 (L)		590	0,0					60288,3		63966,7 3,1
Level 2	25 HEATING: R		TPv4 22-412 10		590	0,0		48,3					3678,4
Level 2	REDUCER	17	Reducer Stra 20/12		640	0,0	0,11				18,0	0,290	64165,7
Level 2	PIPE	17	EN 1057 - R212 (L)	0,4	640	0,0	0,35	48,3	3,8	219,1	81,5		64147,7
Level 2	BEND-90	17	Elbow Solder 12		640	0,0	0,35				22,5	0,363	64066,2
Level 2	PIPE	17	EN 1057 - R212 (L)	0,2	640	0,0	0,35	48,3	1,7	219,1	35,2		64043,6
Level 2	BEND-90	17	Elbow Solder 12		640	0,0	0,35				22,5	0,363	64008,5
Level 2	PIPE	17	EN 1057 - R212 (L)	0,1	640	0,0	0,35	48,3	0,6	219,1	12,3		63985,9
Level 2	26 RADIATOR V17		RA-N_Straig 10 (L)		640	0,0					60295,5		63973,6 3,3
Level 2	27 HEATING: R		TPv4 22-318 10		640	0,0		48,3					3678,1
Level 2	REDUCER	17	Reducer Stra 20/16		1280	0,1	0,22				10,7	0,166	64256,8
Level 2	PIPE	17	EN 1057 - R216	0,1	1280	0,1	0,36	48,3	0,9	147,7	9,3		64246,0
Level 2	BEND-90	17	Elbow Solder 16		1280	0,1	0,36				25,6	0,396	64236,7
Level 2	PIPE	17	EN 1057 - R216	0,2	1280	0,1	0,36	48,3	2,9	147,7	31,4		64211,1
Level 2	BEND-90	17	Elbow Solder 16		1280	0,1	0,36				25,6	0,396	64179,6
Level 2	PIPE	17	EN 1057 - R216	2,9	1280	0,1	0,36	48,3	39,9	147,7	429,1		64154,0
Level 2	BEND-90	17	Elbow Solder 16		1280	0,1	0,36				25,6	0,396	63724,9
Level 2	PIPE	17	EN 1057 - R216	0,2	1280	0,1	0,36	48,1	2,1	147,7	22,8		63699,2
Level 2	28 BRANCH	17	TEE Soldered 16/16		1280	0,1	0,36				64,7	1,000	63676,4
Level 2	REDUCER	17	Reducer Stra 16/12 (L)		610	0,0	0,17				11,6	0,206	63611,7
Level 3	PIPE	17	EN 1057 - R212 (L)	0,4	610	0,0	0,34	48,1	3,9	201,7	77,8		63600,1
Level 3	29 RADIATOR V17		RA-N_Straig 10 (L)		610	0,0					59306,9		63522,3 3,2
Level 3	30 HEATING: R		TPv4 22-412 10		610	0,0		48,1					4215,5
Level 2	REDUCER	17	Reducer Stra 16/12 (L)		670	0,0	0,19				14,0	0,206	63611,7
Level 3	PIPE	17	EN 1057 - R212 (L)	0,7	670	0,0	0,37	48,1	6,7	237,1	154,3		63597,7
Level 3	31 RADIATOR V17		RA-N_Straig 10 (L)		670	0,0					59122,7		63443,4 3,4
Level 3	32 HEATING: R		TPv4 22-318 10		670	0,0		48,1					4320,7
Level 1	REDUCER	17	Reducer Stra 32/25		4620	0,2	0,28				20,0	0,173	65541,7
Basement	PIPE	17	EN 1057 - R225	2,0	4620	0,2	0,48	48,7	42,8	131,1	258,3		65521,7
Level 3	BEND-90	17	Elbow Solder 25		4620	0,2	0,48				49,6	0,428	65263,5
Level 3	PIPE	17	EN 1057 - R225	0,5	4620	0,2	0,48	48,6	11,0	131,1	66,5		65213,9
Level 1	33 BRANCH	17	TEE Soldered 25/25		4620	0,2	0,48				115,7	1,000	65147,4
Level 1	REDUCER	17	Reducer Stra 25/10		490	0,0	0,05				32,8	0,369	65031,7
Level 1	PIPE	17	EN 1057 - R210	0,2	490	0,0	0,42	48,6	2,1	397,2	97,4		64998,9

Level 3	PIPE	17	EN 1057 - R225		3800	0,2	0,40	48,5	65,3	93,0	281,2		63642,1
Level 3	BEND-90	17	Elbow Solder 25		3800	0,2	0,40				33,5	0,428	63360,9
Tak	PIPE	17	EN 1057 - R225	0,3	3800	0,2	0,40	48,4	7,3	93,0	31,7		63327,4
Tak	BEND-90	17	Elbow Solder 25		3800	0,2	0,40				33,5	0,428	63295,6
Tak	PIPE	17	EN 1057 - R225	0,6	3800	0,2	0,40	48,4	13,3	93,0	57,4		63262,1
Tak	78 BRANCH	17	Tee Soldered 25/25		3800	0,2	0,40				78,3	1,000	63204,7
Tak	REDUCER	17	Reducer Stra 25/16 (L)		1900	0,1	0,20				37,7	0,264	63126,4
Tak	PIPE	17	EN 1057 - R216 (L)	0,2	1900	0,1	0,54	48,4	2,3	292,7	49,1		63088,7
Tak	79 RADIATOR V17		RA-N_Straig 10 (L)		1900	0,1					57338,1		63039,6 7,1
Vind	80 HEATING: R		TPv4 22-626 10		1900	0,1		48,4					5701,5
Tak	REDUCER	17	Reducer Stra 25/16 (L)		1900	0,1	0,20				37,7	0,264	63126,4
Tak	PIPE	17	EN 1057 - R216 (L)	0,3	1900	0,1	0,54	48,4	4,1	292,7	87,6		63088,7
Tak	BEND-90	17	Elbow Solder 16		1900	0,1	0,54				56,5	0,396	63001,1
Tak	PIPE	17	EN 1057 - R216 (L)	1,2	1900	0,1	0,54	48,4	16,0	292,7	339,9		62944,7
Tak	BEND-59	17	Elbow Solder 16		1900	0,1	0,54				22,6	0,159	62604,7
Tak	PIPE	17	EN 1057 - R216 (L)	2,5	1900	0,1	0,54	48,3	34,1	292,7	728,0		62582,1
Tak	BEND-31	17	Elbow Solder 16		1900	0,1	0,54						61854,1
Tak	PIPE	17	EN 1057 - R216 (L)	0,2	1900	0,1	0,54	48,2	2,5	292,7	53,1		61854,1
Tak	BEND-90	17	Elbow Solder 16		1900	0,1	0,54				56,5	0,396	61800,9
Tak	PIPE	17	EN 1057 - R216 (L)	2,5	1900	0,1	0,54	48,2	33,6	292,7	720,9		61744,5
Tak	BEND-90	17	Elbow Solder 16		1900	0,1	0,54				56,5	0,396	61023,5
Tak	PIPE	17	EN 1057 - R216 (L)	0,3	1900	0,1	0,54	48,1	4,3	292,7	93,1		60967,1
Tak	BEND-90	17	Elbow Solder 16		1900	0,1	0,54				56,5	0,396	60874,0
Tak	PIPE	17	EN 1057 - R216 (L)	0,2	1900	0,1	0,54	48,1	3,0	292,7	65,0		60817,5
Tak	81 RADIATOR V17		RA-N_Straig 10 (L)		1900	0,1					52700,4		60752,6 7,1
Vind	82 HEATING: R		TPv4 22-626 10		1900	0,1		48,1					8052,1
Basement	REDUCER	17	Reducer Stra 40/25		3400	0,1	0,13				16,7	0,266	66838,1
Level 1	PIPE	17	EN 1057 - R225	0,7	3400	0,1	0,36	48,8	14,4	76,5	50,3		66821,4
Level 1	BEND-90	17	Elbow Solder 25		3400	0,1	0,36				26,9	0,428	66771,1
Level 1	PIPE	17	EN 1057 - R225	0,5	3400	0,1	0,36	48,8	11,0	76,5	38,5		66744,2
Level 1	83 BRANCH	17	Tee Soldered 25/25		3400	0,1	0,36				62,7	1,000	66705,8
Level 1	REDUCER	17	Reducer Stra 25/16		1000	0,0	0,10				10,4	0,264	66643,1
Level 1	PIPE	17	EN 1057 - R216 (L)	0,9	1000	0,0	0,28	48,8	11,9	96,3	82,3		66632,6
Level 1	84 RADIATOR V17		RA-N_Straig 10 (L)		1000	0,0					65048,0		66550,3 4,5
Level 1	85 HEATING: R		TPv4 22-420 10		1000	0,0		48,7					1502,4
Level 1	REDUCER	17	Reducer Stra 25/20		2400	0,1	0,25				13,5	0,163	66705,8
Level 1	PIPE	17	EN 1057 - R220	3,0	2400	0,1	0,41	48,8	52,7	133,3	402,2		66692,2
Level 2	86 BRANCH	17	Tee Soldered 20/20		2400	0,1	0,41				83,2	1,000	66290,0
Level 2	REDUCER	17	Reducer Stra 20/16		1000	0,0	0,17				6,6	0,166	66206,7
Level 2	PIPE	17	EN 1057 - R216 (L)	0,8	1000	0,0	0,28	48,7	11,5	96,3	79,9		66200,2
Level 2	87 RADIATOR V17		RA-N_Straig 10 (L)		1000	0,0					64192,6		66120,3 4,5
Level 2	88 HEATING: R		TPv4 22-420 10		1000	0,0		48,6					1927,6
Level 2	REDUCER	17	Reducer Stra 20/16 (L)		1400	0,1	0,24				12,8	0,166	66290,0
Level 1	PIPE	17	EN 1057 - R216 (L)	3,0	1400	0,1	0,40	48,7	42,1	172,5	522,2		66277,1
Level 1	BEND-90	17	Elbow Solder 16		1400	0,1	0,40				30,7	0,396	65755,0
Level 3	PIPE	17	EN 1057 - R216 (L)	0,8	1400	0,1	0,40	48,5	11,7	172,5	145,9		65724,3
Level 3	89 RADIATOR V17		RA-N_Straig 10 (L)		1400	0,1					62859,1		65578,4 6,0
Level 3	90 HEATING: R		TPv4 22-620 10		1400	0,1		48,5					2719,3

Figure 61. Balancing and sizes of the supply piping, with an illustration of the critical path in building B.

Appendix I

Table 29. Detailed description of the retrofitting costs related to building B.

Type	Specification	Price /SEK	Note	Source
Ventilation	AHU	100 000	Replaced every 20 years.	Wikells
	Ducts and bends	150 000	(-)	Lindab webshop
	Diffusers	31 000	(-)	Lindab webshop
	Inlet & outlet	7 000	(-)	Lindab webshop
	Filter	1 500	Replaced every year.	Luftbutikens webshop
	Core drilling	162 000	Includes labor.	GK
	Fire sealant	7 000	Includes labor.	Wikells
	Adjustment of system	16 000	Performed every 20 years.	GK
	Labor	88 000	All except core drilling, adjustment, and fire sealant.	Wikells
Heating	HP & tank	373 000	Replaced once during the calculation period.	Wikells, Velltra, VVSButiken
	Radiators	157 000	(-)	Bygghemma
	Pipes & bends	36 000	(-)	Bauhaus, Golvvarmebutiken
	Thermostats	8 000	Replaced every 10 years.	Amazon
	Circulation pumps	24 000	Replaced every 10 years.	Bygghemma
	Core drilling	28 000	Includes labor.	GK
	Fire sealant	5 000	Includes labor.	Wikells
	Labor	184 000	All except core drilling, and fire sealant.	Wikells
Façade	Scaffolding	49 000	Included in each façade retrofitting.	Wikells
	Rockwool 50 /mm	317 000	Serporoc system	Wikells
	Rockwool 80 /mm	326 000	Serporoc system	Wikells
	Rockwool 100 /mm	333 000	Serporoc system	Wikells
	EPS 50 /mm	241 000	StoTherm Vario	Wikells
	EPS 80 /mm	246 000	StoTherm Vario	Wikells
	EPS 100 /mm	263 000	StoTherm Vario	Wikells
	Labor	(-)	Is included in each set.	
Roof	Scaffolding	(-)	The work was performed from the interior.	Wikells
	Mineral wool	38 000	(-)	Wikells/Bygghemma
	Rockwool	46 000	(-)	Wikells/Bygghemma
	Cellulose	37 000	(-)	Wikells/Bygghemma
	PE-membrane, duct-tape	34 000	Included in each roof retrofitting.	Wikells
	Gypsum board	35 000	Included in each roof retrofitting.	Wikells
	Labor	(-)	Included in each set.	
Window	Scaffolding	65 000	The windows are only being replaced on one façade.	Wikells
	Demolition of existing windows	15 000	Included in each retrofitting.	Wikells
	Painted <i>U-value</i> : 1.2	344 000	Painted once during the calculation period.	Beijerbygg
	Painted <i>U-value</i> : 0.9	363 000	Painted once during the calculation period.	Beijerbygg
	Alu <i>U-value</i> : 1.2	411 000	No maintenance.	Beijerbygg
	Alu <i>U-value</i> : 0.9	425 000	No maintenance.	Beijerbygg
	Labor	145 000	A complete package for finishing a window installation. Included in each window retrofitting.	Wikells

Appendix

Table 30. AI and its role in this thesis.

Questions	Answer: Yes/no	Details
I used Generative AI tool (e.g. ChatGPT or similar) in my report.	Yes	Only ChatGPT was used.
I used a GAI tool as language editor (i.e. to correct grammar mistakes, etc.).	No	
I used GAI to retrieve information.	No	
I used GAI to get help in writing code	No	
I used GAI for translations	Yes	ChatGPT was used to generate synonyms and typical words that enhance the flow of the text. All information were cross-checked with literature before it was used. The tool were used in background and method.
I used GAI to generate graphs/images	No	
I used GAI to help structuring my content	No	



LUND UNIVERSITY

Divisions of Energy and Building Design, Building Physics and Building Services
Department of Building and Environmental Technology